The statistical theory of stationary turbulence

H. O. Rasmussen

A thesis submitted for the degree of Doctor of Philosophy

at the University of Cambridge, March 1995.

Statement

The work in this thesis is entirely my own, except where explicit reference is made to others, and includes nothing done in collaboration. No part of this work has been submitted or is being submitted for any degree other than that of Doctor of Philosophy at the University of Cambridge.

Acknowledgement

I am grateful to my supervisor during the first two years, Prof. J. C. R. Hunt, for suggesting the Lagrangian structure of turbulence as a topic for research (Chapter 5), and for comments on other chapters. Moreover, I am grateful to Prof. H. K. Moffatt, my supervisor since Prof. Hunt's departure, for general advice, comments, and references.

Furthermore, I would like to thank the following for advice or discussions: Dr. S. Cowley, Dr. L. Fradkin, Dr. J–M. Ghez, Dr. A. D. Gilbert, Dr. M. Holschneider, Dr. N. Kevlahan, Prof. T. Körner, Dr. B. Legras, Prof. M. E. McIntyre, Dr. R. Ricca, Dr. D. J. Thomson, and Dr. S. Vaienti. The topic of Chapter 7, the wavelet Gibbs phenomenon, was suggested by Dr. J. C. Vassilicos. Finally, it is a pleasure to thank Prof. V. L. Hansen, at the Technical University of Denmark, for support and encouragement.

I have been supported by the Carlsberg Foundation, the Science and Engineering Research Council, Schlumberger Research Cambridge, the Danish Research Academy, and the Department of Applied Mathematics and Theoretical Physics.

Some of the work in this thesis has been published (1993a,b); the rest has either been submitted or is in preparation (1995a,b,c,d,e,f,g).

Contents

Chapter 1

General introduction

This thesis is mainly on stationary turbulence, but two chapters on wavelet transforms are also included. Wavelet transforms are better than Fourier transforms at characterising local structure (since they use localised waves instead of Sine waves). Local structure in turbulence is not well understood, and this motivates the study of wavelet transforms in connection with turbulence.

This chapter reviews main results in these two fields and summarises the contents of later chapters. Each chapter contains a more exhaustive introduction, and is either self–contained or, in the case of Chapter 3, continues the previous chapter.

1.1 Part 1: Turbulence

1.1.1 A short history

Turbulence was described already by Leonardo da Vinci, but systematic study of this phenomenon did not begin until 1883. That year, Osborne Reynolds gave a talk at the Royal Society and published a paper on turbulence in cylindrical pipes. Reynolds (1894) soon realised that the random nature of turbulence requires a statistical approach for its analysis. He derived an equation for the mean momentum directly from the Navier–Stokes equation by separating the velocity field into mean and fluctuating parts. However, there was little progress the next 40 years in deriving results directly from the Navier–Stokes equation.

The kinetic theory of gasses inspired much early work on the statistical theory of turbulence. For instance, work on turbulent diffusion (Taylor, 1921). Einstein had described, in one of his famous 1905 papers, molecular diffusivity in terms of the random motion of molecules. Taylor showed that turbulent diffusion resembles molecular diffusion only asymptotically at times much larger than those characterising velocity disturbances. At small times, on the other hand, fluid elements are displaced from initial positions by the

mean flow. Velocity disturbances alone determine the rate at which pairs of fluid elements separate. Richardson (1926) measured this rate of separation by releasing pairs of balloons in the atmosphere. He found that the separation l satisfies

$$\frac{dl^2}{dt} \sim K\, l^{4/3}, \tag{1.1}$$

where t is the separation in time and K is a dimensional constant. It was crucial to discover that turbulent diffusivity, in contrast to molecular diffusivity, increases with the separation. Balloons with separation in the inertial range move apart mainly through velocity disturbances at the corresponding length scale. An estimate for the magnitude of these velocity disturbances is readily derived from Eq. 1.1. But it took another 15 years before this estimate was derived by Kolmogorov (1941 a, b) and Obukhov (1941).

Richardson (1922) observed that turbulence 'cascades' kinetic energy from large scales to small scales. Kolmogorov (1941 a) and Obukhov (1941) based their theory of turbulence in statistical equilibrium on this picture. It was suggested by Kolmogorov (1941 a) that turbulence at high Reynolds number has an approximately universal form in the inertial range that depends only on the mean rate of viscous energy dissipation ϵ per unit mass. The equilibrium energy spectrum $E(k)$ is then given by

$$E(k) \sim C\, \epsilon^{2/3}\, k^{-5/3}, \tag{1.2}$$

when the wavenumber k lies in the inertial range. This result has been confirmed in many experiments and numerical simulations. Most recently, Zocchi *et al.* (1994) find that there is no noticeable deviation from $-5/3$ at the rather high Taylor micro–scale Reynolds number of $R_\lambda \approx 1900$ (using helium gas). Note that the dimensional constant K in Richardson's 4/3–law has the dimension of $\epsilon^{1/3}$. With the wisdom of hindsight, it is striking that Richardson did not use his idea of an energy cascade to explain the 4/3–law.

Taylor (1935) suggested that the distribution of velocities in turbulence is approximately homogeneous and isotropic when the Reynolds number is high. Homogeneity denotes invariance under translations. Isotropy denotes invariance under both rotations of the coordinate system and reflections of the coordinate axes. It was shown that turbulence in a wind tunnel is approximately homogeneous and isotropic. Dynamical consequences of homogeneity and isotropy for velocity correlations were deduced by von Kármán & Howarth (1938). These authors obtained an equation for the energy transfer during the decay of homogeneous and isotropic turbulence. The methods used in deriving this equa-

tion (see Chapter 2) form the basis for most analytical work on the statistical theory of turbulence.

Kolmogorov (1941 b) extended, without proof, the equation of von Kármán & Howarth to turbulence in statistical equilibrium. Kolmogorov's equation admits an approximate solution at inertial scales (see Chapter 2). This solution depends only on the scale and the mean rate of viscous energy dissipation ϵ per unit mass; it then partially confirms the hypothesis made in the two previous papers (Kolmogorov, 1941 a; Obukhov, 1941). This solution is so far the only result for the equilibrium structure of turbulence obtained directly from the Navier–Stokes equation.

One of the most important experimental results since 1941 is that turbulence is intermittent (Batchelor & Townsend, 1949). That is, regions with large velocity derivatives occupy only a small fraction of total space. The Kolmogorov–Obukhov theory then describes accurately only the distribution of velocity differences near the root–mean–square velocity difference. There is still no adequate theory for the entire distribution of velocity differences. However, numerical simulations can now resolve the small–scale structure of homogeneous turbulence. These simulations show that intermittency at small scales is associated with intense vortex tubes.

The Kolmogorov–Obukhov theory fails also for two–dimensional turbulence. Von Neumann realised this already in 1949. But there has apparently not been any attempt so far to construct a theory of two–dimensional turbulence from first principles, as done by von Kármán & Howarth (1938) and Kolmogorov (1941 b) for three–dimensional turbulence. Suggestions for dimensional hypotheses (e.g., Bray, 1966; Kraichnan, 1967; Leith, 1968; Batchelor, 1969), which at any rate are not complete explanations, cannot account for all the results observed in experiments and numerical simulations.

1.1.2 Overview

The main purpose of this thesis is to develop the statistical theory of forced turbulence. It is, in my opinion, remarkable that the theory of homogeneous turbulence in statistical equilibrium has been developed so far without much attention to the forcing required to maintain the turbulence against viscous energy dissipation. Forcing has of course been considered in many contexts, such as various closure models, but the most important analytical work in the subject — that of Kolmogorov (1941 b) — still has not been extended rigorously to forced turbulence. Moreover, it seems that proper analysis of the contribution from forcing leads to the solution of several important problems in the statistical theory of turbulence.

Chapter 2 extends Kolmogorov's equation for the energy cascade in three–dimensional turbulence to forced turbulence of dimension d_0 (where $d_0 = 2$ or $d_0 = 3$). The turbulence is assumed homogeneous, isotropic, and stationary. It is shown that Kolmogorov's equation is the leading–order approximation at small scales in three–dimensional turbulence. The general equation is solved for three–dimensional turbulence, both when forced at a single wavenumber and for general (smooth) forcing. The former extends Kolmogorov's solution to all scales at which viscous forces are negligible. The physical meaning of the general solution is briefly discussed.

Chapter 3 begins with a discussion of two–dimensional turbulence. The equation derived in the previous section is then solved for two–dimensional turbulence under general forcing. It is assumed that the forcing injects kinetic energy at small scales and extracts some of it again at large scales. This leads to a prediction for the third–order moment of two–dimensional turbulence in statistical equilibrium. The structure at large scales corresponds to an inverse energy cascade and, as the scale increases, to an inverse enstrophy cascade. The structure at small scales corresponds first to a palinstrophy cascade (mean–square vorticity gradient), and, as the scale decreases, to an enstrophy cascade. When the characteristic Reynolds number of those structures in the vorticity field responsible for viscous energy dissipation increases, the enstrophy cascade to small scales is inhibited and the enstrophy cascade to large scales is enhanced. The energy spectrum is determined by considering the effects of intermittency. This energy spectrum is in good agreement with experimental and numerical results.

Chapter 4 presents an exact theory for the energy cascade in a particular type of anisotropic turbulence in statistical equilibrium. The turbulence is assumed homogeneous. But instead of isotropy, only reflectional invariance in a plane is required. Reflectional invariance in a plane is much easier to justify than full isotropy. For instance, turbulence in cylindrical pipes can presumably be considered reflectionally invariant in the plane normal to the mean flow, provided that the Reynolds number is high and the separations considered are much smaller than the distance to the wall. The third–order moment is derived. The tensor analysis of von Kármán & Howarth (1938) is avoided by deriving instead equations for the transfer of both kinetic energy and mean–square angular momentum.

Chapter 5 concerns the Lagrangian structure of homogeneous turbulence in statistical equilibrium (i.e., stationary; I use the terms interchangeably). It is argued that the Lagrangian acceleration decorrelates rapidly along fluid trajectories. This agrees with recent numerical results. I then derive the Lagrangian velocity correlation at inertial–range sepa-

rations. This correlation falls off linearly, as first conjectured by Landau & Lifshitz (1944). But the rate of fall off equals the integral over positive time separations of the forcing correlation. In particular, the rate of fall off depends on the conditions at large scales and is not a universal function of the energy dissipation ϵ. Kolmogorov's hypothesis of a universal equilibrium structure of three–dimensional turbulence at high Reynolds numbers, therefore, is not entirely correct for the Lagrangian velocity correlation. Moreover, this result explains why different experiments often give different constants of proportionality when ϵ is used for comparison.

I finally consider applications to turbulent diffusion. First, Taylor's result for the mean–square displacement of fluid elements is extended to orders at which turbulent velocity disturbances contribute. Next, I derive a version of Richardson's 4/3–law for the rate at which the actual and expected position of a fluid element, where the expected position is that based on initial position and velocity, diverges. This is apparently the first derivation of such a 4/3–law directly from the Navier–Stokes equation.

Chapter 6 presents a heuristic model for intermittency in homogeneous turbulence. It is first pointed out that the kinetic energy associated with intermittency remains at scales much larger than the Kolmogorov dissipation scale. I suggest instead that intermittency is associated with helicity transfer to small scales. Predictions are then derived for the Reynolds numbers of vortex tubes and the asymptotic behaviour of structure functions as the order tends to infinity. The agreement with experimental and numerical results is good. In an appendix, it is argued that spiral–shaped vorticity distributions assumed by Lundgren (1982) are far too unstable to exist in turbulence at high Reynolds number. The roll–up of such spirals has been proposed as a model for the energy cascade by several authors.

1.2 Part 2: Wavelet transforms

1.2.1 Definitions and previous works

This section reviews previous work on wavelet transforms. Each chapter on wavelet transforms contains a more exhaustive review and general reviews can be found in the book by Meyer (1990) (the construction of orthogonal wavelet bases, in particular, is described in detail in these books). Applications to turbulence are discussed in the review by Farge (1992).

Wavelet transforms generalise Fourier transforms and they arise by using localised waves instead of Sine waves. These localised waves are known as *analysing wavelets* and are usually denoted by $g(t)$ (for the continuous wavelet transform) and by $\psi(t)$ (for the discrete wavelet transform). Wavelets are formed from the analysing wavelet by two transformations. The first transformation is to scale the analysing wavelet by a positive parameter $\lambda > 0$,

$$g(t) \mapsto g\left(\frac{t}{\lambda}\right). \tag{1.3}$$

The inverse, λ^{-1}, is then similar to a wavenumber or a frequency in Fourier analysis. The second transformation is to translate the scaled analysing wavelet,

$$g(t) \mapsto g\left(\frac{t-r}{\lambda}\right). \tag{1.4}$$

Translations are required to reconstruct the function $f(t)$. The wavelet transform is defined by (Grossman & Morlet, 1984; Holschneider & Tchamitchian, 1991),

$$\begin{aligned} W(\lambda, r) &= \frac{1}{\lambda}\int_{-\infty}^{+\infty} f(t)\, g^*\left(\frac{t-r}{\lambda}\right) dt \\ &= \int_{-\infty}^{+\infty} \tilde{f}(\omega)\, \tilde{g}^*(\lambda\omega)\, \exp[ir\omega]\, d\omega \end{aligned} \tag{1.5}$$

where r is a real number, λ is positive and the complex conjugate of $g(t)$ is denoted by $g^*(t)$. The wavelet transform focusses at $t = r$ as the scale λ decreases. The behaviour of the wavelet transform in this limit is similar to the procedure for constructing the delta–function, except that the total integral of the analysing wavelet $g(t)$ should be zero. In fact, the analysing wavelet should generally satisfy the following three conditions,

$$(1) \qquad 0 < \int |g(t)|^2\, dt < \infty$$

$$(2) \qquad \int_{-\infty}^{+\infty} g(t)\,dt = 0$$

$$(3) \qquad 0 < c_g \stackrel{\text{def}}{=} 2\,\pi \int_0^{\infty} \frac{|\tilde{g}(\omega)|^2}{\omega}\,d\omega < \infty.$$

where the Fourier transform $\tilde{g}(\omega)$ is defined as follows,

$$\tilde{g}(\omega) = \frac{1}{\sqrt{2\,\pi}} \int_{-\infty}^{+\infty} g(t)\,e^{i\,\omega\,t}\,dt. \tag{1.6}$$

The analysing wavelet is said to be 'admissible' (Grossman & Morlet, 1984) and the wavelet transform is then invertible (e.g., Holschneider & Tchamitchian, 1991). The so–called Mexican Hat wavelet satisfies these conditions,

$$g(t) = \frac{1}{\sqrt{2\pi}} \int_0^{\infty} \omega^2 e^{-\omega^2/2 + i\omega t}\,d\omega. \tag{1.7}$$

This analysing wavelet is *progressive*: the Fourier transform vanishes for all negative frequencies. If $g(t)$ is progressive, the imaginary part of $g(t)$ is the Hilbert transform of the real part (Zygmund, 1959). Progressive analysing wavelets often simplify the wavelet transform for the same reason as the exponential of imaginary argument often simplifies the Fourier transform (when compared with, say, the Cosine transform). Another example (see Figures 1.1 and 1.2 below) are the wavelets defined by

$$g_m(t) = \frac{1}{2\pi}(1 - it)^{-m-1}, \quad m > 0. \tag{1.8}$$

We call these *Poisson wavelets*, because they are proportional to derivatives of the Poisson kernels used in Fourier analysis. The Mexican Hat wavelet and the Poisson wavelets are considered in Chapter 7.

As the Fourier transform, the wavelet transform has a discrete and a continuous version. Following the naming in Fourier theory, we call the discrete representation a *wavelet series* and the continuous representation a *wavelet integral*. The discrete wavelet transform is formed in the same way as the continuous wavelet transform, but using only scales and positions of the form

$$\lambda_j = 2^{-j} \tag{1.9}$$

$$r_{ij} = 2^{-j}\,i \tag{1.10}$$

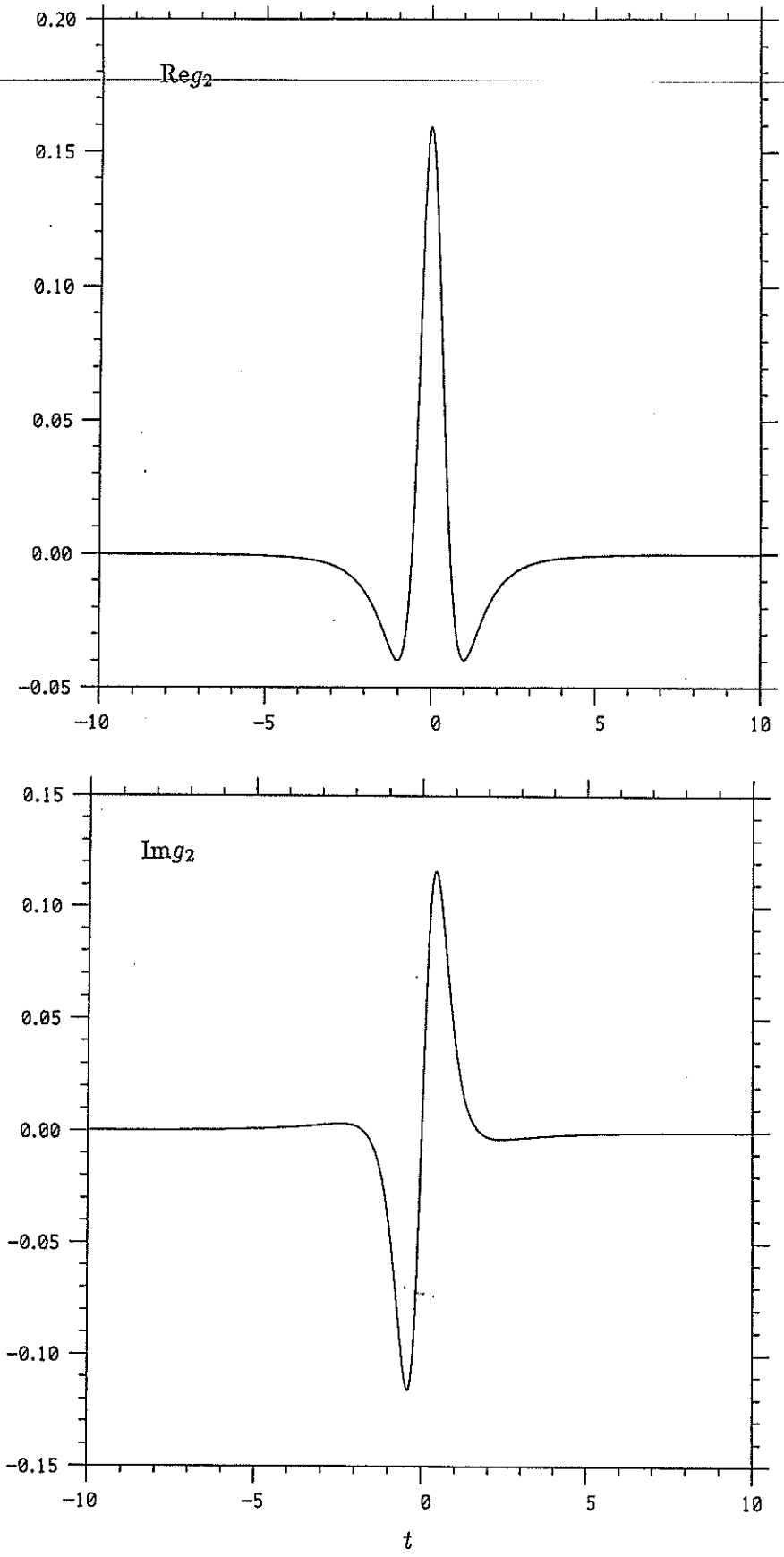

Figure 1.1: The real and imaginary parts of the Poisson wavelet with $m = 2$.

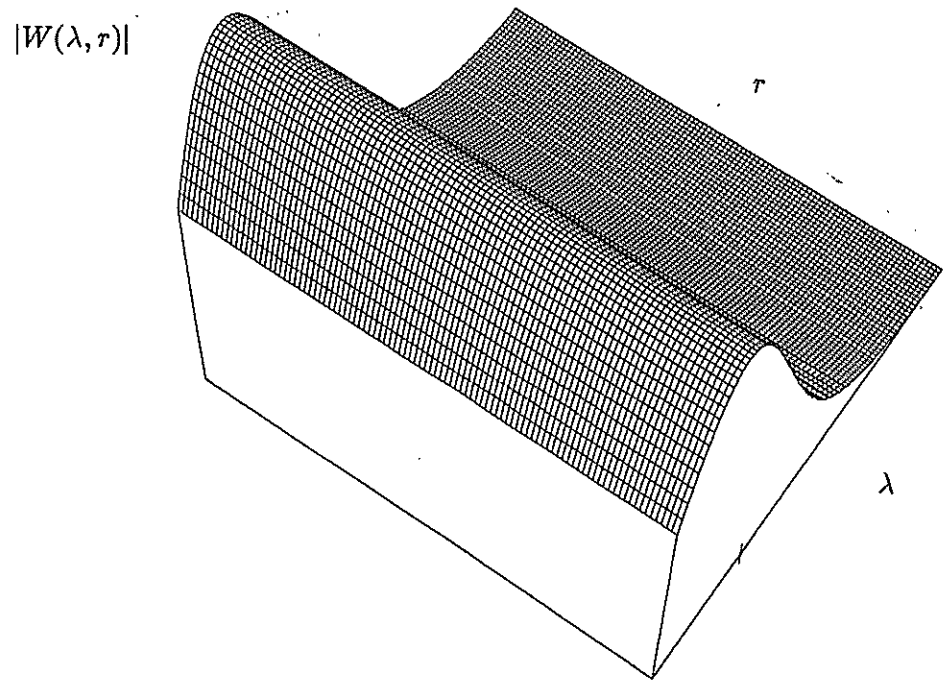

Figure 1.2: The wavelet transform of a Sine wave; the position of the ridge depends linearly on the frequency of the Sine wave.

where $i, j \in \mathbb{Z}$. In this case, the analysing wavelet, which is usually denoted by $\psi(t)$, must satisfy much stricter conditions (see, for instance, Meyer, 1990).

An important property of wavelet transforms is the ability to characterise the Hölder continuity of functions. Recall that a function $f : \mathbb{R} \to \mathbb{R}$ is Hölder continuous with exponent α, $0 < \alpha \leq 1$, if there exists a $C > 0$ such that

$$\sup_{|x-y| \leq h} |f(x) - f(y)| \leq C\, h^{\alpha} \tag{1.11}$$

for all $h > 0$. For bounded functions, this condition holds for all $h > 0$ whenever it holds for $h > 0$ sufficiently small (though generally with a different constant). To determine the Hölder continuity by means of wavelet transforms, the analysing wavelet must be continuously differentiable and satisfy the following conditions

(1) there exist C > 0, C′ > 0, $\epsilon > 0$, and m > 0, such that

$$|g(t)| \leq C\,(1+|t|)^{-m-2} \quad \text{and} \quad |g'(t)| \leq C'(1+|t|)^{-\epsilon-2}$$

(2) the following relations are satisfied :

$$\int_{-\infty}^{+\infty} g(t)\,dt = 0 \quad \text{and} \quad \int_{-\infty}^{+\infty} t\,g(t)\,dt = 0$$

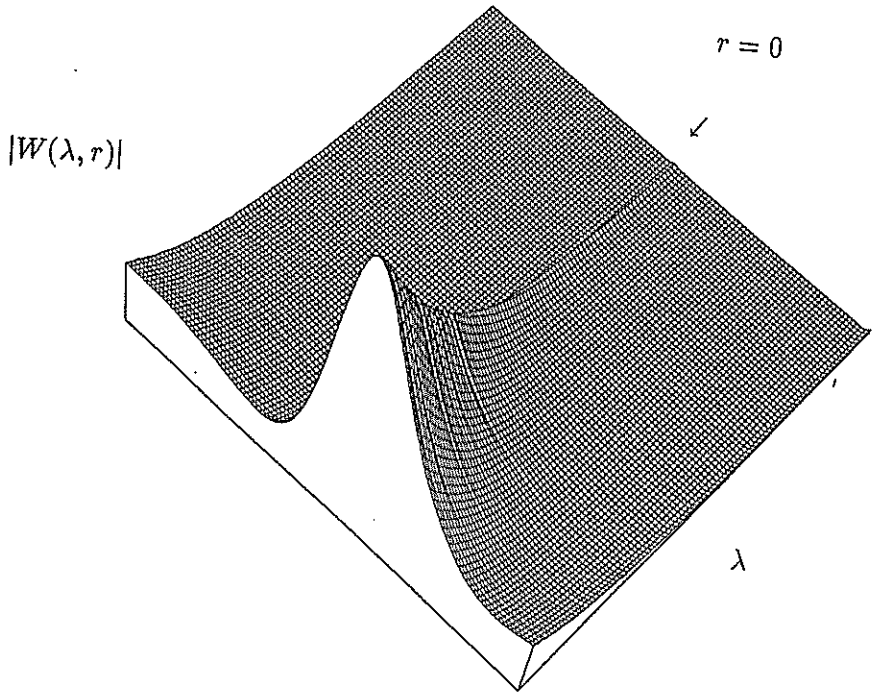

Figure 1.3: The wavelet transform of the function $f(t) = t^{1/2} \exp(-t)\, H(t)$, where $H(t)$ is Heaviside's function, with the complex–valued Mexican Hat wavelet. The discontinuity in the derivative is clearly detected.

When these conditions are satisfied, the wavelet transform characterises the Hölder continuity.

Theorem 1.1 *Suppose that the function $f(t)$ to be analysed is square integrable and continuous. Let the analysing wavelet satisfy the two above conditions with $m > \alpha$ for some $\alpha \in]0, 1[$. Then the function is Hölder continuous with exponent α if and only if*

$$W(\lambda, r) = O(\lambda^\alpha) \tag{1.12}$$

holds uniformly in r.

This theorem translates a result due to Calderón & Zygmund (1961) into wavelet terminology. The version here is due to Holschneider & Tchamitchian (1991), although they forget the condition of continuity.

1.2.2 Overview

Chapter 7 contains a proof of the existence of a Gibbs phenomenon for wavelet integrals. The Gibbs phenomenon for the orthogonal wavelet transforms was considered earlier by

Jaffard (1989). But it is necessary to consider the Gibbs phenomenon for wavelet integrals separately, because the class of admissible analysing wavelets for wavelet integrals is much larger than the class of admissible analysing for orthogonal wavelet series. Furthermore, the discretisation of wavelet transforms influences the convergence properties of truncated wavelet series near singular points. The Gibbs pheomenon for wavelet integrals may therefore be different from the Gibbs phenomenon for wavelet series. In Chapter 7, it is shown that there is a Gibbs phenomenon for wavelet integrals and that the overshoot is always less than the overshoot for Fourier integrals (whereas, the overshoot may be infinite for orthogonal wavelet series; Jaffard, 1989). The overshoot is expressed in terms of the analysing wavelet, and the asymptotic number of oscillations in the truncated wavelet integral around the original function is determined (this number may be finite, even zero, whereas the Fourier Gibbs phenomenon asymptotically has an infinite number of oscillations).

Chapter 8 concerns the wavelet analysis of fractals represented by continuous functions on the unit interval. It is shown that the decay of wavelet transforms of continuous functions defined on finite intervals, as the scale tends to zero, typically determines the box dimensions of the graphs (the existence of these box dimensions follows). Such a result was basically conjectured, though not stated explicitly in this form, by Holschneider (1988). It is then easy, for instance, to determine box dimensions of graphs of Weierstrass functions.

Part I

Turbulence

Chapter 2

The energy transfer in forced turbulence

An equation is derived for the energy transfer in forced turbulence in statistical equilibrium; the turbulence is assumed homogeneous and isotropic, and may be either two–dimensional or three–dimensional. The equation for three–dimensional turbulence has Kolmogorov's equation as a leading–order approximation at small scales and corrects a similar equation obtained by Yakhot (1992). In addition, the equation for three–dimensional turbulence is solved, both for forcing that acts at a single wavenumber and for general forcing. The equation for two–dimensional turbulence is solved in Chapter 3.

2.1 Introduction

The only analytical result, so far, for the inertial–range structure of stationary turbulence was obtained by Kolmogorov (1941 b) from an equation for the energy transfer in locally isotropic turbulence. The inertial–range solution of this equation is the third–order moment of velocity differences u_r,

$$\langle u_r^3 \rangle \sim -\frac{4}{5}\,\epsilon\, r, \tag{2.1}$$

where ϵ is the mean rate of viscous energy dissipation per unit mass and the brackets $\langle\cdot\rangle$ denote an ensemble average. The velocity difference u_r is defined as follows,

$$\mathrm{u}_r = \Big[\mathbf{u}(\mathbf{x}+r\mathbf{e},t) - \mathbf{u}(\mathbf{x},t)\Big]\cdot\mathbf{e}, \tag{2.2}$$

where $\mathbf{e}$ is an arbitrary unit vector. Local isotropy means, basically, that the distribution of u_r is independent of $\mathbf{x}$, $\mathbf{e}$, and t. However, the approximation denoted by $\sim$ requires both that $R \to \infty$ and that $r/L \to 0$ (where R is the Reynolds number and L is the integral scale). The last limit is necessary because forcing is ignored. Moreover, it must be possible to derive an equation for the energy transfer in forced turbulence in two dimensions. Therefore, let us derive a general equation for the energy transfer in forced turbulence, of dimension either two or three.

The outline is as follows. In section 2, the kinematical consequences of homogeneity and isotropy are first extended from turbulence in three dimensions to turbulence in dimension d_0 (where $d_0 = 2$ or $d_0 = 3$); these relations then lead to an equation for the energy transfer in forced turbulence with dimension d_0. In section 3, the equation is solved for $d_0 = 3$, extending the solution of Kolmogorov (1941 b) from inertial scales to all scales where viscous forces are negligible; the equation for $d_0 = 2$ is solved in Chapter 3. Recently, Yakhot (1992) derived an equation for the energy transfer in forced turbulence in three dimensions, apparently the first attack on this problem; but the analysis in the present chapter indicates that his equation, for which no complete proof is given, requires correction.

2.2 The general equation for energy transfer in forced turbulence

Assume the turbulence homogeneous and isotropic in the sense of Taylor (1935) (i.e., the distribution of velocity components is invariant under translations in both time and space, as well as under rotations of the coordinate system and reflections of coordinate axes). The energy transfer in homogeneous and isotropic is the simplest possible, and is therefore the natural starting point. Two–dimensional turbulence is approximately homogeneous at small scales whenever this is true about the energy injection at large scales (the arguments are similar to those for turbulence in three dimensions, and rely on the empirical result that inertial forces increase as the length scale decreases from the largest scale to the scale at which energy is injected). Isotropy includes invariance under reflections of the coordinate axes and thus excludes, for instance, turbulence with mean rotation.

2.2.1 *Kinematical consequences of homogeneity and isotropy*

Von Kármán & Howarth (1938) express double and triple correlations for homogeneous isotropic turbulence in three dimensions through correlations of the velocity component parallel to the separation. Let us extend these relations to turbulence of dimension d_0. Define first the correlation between velocity components u_i and u_j,

$$R_{ij}(\mathbf{r}) = \langle u_i(\mathbf{x})\, u_j(\mathbf{x}+\mathbf{r}) \rangle, \tag{2.3}$$

where the brackets $\langle \cdot \rangle$ denote an ensemble average. Since the turbulence is isotropic, this correlation has the form (Batchelor, 1953, p. 45)

$$R_{ij}(\mathbf{r}) = F(r)\, r_i\, r_j + G(r)\, \delta_{ij}, \tag{2.4}$$

where $F(r)$ and $G(r)$ are scalar functions. Incompressibility gives

$$\frac{\partial R_{ij}}{\partial r_i} = r_j [\, (d_0+1)\, F + r\, F' + r^{-1}\, G' \,] = 0, \tag{2.5}$$

where F' denotes the derivative with respect to r and where the summation convention applies to repeated indices. This equation is satisfied only if

$$(d_0+1)\, F + r\, F' + r^{-1}\, G' = 0, \tag{2.6}$$

Define longitudinal and lateral correlations,

$$\begin{aligned} f(r) &= \langle u_1(\mathbf{x})\, u_1(\mathbf{x}+r\,\mathbf{e}_1) \rangle \\ g(r) &= \langle u_2(\mathbf{x})\, u_2(\mathbf{x}+r\,\mathbf{e}_1) \rangle, \end{aligned} \tag{2.7}$$

where $\mathbf{e}_1$ is the first reference vector. It then follows from Eq. 2.4 that

$$\begin{aligned} f &= r^2\, F + G \\ g &= G, \end{aligned} \tag{2.8}$$

and from Eq. 2.6,

$$g = f + \frac{r}{d_0 - 1}\, f'. \tag{2.9}$$

The auto–correlation is the contraction,

$$R(\mathbf{r}) = R_{ii}(\mathbf{r}). \tag{2.10}$$

Equation 2.9 then gives,

$$R(\mathbf{r}) = f + (d_0 - 1)\, g = d_0\, f + r\, f'. \tag{2.11}$$

Consider next the third–order correlation

$$S_{ijl}(\mathbf{r}) = \langle u_i(\mathbf{x})\, u_j(\mathbf{x})\, u_l(\mathbf{x}+\mathbf{r})\rangle. \tag{2.12}$$

Since the turbulence is isotropic, the third–order correlation can be written in terms of even scalar functions (A, B, and C)

$$S_{ijl}(\mathbf{r}) = A\, r_i\, r_j\, r_l + B\,(r_i\, \delta_{jl} + r_j\, \delta_{il}) + C\, r_l\, \delta_{ij}. \tag{2.13}$$

Since $A(r)$ depends only on $r = |\mathbf{r}|$,

$$\begin{aligned} \nabla \cdot (A\,\mathbf{r}) &= d_0\, A + r\, A' \\ \frac{dA}{dr_l} &= \frac{r_l}{r}\,\frac{dA}{dr}. \end{aligned} \tag{2.14}$$

Incompressibility then implies that

$$\frac{\partial S_{ijl}(\mathbf{r})}{\partial r_l} = \left[(d_0+2)\, A + r\, A' + \frac{2}{r}\, B'\right] r_i\, r_j + \left[2\, B + d_0\, C + r\, C'\right] \delta_{ij} = 0. \tag{2.15}$$

And this is the case only if

$$\begin{aligned} (d_0+2)\, A + r\, A' + 2\, r^{-1}\, B' &= 0 \\ 2\, B + d_0\, C + r\, C' &= 0. \end{aligned} \tag{2.16}$$

The tensor $S_{iil}(\mathbf{r})$ is first–order, solenoidal, and isotropic; any such tensor is easily shown to vanish if bounded. That is,

$$A\, r^2 + 2\, B + d_0\, C = 0. \tag{2.17}$$

This equation and Eq. 2.16 together show that

$$A = \frac{C'}{r}. \tag{2.18}$$

Equation 2.17 then gives

$$B = -\frac{d_0}{2}\, C - \frac{1}{2}\, r\, C'. \tag{2.19}$$

Define

$$\begin{aligned} k(r) &= \langle u_1^2(\mathbf{x})\, u_1(\mathbf{x}+r\,\mathbf{e}_1)\rangle \\ &= S_{111}(r\,\mathbf{e}_1). \end{aligned} \tag{2.20}$$

The above results give

$$\begin{aligned} k(r) &= A\,r^3 + 2\,B\,r + C\,r \\ &= -(d_0-1)\,r\,C(r). \end{aligned} \tag{2.21}$$

The third–order correlation is now completely determined by $k(r)$,

$$S_{ijl}(\mathbf{r}) = \left[\frac{k - r\,k'}{(d_0-1)\,r^3}\right] r_i\,r_j\,r_l + \left[\frac{(d_0-1)\,k + r\,k'}{2\,(d_0-1)\,r}\right](r_i\,\delta_{jl} + r_j\,\delta_{il}) - \frac{k}{r\,(d_0-1)}\,r_l\,\delta_{ij}. \tag{2.22}$$

On setting $l = i$ and summing over i,

$$S_{iji}(\mathbf{r}) = \frac{1}{2}\left[k' + \frac{(d_0+1)\,k}{r}\right] r_j. \tag{2.23}$$

For $d_0 = 3$, this relation agrees with that derived by von Kármán & Howarth (1938); see also Eq. 3.4.35 in Batchelor (1953). It is convenient to express the above results in terms of the velocity differences u_r. Note first that

$$\begin{aligned} f(r) &= \langle u_1^2\rangle - \frac{\langle u_r^2\rangle}{2} \\ k(r) &= \frac{\langle u_r^3\rangle}{6}. \end{aligned} \tag{2.24}$$

Equations 2.11 and 2.23 then give

$$\begin{aligned} R(\mathbf{r}) &= \langle \mathbf{u}^2\rangle - \frac{1}{2}\left(r\,\frac{d}{dr} + d_0\right)\langle u_r^2\rangle \\ S_{iji}(\mathbf{r}) &= \frac{1}{6}\left(\frac{d}{dr} + \frac{d_0+1}{r}\right)\langle u_r^3\rangle\, r_j, \end{aligned} \tag{2.25}$$

as functions of r

where $r = |\mathbf{r}|$. The auto–correlation is even and the third–order moment is odd. Having extended the tensor analysis of von Kármán & Howarth (1938) to turbulence of dimension d_0, it is now straightforward to extend the work of Kolmogorov (1941 b) similarly.

2.2.2 Dynamical consequences of homogeneity and isotropy

We now extend the equations of von Kármán & Howarth (1938) and Kolmogorov (1941 b) to forced turbulence in statistical equilibrium (i.e., stationary turbulence). We then consider an incompressible velocity field $\mathbf{u}(\mathbf{x},t)$ that satisfies the Navier–Stokes equation with forcing $\mathbf{f}(\mathbf{x},t)$,

$$\begin{aligned} \frac{\partial \mathbf{u}}{\partial t} + (\mathbf{u}\cdot\nabla)\mathbf{u} &= \nu\,\nabla^2\mathbf{u} - \frac{1}{\rho}\nabla p + \mathbf{f} \\ \nabla\cdot\mathbf{u} &= 0, \end{aligned} \tag{2.26}$$

Consider next two points, $\mathbf{x}_0$ and $\mathbf{x}_1$, and regard each point as independent of the other. Let the subscripts 0 and 1 denote conditions at the corresponding points; for instance, $\mathbf{u}_0 = \mathbf{u}(\mathbf{x}_0)$. On multiplying the equation at $\mathbf{x}_0$ by $\mathbf{u}_1$, and the equation at $\mathbf{x}_1$ by $\mathbf{u}_0$, and then adding the results,

$$\begin{aligned} \frac{\partial}{\partial t}\langle \mathbf{u}_0\cdot\mathbf{u}_1\rangle + \nabla_{\mathbf{r}}\cdot\langle(\mathbf{u}_0\cdot\mathbf{u}_1)\,\mathbf{u}_1 - (\mathbf{u}_0\cdot\mathbf{u}_1)\,\mathbf{u}_0\rangle &= 2\,\nu\,\nabla_{\mathbf{r}}^2\langle\mathbf{u}_0\cdot\mathbf{u}_1\rangle \\ &\quad + \frac{1}{\rho}\langle\mathbf{u}_1\cdot\nabla_0 p_0 + \mathbf{u}_0\cdot\nabla_1 p_1\rangle \\ &\quad + \langle\mathbf{u}_1\cdot\mathbf{f}_0 + \mathbf{u}_0\cdot\mathbf{f}_1\rangle, \end{aligned} \tag{2.27}$$

where the divergence and the Laplacian are with respect to the relative position $\mathbf{r} = \mathbf{x}_1 - \mathbf{x}_0$. Von Kármán & Howarth (1938) use the identity $\partial/\partial\mathbf{r} = \partial/\partial\mathbf{x}_1 - \partial/\partial\mathbf{x}_0$ to transform differential operators in $\mathbf{x}_0$ and $\mathbf{x}_1$ into differential operators in $\mathbf{r}$. But simple examples show that this identity generally fails when the two points $\mathbf{x}_0$ and $\mathbf{x}_1$ vary independently. The correct argument is that ensemble averages in homogeneous turbulence depend only on the relative position $\mathbf{r}$.

Moreover, von Kármán & Howarth (1938) use both homogeneity and isotropy to show that the pressure terms in Eq. 2.27 either vanish or tend to infinity as r tends to zero. But homogeneity suffices, provided that averaging over ensembles with $\mathbf{x}_0$ varying and $\mathbf{x}_1$ fixed is equivalent to averaging over space with $\mathbf{x}_0$ varying and $\mathbf{r}$ fixed. (This assumption does *not* require a type of ergodic hypothesis, as often claimed, but rather that the velocity field in widely separated regions can be regarded as independent realisations; but the details of this question are beyond the compass of the present paper). The average over space may be performed by integrating over spheres centered at the origin, dividing by the volume, and then letting the radius tend to infinity.

Suppose now that we seek the average of a divergence. We may then transform the integral over the interior of the sphere into an integral over the surface. The surface integral will generally increase no faster than the surface area as the volume tends to infinity, so that the average of any divergence is zero (it suffices that the absolute value of the vector, whose divergence is averaged, has finite average). Incompressibility implies that both pressure terms in Eq. 2.27 are divergences. For instance,

$$\langle \mathbf{u}_1 \cdot \nabla_0 p_0 \rangle = \langle \nabla_0 \cdot [\mathbf{u}_1 \, p_0] \rangle. \tag{2.28}$$

The two pressure terms then vanish. The physical interpretation is that pressure fluctuations transfer kinetic energy between different regions without changing the total kinetic energy (Batchelor, 1953). In addition, the time derivative on the left side of Eq. 2.27 vanishes by stationarity. We then obtain

$$\nabla_{\mathbf{r}} \cdot \langle (\mathbf{u}_0 \cdot \mathbf{u}_1) \, \mathbf{u}_1 - (\mathbf{u}_0 \cdot \mathbf{u}_1) \, \mathbf{u}_0 \rangle = 2 \nu \nabla^2 R(\mathbf{r}) + \langle \mathbf{u}_1 \cdot \mathbf{f}_0 + \mathbf{u}_0 \cdot \mathbf{f}_1 \rangle. \tag{2.29}$$

The two relations in Eq. 2.25 show that

$$\frac{1}{6} \left(r \frac{d}{dr} + d_0 \right) \left(\frac{d}{dr} + \frac{d_0 + 1}{r} \right) \langle u_r^3 \rangle = \nu \left(\frac{d^2}{dr^2} + \frac{d_0 - 1}{r} \frac{d}{dr} \right) \left(r \frac{d}{dr} + d_0 \right) \langle u_r^2 \rangle - \langle \mathbf{u}_1 \cdot \mathbf{f}_0 + \mathbf{u}_0 \cdot \mathbf{f}_1 \rangle. \tag{2.30}$$

To simplify this equation, use the following identity to write the viscous term in a form similar to the term in which the third–order moment occurs (where the constant d_0 should be regarded not as a function, which vanishes on differentiation, but as the operator of multiplication),

$$\left(\frac{d^2}{dr^2} + \frac{d_0 - 1}{r} \frac{d}{dr} \right) \left(r \frac{d}{dr} + d_0 \right) = \left(r \frac{d}{dr} + d_0 \right) \left(\frac{d^2}{dr^2} + \frac{d_0 + 1}{r} \frac{d}{dr} \right). \tag{2.31}$$

It is easily shown that the differential operator $r d/dr + d_0$ has unique inverse within the class of functions bounded at the origin; this class of functions is appropriate because velocity differences in realistic flows are bounded at all scales. The first integral of Eq. 2.30 then gives an equation for the energy transfer,

$$\left(\frac{d}{dr} + \frac{d_0 + 1}{r} \right) \langle u_r^3 \rangle = 6 \nu \left(\frac{d^2}{dr^2} + \frac{d_0 + 1}{r} \frac{d}{dr} \right) \langle u_r^2 \rangle - 6 \, F(r), \tag{2.32}$$

where

$$F(r) = r^{-d_0} \int_0^r x^{d_0 - 1} \langle \mathbf{u}_1 \cdot \mathbf{f}_0 + \mathbf{u}_0 \cdot \mathbf{f}_1 \rangle \, dx. \tag{2.33}$$

[not to be confused with F(r) in (2.4)]

(The correlation between velocity and forcing is here considered a function of x). Since the turbulence is stationary, viscous energy dissipation equals energy transfer through forcing,

$$\begin{aligned} \epsilon &= -\nu \langle \mathbf{u} \cdot \nabla^2 \mathbf{u} \rangle \\ &= \langle \mathbf{u} \cdot \mathbf{f} \rangle. \end{aligned} \tag{2.34}$$

Then $F(0) = 2\,\epsilon/d_0$. The left side of Eq. 2.32 represents inertial energy transfer in velocity disturbances with characteristic length scale r; on the right side, the first term represents viscous energy dissipation and the second represents energy transfer from velocity disturbances at other length scales. Yakhot (1992) similarly obtains an equation for the energy transfer in forced turbulence in three dimensions (i.e., $d_0 = 3$). But he apparently overlooks the step in which the divergence is inverted, and consequently ends up with an equation that, wrongly, has $d_0 = 0$ in the expression for $F(r)$ in Eq. 2.33.

We now see, as was first pointed out by Yakhot (1992), that Kolmogorov's equation arises for three–dimensional turbulence by assuming $F(r) \approx F(0)$. To justify this approximation, suppose that the Fourier transform of forcing concentrates around the wavenumber $2\,\pi/L$. Suppose that the forcing is smooth, so that we may approximate the following correlation by its Taylor series,

$$\langle \mathbf{u}_0 \cdot \mathbf{f}_1 + \mathbf{u}_1 \cdot \mathbf{f}_0 \rangle \sim \sum_{n=0}^{\infty} a_n\, r^n. \tag{2.35}$$

whenever $r = |\mathbf{r}|$ is much smaller than the forcing scale L. Suppose that the turbulence transfers kinetic energy mainly to small scales and that the forcing $\mathbf{f}$ varies significantly only over scales larger than some length scale L. A simple dimensional argument then shows that a_n is of order U^3/L^{2n+1}. Therefore, when $r << L$, the first term, a_0, dominates, giving Kolmogorov's equation. Let us now solve the equation for energy transfer in three–dimensional turbulence without any approximation; this solution is of independent interest and, moreover, helps prepare the discussion of two–dimensional turbulence.

2.3 Solution for three–dimensional turbulence

2.3.1 *Sine wave forcing*

Consider first the simplest case of forcing at a single wavenumber. The forcing function $F(r)$ can then be written as a combination of algebraic and trigonometric functions, giving an inertial–range solution of Eq. 2.32 that is exact in the limit of zero viscosity. The analysis proceeds by expressing $F(r)$ as an integral over Fourier transforms of velocity and forcing. Define these Fourier transforms as follows,

$$\begin{aligned} T\mathbf{u}(\mathbf{k}) &= \frac{1}{8\,\pi^3} \int_{\mathbb{R}^3} \mathbf{u}(\mathbf{x})\, \exp[-i\,\mathbf{k}\,\mathbf{x}]\, d\mathbf{x} \\ T\mathbf{f}(\mathbf{k}) &= \frac{1}{8\,\pi^3} \int_{\mathbb{R}^3} \mathbf{f}(\mathbf{x})\, \exp[-i\,\mathbf{k}\,\mathbf{x}]\, d\mathbf{x}. \end{aligned} \tag{2.36}$$

The time–coordinate is ignored here because the Fourier transforms are used only for averages that are independent of time. Assume that both the velocity $\mathbf{u}$ and the forcing $\mathbf{f}$ are convolutes, that is, tempered distributions for which the convolution theorem on Fourier transforms holds. Then

$$\langle \mathbf{u}_0 \cdot \mathbf{f}_1 + \mathbf{u}_1 \cdot \mathbf{f}_0 \rangle = 16\,\pi^3 \int_{\mathbb{R}^3} \cos(\mathbf{k}\cdot\mathbf{r})\, \langle T\mathbf{u}(\mathbf{k}) \cdot T\mathbf{f}(\mathbf{k})^* \rangle\, d\mathbf{k}. \tag{2.37}$$

The average on the left side is invariant under rotations of the coordinate system and is therefore unchanged by averaging over the sphere with radius $r = |\mathbf{r}|$, centered at the origin. Define the angle θ by $\mathbf{k}\cdot\mathbf{r} = k\,r\,\cos\theta$. The Cosine has integral

$$\begin{aligned} \int_{|\mathbf{r}|=r} \cos(\mathbf{k}\cdot\mathbf{r})\, d\mathbf{r} &= 2\,\pi\,r^2 \int_0^\pi \cos(\,k\,r\,\cos\theta\,)\,\sin\theta\, d\theta \\ &= 2\,\pi\,r^2 \int_{-1}^{1} \cos(k\,r\,x)\, dx \\ &= 4\,\pi\,r\,k^{-1}\,\sin(k\,r). \end{aligned} \tag{2.38}$$

The average over the sphere is then (see also p. 36, Batchelor, 1953)

$$\langle \mathbf{u}_0 \cdot \mathbf{f}_1 + \mathbf{u}_1 \cdot \mathbf{f}_0 \rangle = 16\,\pi^3 \int_{\mathbb{R}^3} \frac{\sin(k\,r)}{k\,r}\, \langle T\mathbf{u}(\mathbf{k}) \cdot T\mathbf{f}(\mathbf{k})^* \rangle\, d\mathbf{k}. \tag{2.39}$$

Note that this relation holds only in three dimensions. Suppose now that the forcing acts only at the wavenumber $k_0 > 0$. The average in the integrand, since the turbulence is

isotropic, depends only on the modulus k and not on the direction of the wavevector. Integrating over the sphere with radius equal to k then gives,

$$\langle \mathbf{u}_0 \cdot \mathbf{f}_1 + \mathbf{u}_1 \cdot \mathbf{f}_0 \rangle = 64\,\pi^4 \int_0^\infty \frac{\sin(k\,r)}{k\,r} \langle T\mathbf{u}(k\,\mathbf{e}) \cdot T\mathbf{f}(k\,\mathbf{e})^* \rangle\, k^2\, dk, \tag{2.41}$$

where $\mathbf{e}$ is an arbitrary unit vector. Since the left side equals $2\,\epsilon$ at $r = 0$, the Fourier transform is given by

$$\langle T\mathbf{u}(\mathbf{k}) \cdot T\mathbf{f}(\mathbf{k})^* \rangle = \frac{\epsilon}{32\,\pi^4\,k^2}\,\delta(k - k_0). \tag{2.42}$$

On substituting this Fourier transform in Eq. 2.41,

$$\langle \mathbf{u}_0 \cdot \mathbf{f}_1 + \mathbf{u}_1 \cdot \mathbf{f}_0 \rangle = 2\,\epsilon\,\frac{\sin(k_0\,r)}{k_0\,r}. \tag{2.43}$$

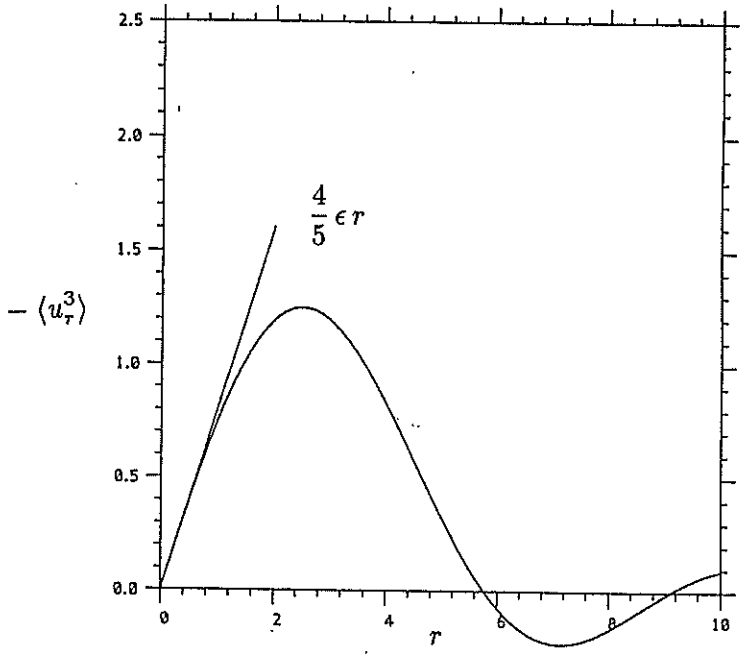

Figure 2.1. Minus the third-order moment $\langle u_r^3 \rangle$ for turbulence forced at a single wavenumber; the straight line is Kolmogorov's asymptotic result $4/5\,\epsilon\,r$. Lengths and velocities are non–dimensionalised such that $k_0 = 1$ and $\epsilon = 1$; the forcing scale is then $L = 2\,\pi$.

On dimensional grounds, the term representing viscous energy dissipation is negligible at scales larger than the Kolmogorov dissipation scale $\eta = \nu^{3/4}\,\epsilon^{-1/4}$. Substituting Eq. 2.43

on the right side of Eq. 2.32 gives the following approximate solution, valid at length scales where viscous forces are negligible,

$$\begin{aligned} \langle u_r^3 \rangle &\sim -12\,\epsilon \sum_{n=0}^{\infty} \frac{(-1)^n\, k_0^{2n}\, r^{2n+1}}{(2n+5)\,(2n+3)\,(2n+1)!} \\ &= -12\,\epsilon\, k_0^{-5}\, r^{-2} \left[\left(\frac{3}{r^2} - k_0^2 \right) \sin(k_0\, r) - \frac{3\, k_0}{r} \cos(k_0\, r) \right]. \end{aligned} \tag{2.43}$$

This solution is exact in the limit of zero viscosity and thus improves, particularly at large scales, on Kolmogorov's result in Eq. 2.1 (see Figure 2.1); the two solutions agree to the leading order as $k_0\, r$ tends to zero. Equation 2.43 holds also when r is larger than the forcing scale $L = 2\,\pi/k_0$, where Kolmogorov's prediction no longer holds. But this part of the solution is only visible in real flows when the forcing scale L is much smaller than the characteristic scale for the flow domain.

2.3.2 *General forcing*

Consider now the general solution at scales where viscous forces are negligible. We seek a simple interpretation of the correlation between velocity and forcing. Define rotation fields by successive applications of the rotation operator,

$$\nabla^n \times \mathbf{u} = \overbrace{\nabla \times \ldots \nabla \times}^{n \text{ times}} \mathbf{u}, \tag{2.44}$$

and similarly for the forcing. The Fourier transforms satisfy

$$\begin{aligned} T[\nabla^n \times \mathbf{u}] &= i\,\mathbf{k} \times T[\nabla^{n-1} \times \mathbf{u}] \\ T[\nabla^n \times \mathbf{f}] &= i\,\mathbf{k} \times T[\nabla^{n-1} \times \mathbf{f}]. \end{aligned} \tag{2.45}$$

Since the velocity field is incompressible, the Fourier transforms of all rotation fields are perpendicular to the wavevector $\mathbf{k}$,

$$\mathbf{k} \cdot T[\nabla^n \times \mathbf{u}](\mathbf{k}) = 0. \tag{2.46}$$

By combining this result with the two previous equations, we see that the scalar product of the two Fourier transforms is given by

$$T[\nabla^n \times \mathbf{u}] \cdot T[\nabla^n \times \mathbf{f}]^* = \mathbf{k}^2\, T[\nabla^{n-1} \times \mathbf{u}] \cdot T[\nabla^{n-1} \times \mathbf{f}]^*. \tag{2.47}$$

Note that the forcing need not be non-divergent for this identity to hold. If we use induction over n to reduce this result further, and assume that ensemble (or space) averaging commutes with integration over wavenumbers,

$$\begin{aligned} \langle\,(\nabla^n \times \mathbf{u})\,(\nabla^n \times \mathbf{f})\,\rangle &= 8\,\pi^3 \int_{\mathbb{R}^3} \langle T[\nabla^n \times \mathbf{u}] \cdot T[\nabla^n \times \mathbf{f}]^* \rangle \, d\mathbf{k} \\ &= 8\,\pi^3 \int_{\mathbb{R}^3} k^{2n}\,\langle T\mathbf{u} \cdot T\mathbf{f}^* \rangle \, d\mathbf{k}. \end{aligned} \tag{2.48}$$

These averages are the rates at which the forcing transfers mean squares of the rotation fields $\nabla^n \times \mathbf{u}$ to the turbulence. From Eq. 2.39,

$$F(r) = 16\,\pi^3 \sum_{n=0}^{\infty} \int_{\mathbb{R}^3} \frac{(-1)^n\,(k\,r)^{2n}}{(2\,n+1)!\,(2n+3)}\,\langle T\mathbf{u}(\mathrm{k}) \cdot T\mathbf{f}(\mathrm{k})^* \rangle \, d\mathbf{k}. \tag{2.49}$$

Then, from Eq. 2.48,

$$F(r) = 2 \sum_{n=0}^{\infty} \frac{(-1)^n\,\langle\,(\nabla^n \times \mathbf{u}) \cdot (\nabla^n \times \mathbf{f})\,\rangle}{(2\,n+1)!\,(2n+3)}\,r^{2n}. \tag{2.50}$$

The forcing, of course, should be smooth. The general solution at scales where viscous forces are negligible is now

$$\langle u_r^3 \rangle \sim -12 \sum_{n=0}^{\infty} \frac{(-1)^n\,\langle\,(\nabla^n \times \mathbf{u}) \cdot (\nabla^n \times \mathbf{f})\,\rangle}{(2\,n+1)!\,(2n+3)\,(2n+5)}\,r^{2n+1}. \tag{2.51}$$

The rate of energy transfer at small scales then depends not only on the rate at which the forcing transfers kinetic energy to the turbulence, as Kolmogorov's equation indicates, but also on the rates at which the forcing transfers all other squares $(\nabla^n \times \mathbf{u})^2$; this is because the mean kinetic energy is non–zero when just one of the mean squares is non–zero. In particular, the lowest order correction to Kolmogorov's prediction in Eq. 2.1 represents enstrophy transfer through forcing,

$$\langle u_r^3 \rangle \sim -\frac{4}{5}\,\epsilon\,r + \frac{2}{35}\,\langle \omega \cdot \nabla \times \mathbf{f} \rangle\,r^3. \tag{2.52}$$

In three–dimensional turbulence, enstrophy transfer through forcing is negligible compared with enstrophy production through advection; this is why Kolmogorov's prediction in Eq. 2.1 holds asymptotically at small scales. But two–dimensional turbulence does not produce enstrophy by advection, so we expect that, in this case, the term representing enstrophy transfer through forcing is important.

Chapter 3

The local structure of two–dimensional turbulence

In chapter 2, an exact equation was derived for the energy transfer in forced turbulence of dimension either two or three, and this equation was solved for the case of three dimensions. We now solve the equation for the case of two dimensions. It is assumed that the Fourier transform of forcing concentrates in two regions, around a wavenumber $2\pi/L_1$ and then at wavenumbers smaller than $2\pi/L_2$, where L_2 is much larger than L_1. At small scales, between the dissipation scale η and the forcing scale L_1, the solution is given by,

$$\langle u_r^3 \rangle \sim \frac{1}{8}\alpha r^3 - \frac{1}{256}\beta r^5, \tag{3.1}$$

where α is the mean rate of viscous enstrophy (mean–square vorticity) dissipation and β is the mean rate of palinstrophy (mean–square vorticity gradient) transfer through forcing. In large scales, between L_1 and L_2, the solution is given by,

$$\langle u_r^3 \rangle \sim \frac{3}{2}(E-\epsilon)r - \frac{1}{8}(A-\alpha)r^3, \tag{3.2}$$

where E and A are, respectively, the rates of energy and enstrophy transfer at the scale L_1 through forcing. The ratio E/ϵ is proportional to the Reynolds number. As the ratio A/α, a free parameter, increases to infinity, the enstrophy range at small scales contracts and the enstrophy range at large scales expands. Physically, this corresponds to the appearance of large vortices. Finally, the energy spectrum is estimated.

3.1 Introduction

The study of two–dimensional turbulence is motivated by the observation that velocity disturbances in both the atmosphere and in oceans rarely exceed 10 kilometers in the vertical direction, yet may extend over several thousand kilometers in horisontal directions. Nevertheless, there are so far no analytical results for the equilibrium distribution of velocity differences u_r in two–dimensional turbulence. This contrasts sharply with three–dimensional turbulence, for which Kolmogorov's 4/5–law has been around for more than 50 years. The equation derived in the previous chapter is almost the solution to this problem,

$$\left(\frac{d}{dr}+\frac{3}{r}\right)\langle u_r^3\rangle = 6\,\nu\left(\frac{d^2}{dr^2}+\frac{3}{r}\,\frac{d}{dr}\right)\langle u_r^2\rangle - 6\,F(r), \tag{3.3}$$

where

$$F(r) = r^{-2}\int_0^r x\,\langle \mathbf{u}_1\cdot\mathbf{f}_0 + \mathbf{u}_0\cdot\mathbf{f}_1\rangle\,dx \tag{3.4}$$

(Recall that the correlation between velocity and forcing is a function of x). All we now need is the correct approximation to the forcing function $F(r)$. The approximation used for turbulence in three dimensions is not valid. Since turbulence in two dimensions does not produce enstrophy through advection, the mean enstrophy $\langle\omega^2\rangle$ for stationary turbulence depends mainly on the forcing. In particular, the mean enstrophy presumably remains bounded as the viscosity ν decreases to zero. This contrasts with three–dimensional turbulence, for which advection produces enstrophy at a rate that increases to infinity as the viscosity decreases to zero. Now, when the turbulence is homogeneous,

$$\epsilon = \nu\,\langle\omega^2\rangle, \tag{3.5}$$

so that $\epsilon \to 0$ as $\nu \to 0$ (Bray, 1966; Batchelor, 1969). Recall that Kolmogorov's equation is based on the approximation $F(r) \approx F(0) = \epsilon$. But it is unlikely that the rate of energy transfer associated with large velocity disturbances, where viscous forces are much smaller than inertial forces, decreases to zero in this limit. This shows that $F(r)$ requires a different approximation when the turbulence is two–dimensional. Physically, this is because the turbulence in two dimensions transfers kinetic energy mainly to large scales (Fjørtoft, 1953; Bray, 1966; Kraichnan, 1967; Batchelor, 1969).

Incidentally, we have resolved a problem raised by von Neumann (1949). He remarked that Kolmogorov's equation must use the dimension in some important manner, because the corresponding equation for two–dimensional turbulence not seem plausible. We

does

see that the important assumption is that the turbulence transfers kinetic energy almost entirely to small scales, which fails in two dimensions. Along the same lines, Hama (1953) derived an equation for the energy transfer in decaying turbulence in two dimensions and concluded, wrongly, that the energy transfer resembles that in three dimensions. This conclusion is only correct if the approximation used in three dimensions holds also in two dimensions, and we have just seen that this is not so. Now, let us find the correct approximation to $F(r)$ for two–dimensional turbulence.

3.2 Basic assumptions

The equation for energy transfer can be solved in complete generality for smooth forcing, and this will be done, but to get physically interesting predictions it is necessary to specify the type of forcing considered. Since ϵ decreases with ν, and since the energy transfer at large scales is only weakly dependent on ν, turbulence in two dimensions transfers kinetic energy from velocity disturbances at the smallest forcing scale to larger velocity disturbances (Bray, 1966; Kraichnan, 1967; Batchelor, 1969). Unless some mechanism extracts kinetic energy from the largest velocity disturbances, the (ensemble–averaged) kinetic energy increases with time and we cannot regard the turbulence as stationary. Let us then suppose that kinetic energy is extracted at large scales at exactly the rate required for stationarity (numerical simulations often model this energy extraction as linear drag at small wavenumbers; e.g., Maltrud & Vallis, 1991). Moreover, when kinetic energy is injected and extracted by separate forcing fields,

$$\mathbf{f} = \mathbf{f}_1 + \mathbf{f}_2, \tag{3.6}$$

where the first term represents energy injection and the second energy extraction. Since $F(r)$ is linear in $\mathbf{f}$,

$$F(r) = F_1(r) + F_2(r), \tag{3.7}$$

with the same use of indices as before. Let us assume that the Fourier transform of $\mathbf{f}_1$ concentrates around the wavenumber $2\pi/L_1$ and the Fourier transform of $\mathbf{f}_2$ concentrates solely at wavenumbers smaller than $2\pi/L_2$. To solve Eq. 3.3 explicitly at scales larger than L_1, we require that L_2 is much larger than L_1. That is, kinetic energy is extracted from velocity disturbances that are much larger than those into which kinetic energy is injected. At small scales, $r << L_1$, inertial forces decrease no slower than $\langle\omega^2\rangle r$, so there is generally no scope for inertial ranges in two–dimensional turbulence (not even at large

scales, because $\mathbf{f}_1$ is generally larger than the inertial forces associated with these scales). Let us now discuss the first three terms in the Taylor series in Eq. 3.37.

3.2.1 Kinetic energy

Let us consider how the three different rates of energy transfer are related: the rate of energy extraction by viscous forces, the rate of energy injection at the scale L_1, and the rate of energy extraction at the scale L_2. From the Navier–Stokes equation, by well known arguments, we get

$$\langle \mathbf{u} \cdot \mathbf{f}_1 \rangle + \langle \mathbf{u} \cdot \mathbf{f}_2 \rangle = \nu \langle \omega^2 \rangle. \tag{3.8}$$

Since vorticity is materially conserved for inviscid flows, the typical velocity variation across a distance L_1 is comparable with $\langle \omega^2 \rangle^{1/2} L_1$. We may then define a Reynolds number R for the motion at scale L_1 as follows,

$$R = \frac{\langle \omega^2 \rangle^{1/2} L_1^2}{\nu}. \tag{3.9}$$

Denote by E the rate at which forcing injects kinetic energy at the scale L_1,

$$E = \langle \mathbf{u} \cdot \mathbf{f}_1 \rangle. \tag{3.10}$$

Then, by a simple dimensional estimate of E,

$$E \propto R\epsilon, \tag{3.11}$$

as R tends to infinity. Now, in the same limit,

$$\langle \mathbf{u} \cdot \mathbf{f}_2 \rangle \sim E, \tag{3.12}$$

so that, as already remarked, two–dimensional turbulence transfers kinetic energy mainly to large scales. This equation shows that the first (non–zero) terms in the Taylor series of $F_1(r)$ and $F_2(r)$ are both much larger than ϵ, but almost cancel on addition.

about

3.2.2 *Enstrophy*

The behaviour of enstrophy is more complicated than the simple transfer to large scales of kinetic energy. Consider first the vorticity equation,

$$\frac{\partial \omega}{\partial t} + \mathbf{u} \cdot \nabla \omega = \nu \nabla^2 \omega + \phi, \tag{3.13}$$

where the vorticity ω is considered a scalar and where ϕ is the component of $\nabla \times \mathbf{f}$ normal to the plane of the flow. Multiply by vorticity and average,

$$\langle \omega \, \phi \rangle = \nu \, \langle (\nabla \omega)^2 \rangle, \tag{3.14}$$

where the viscous term was transformed by Green's first identity. Define,

$$\alpha = \nu \, \langle (\nabla \omega)^2 \rangle. \tag{3.15}$$

Then, using the above notation,

$$\alpha = \langle \omega \, \phi_1 \rangle + \langle \omega \, \phi_2 \rangle. \tag{3.16}$$

Suppose that $\mathbf{f}_2$ acts, for instance, only at wavenumbers in the range from $2\pi/L_2$ to $4\pi/L_2$. The second term on the right side of Eq. 3.16 would then seem to be negligible, so that

$$\alpha \sim \langle \omega \, \phi_1 \rangle, \tag{3.17}$$

as L_1/L_2 tends to zero. In this case, the turbulence transfers enstrophy mainly to small scales (as some previous authors have suggested; Bray, 1966; Kraichnan, 1967; Batchelor, 1969). But it turns out that this assumption on the forcing at scale L_2 is too restrictive.

3.2.3 The rôle of vortices

Two–dimensional turbulence often has large vortices (e.g., Fornberg, 1977; McWilliams, 1984; Melander *et al.*, 1987; Legras, Santangelo, & Benzi, 1988; Santangelo, Benzi, & Legras, 1989; Maltrud & Vallis, 1991; Dritschel, 1993; Borue, 1994; Boubnov, Dalziel, & Linden, 1994). That is, the vorticity field has patches with diameters comparable with the forcing scale L_1 (Maltrud & Vallis, 1991).

When the fraction of the vorticity field associated with vortices increases, the mean palinstrophy $\langle (\nabla \omega)^2 \rangle$ decreases and, thereby, the mean rate of viscous enstrophy dissipation α. Let us then compare the rate at which the forcing injects enstrophy at the scale L_1 with the mean rate of viscous enstrophy dissipation α,

$$Q = \frac{\langle \omega^2 \rangle^{3/2}}{\alpha}, \tag{3.18}$$

where the numerator scales like the mean rate of enstrophy injection at the forcing scale L_1. (In general, Q cannot be interpreted as a Reynolds number for structures in the

vorticity field, as it depends also on the fraction of total space occupied by the smallest structures). Let us consider the enstrophy budget when Q is large. Define,

$$A = \langle \omega \, \phi_1 \rangle, \tag{3.19}$$

and note,

$$A \propto \langle \omega^2 \rangle^{3/2}, \tag{3.20}$$

so that,

$$A \propto Q \, \alpha. \tag{3.21}$$

as Q tends to infinity. In this limit, Eq. 3.16 becomes,

$$\langle \omega \, \phi_2 \rangle \sim -A. \tag{3.22}$$

Enstrophy extraction from velocity disturbances at the scale L_2 is then comparable with enstrophy injection at the scale L_1, so enstrophy indeed flows increasingly to large scales as Q increases. Since the rate of viscous enstrophy dissipation α is determined by the mean palinstrophy $\langle (\nabla\omega)^2 \rangle$, let us finally consider the averaged equation for palinstrophy transfer.

3.2.4 *Palinstrophy*

Palinstrophy, in contrast to kinetic and enstrophy, is not conserved for inviscid flows in two dimensions. But it turns out that vortices reduce the rate of palinstrophy production by inertial forces, so that the equation for palinstrophy resembles the equation for a quantity that is conserved in the inviscid limit. The averaged equation for palinstrophy transfer is easily obtained,

$$\langle \nabla\omega \cdot \nabla\phi \rangle = \langle \nabla\omega \cdot (\nabla\omega \cdot \nabla)\mathbf{u} \rangle + \nu \langle (\nabla^2\omega)^2 \rangle. \tag{3.23}$$

The first term on the right side represents extension of isovorticity lines by inertial forces (Batchelor, 1969; Tatsumi, 1980). The extension of isovorticity lines is then produces palinstrophy — just as the extension of vortex lines in three–dimensional turbulence produces enstrophy. Denote by β the mean rate of palinstrophy transfer through forcing,

$$\beta = \langle \nabla\omega \cdot \nabla\phi \rangle. \tag{3.24}$$

To evaluate the rate of palinstrophy production, denote by s the non–negative eigenvalue of strain (assuming this eigenvalue non–zero), and by g_1 and g_2 the components of the vorticity gradient $\nabla\omega$ along the two eigenvectors of strain. Then

$$\langle \nabla\omega \cdot (\nabla\omega \cdot \nabla)\mathbf{u} \rangle = \langle s \, (g_1^2 - g_2^2) \rangle. \tag{3.25}$$

The two components of the mean palinstrophy, g_1^2 and g_2^2, and hence the inertial term in Eq. 3.25, decreases as the characteristic length scale for vortices increases. Consider the extreme case where the mean palinstrophy is associated with the vorticity field at large scales. The mean rate of palinstrophy transfer through forcing is unchanged and is then comparable with the mean rate of viscous palinstrophy dissipation,

$$\beta \sim \nu \langle (\nabla^2 \omega)^2 \rangle, \tag{3.26}$$

and palinstrophy can be regarded as an 'approximate invariant' in the inviscid limit. Introducing vortices is then analogous to reducing the dimension from three to two: the former prevents the extension of isovorticity lines and the latter prevents the extension of vortex lines.

Suppose now that the turbulence transfers palinstrophy mainly to small scales, in the sense that the forcing at scale L_2 does not contribute to β. The only contribution is then from the forcing at scale L_1, so that β satisfies,

$$\beta \propto U^3 / L_1^5, \tag{3.27}$$

where U is the characteristic velocity differences at the scale L_1. Equation 3.27 holds generally when L_2/L_1 is sufficiently large. The physical picture is that the mean–square vorticity gradients is associated with length scales much smaller than L_2, which, evidently, is correct when the Fourier transform of $\mathbf{f}_1$ concentrates around $2\,\pi/L_1$.

3.3 Formal expression for the forcing function

We now determine the forcing function $F(r)$ by considering the Fourier transforms of velocity and forcing. The arguments are analogous to those for three–dimensional turbulence, in the previous chapter. Once more, we seek the Taylor series of $F(r)$. The Fourier transforms are now defined as follows,

$$\begin{aligned} T\mathbf{u}(\mathrm{k}) &= \frac{1}{4\,\pi^2} \int_{\mathrm{IR}^2} \mathbf{u}(\mathrm{x}) \exp[-i\,\mathrm{k}\,\mathrm{x}]\, d\mathrm{x} \\ T\mathbf{f}(\mathrm{k}) &= \frac{1}{4\,\pi^2} \int_{\mathrm{IR}^2} \mathbf{f}(\mathrm{x}) \exp[-i\,\mathrm{k}\,\mathrm{x}]\, d\mathrm{x}. \end{aligned} \tag{3.28}$$

Then

$$\langle \mathbf{u}_0 \cdot \mathbf{f}_1 + \mathbf{u}_1 \cdot \mathbf{f}_0 \rangle = 8\,\pi^2 \int_{\mathrm{IR}^2} \cos(\mathrm{r}\,\mathrm{k})\, \langle T\mathbf{u}(\mathrm{k}) \cdot T\mathbf{f}(\mathrm{k})^* \rangle\, d\mathrm{k}, \tag{3.29}$$

and isotropy again implies that the ensemble average in the integrand depends only on the magnitude of the wavevector $k = |\mathbf{k}|$. To average over the angle θ, defined by $\mathbf{k} \cdot \mathbf{r} = k\, r\, \cos\theta$, note first that

$$\frac{1}{2\,\pi} \int_0^{2\,\pi} \cos(k\, r\, \cos\theta)\, d\theta = \frac{1}{2\,\pi} \sum_{n=0}^{\infty} \frac{(-1)^n}{(2n)!}\, k^{2n}\, r^{2n} \int_0^{2\,\pi} \cos^{2n}\theta\, d\theta. \tag{3.30}$$

It is also possible to write the integral on the left side as a Bessel function, but the Taylor series is more helpful here. Since (e.g., Gradshteyn & Ryzhik, 1980),

$$\cos^{2n}\theta = 2^{-2n} \left\{ \sum_{k=0}^{n-1} 2 \left(\begin{array}{c} 2n \\ k \end{array} \right) \cos 2\,(n-k)\,\theta + \left(\begin{array}{c} 2n \\ n \end{array} \right) \right\}, \tag{3.31}$$

we get

$$\int_0^{2\,\pi} \cos^{2n}\theta\, d\theta = 2^{-2n+1} \left(\begin{array}{c} 2n \\ n \end{array} \right) \pi, \tag{3.32}$$

where n is any non–negative integer. (Gradshteyn & Ryzhik [1980, p. 369] then seem to be mistaken on the value of this integral — as can also be seen by direct calculation when n is small). After substituting in Eq. 3.30,

$$\frac{1}{2\,\pi} \int_0^{2\,\pi} \cos(k\, r\, \cos\theta)\, d\theta = \sum_{n=0}^{\infty} \frac{(-1)^n}{(n!)^2}\, 2^{-2n}\, k^{2n}\, r^{2n}. \tag{3.33}$$

Equation 3.29 can then be written as follows, assuming, once more, that integration and summation commute,

$$\langle \mathbf{u}_0 \cdot \mathbf{f}_1 + \mathbf{u}_1 \cdot \mathbf{f}_0 \rangle = 8\,\pi^2 \sum_{n=0}^{\infty} \frac{(-1)^n}{(n!)^2\, 2^{2n}}\, r^{2n} \int_{\mathbb{R}^2} k^{2n}\, \langle T\mathbf{u}(\mathbf{k})\, T\mathbf{f}(\mathbf{k})^* \rangle\, d\mathbf{k}. \tag{3.34}$$

The follwing identity is obtained in the same way as for three–dimensional turbulence,

$$\langle\, (\nabla^n \times \mathbf{u}) \cdot (\nabla^n \times \mathbf{f})\, \rangle = 4\,\pi^2 \int_{\mathbb{R}^2} k^{2n}\, \langle T\mathbf{u} \cdot T\mathbf{f}^* \rangle\, d\mathbf{k}, \tag{3.35}$$

so that

$$\langle \mathbf{u}_0 \cdot \mathbf{f}_1 + \mathbf{u}_1 \cdot \mathbf{f}_0 \rangle = 2 \sum_{n=0}^{\infty} \frac{(-1)^n\, \langle\, (\nabla^n \times \mathbf{u}) \cdot (\nabla^n \times \mathbf{f})\, \rangle}{2^{2n}\, (n!)^2}\, r^{2n}. \tag{3.36}$$

Finally, by the definition of $F(r)$,

$$F(r) = \sum_{n=0}^{\infty} \frac{(-1)^n \left\langle (\nabla^n \times \mathbf{u}) \cdot (\nabla^n \times \mathbf{f}) \right\rangle}{2^{2n}\,(n+1)\,(n!)^2}\, r^{2n}. \tag{3.37}$$

Let us note, in passing, that Eq. 3.3 has the following formal solution, at scales where viscous forces are negligible,

$$\langle u_r^3 \rangle \sim -3 \sum_{n=0}^{\infty} \frac{(-1)^n \left\langle (\nabla^n \times \mathbf{u}) \cdot (\nabla^n \times \mathbf{f}) \right\rangle}{2^{2n}\,(n+1)\,(n+2)\,(n!)^2}\, r^{2n+1}. \tag{3.38}$$

As in three dimensions, we see that the energy transfer depends not only on the rate at which forcing transfers kinetic energy to the turbulence, but also on the rates at which it transfers the squares of all other rotation fields $(\nabla^n \times \mathbf{u})^2$. We shall now see that the transfer of higher order rotation fields ($n \geq 1$) dominates the energy transfer at small scales in two–dimensional turbulence. But, first, it is useful to check the above Taylor series of $F(r)$ by solving Eq. 3.3 in the dissipation range.

3.4 Solution in the dissipation range

At small scales, the dissipation term and the forcing term are of equal magnitudes, but the inertial term is small. To satisfy Eq. 3.3 at small scales, the first terms in the Taylor series of the dissipation and the forcing term should then cancel. It is useful to check this condition by calculating the Taylor series of the dissipation term. The Taylor series of $F(r)$ in Eq. 3.37 serves as comparison.

Consider the inertial term in Eq. 3.3 as r tends to zero. Assume that the Taylor series of u_r converges uniformly with respect to variations in both position and ensemble. The terms in the Taylor series of u_r^3 may then be averaged individually. Hence,

$$\begin{aligned} \langle u_r^3 \rangle \;\sim\; & \left\langle \left(\frac{\partial u_1}{\partial x_1}\right)^3 \right\rangle r^3 + \frac{3}{2} \left\langle \left(\frac{\partial u_1}{\partial x_1}\right)^2 \frac{\partial^2 u_1}{\partial x_1^2} \right\rangle r^4 \\ & + \frac{3}{4} \left\langle \frac{\partial u_1}{\partial x_1} \left(\frac{\partial^2 u_1}{\partial x_1^2}\right)^2 \right\rangle r^5 + \frac{1}{2} \left\langle \left(\frac{\partial u_1}{\partial x_1}\right)^2 \frac{\partial^3 u_1}{\partial x_1^3} \right\rangle r^5, \end{aligned} \tag{3.39}$$

as r tends to zero. The coefficient of r^4 changes sign under the reflection $\mathbf{e}_1 \mapsto -\mathbf{e}_1$ and then vanishes by isotropy. To see that the coefficient of r^3 also vanishes, consider an arbitrary point at which the strain matrix does not vanish. Denote by s the non–negative

eigenvalue of strain at this point (the other eigenvalue is then $-s$ by incompressibility). The strain rate along the first reference vector $\mathbf{e}_1$ is given by

$$\frac{\partial u_1}{\partial x_1} = s\,\cos\theta - s\,\sin\theta, \tag{3.40}$$

where θ is the angle between $\mathbf{e}_1$ and the eigenvector for the eigenvalue s. Since the flow is isotropic, the distribution of θ is uniform in the interval $[0, 2\,\pi]$ and independent of the strain eigenvalue s. The average over ensembles may then be carried out by averaging first over angles θ and then over eigenvalues s. Hence,

$$\left\langle \left(\frac{\partial u_1}{\partial x_1}\right)^3 \right\rangle = 0. \tag{3.41}$$

For comparison, the strain rate cubed has non–zero average in three dimensions because the turbulence produces enstrophy through the extension of vortex lines (Batchelor & Townsend, 1947).

To derive a Taylor series for the dissipation term in Eq. 3.3, note first that the correlations of higher–order rotation fields $\nabla^n \times \mathbf{u}$ are derivatives of the velocity correlation,

$$\langle\, (\nabla^n \times \mathbf{u})(\mathbf{x}) \cdot (\nabla^n \times \mathbf{u})(\mathbf{x}+\mathbf{r})\,\rangle = (-1)^n\, \nabla^{2n} R(\mathbf{r}), \tag{3.42}$$

where ∇^2 is the Laplacian in two dimensions (Batchelor, 1953). Batchelor derives this result for turbulence in three dimensions, but the extension to two dimensions is straightforward. The Taylor series of the velocity correlation $R(\mathbf{r})$ is then

$$R(\mathbf{r}) = \sum_{n=0}^{\infty} \frac{(-1)^n\, \langle\, (\nabla^n \times \mathbf{u})^2\,\rangle}{(2n)^2\,(2n-2)^2 \cdot \ldots \cdot 2^2}\, r^{2n}. \tag{3.43}$$

This Taylor series presumably converges everwhere, provided that the forcing $\mathbf{f}$ is smooth; though, the exact radius of convergence is of no consequence and the series need only be an asymptotic expansion. It was shown above that

$$R(\mathbf{r}) = \langle \mathbf{u}^2 \rangle - \left(1 + \frac{r}{2}\,\frac{d}{dr}\right) \langle u_r^2 \rangle. \tag{3.44}$$

We then obtain the following Taylor series for the second–order moment $\langle u_r^2 \rangle$,

$$\langle u_r^2 \rangle = \sum_{n=1}^{\infty} \frac{(-1)^{n+1}\, \langle\, (\nabla^n \times \mathbf{u})^2\,\rangle}{(n+1)\,(2n)^2\,(2n-2)^2 \cdot \ldots \cdot 2^2}\, r^{2n}, \tag{3.45}$$

and the dissipation term in Eq. 3.3 has the following Taylor series,

$$\nu \left(\frac{d^2}{dr^2} + \frac{3}{r} \frac{d}{dr} \right) \langle u_r^2 \rangle = 2\nu \sum_{n=0}^{\infty} \frac{(-1)^n \langle (\nabla^{n+1} \times \mathbf{u})^2 \rangle}{(2n+2)(2n)^2 \cdot \ldots \cdot 2^2} r^{2n}. \tag{3.46}$$

Equation 3.3 must hold separately at each order as the scale r tends to zero. Since only the dissipation term and the forcing term contribute at orders r^0 and r^2, Eq. 3.3 gives the following conditions on the first coefficients,

$$\nu \langle \omega^2 \rangle = \langle \mathbf{u} \cdot \mathbf{f} \rangle \qquad \nu \langle (\nabla \omega)^2 \rangle = \langle \omega \phi \rangle. \tag{3.47}$$

We have already seen that these equations are satisfied when the turbulence is two–dimensional and stationary (they represent stationarity of the mean kinetic energy and the mean enstrophy). The conclusion is that the first two terms in the Taylor series of $F(r)$ have the form imposed by the dissipation term in Eq. 3.3, which of course indicates that this Taylor series is correct.

3.5 Solution at small scales

We now solve Eq. 3.3 at scales r for which the viscous term is negligible, yet smaller than L_1. (Since inertial forces, on dimensional grounds, decrease no slower than $\langle \omega^2 \rangle r$ as r tends to zero, the forcing $\mathbf{f}_1$ dominates in this range). Equation 3.27 implies that the Taylor series in Eq. 3.37, when $r << L_1$, can be approximated as follows,

$$F(r) \sim \epsilon - \frac{1}{8} \alpha r^2 + \frac{1}{192} \beta r^4. \tag{3.48}$$

Simplify the notation,

$$\begin{aligned} I(r) &= \left(\frac{d}{dr} + \frac{3}{r} \right) \langle u_r^3 \rangle \\ D(r) &= \nu \left(\frac{d^2}{dr^2} + \frac{3}{r} \frac{d}{dr} \right) \langle u_r^2 \rangle, \end{aligned} \tag{3.49}$$

so that,

$$I(r) = 6\, D(r) - 6\, F(r). \tag{3.50}$$

It is shown in the appendix that $F(r) - \epsilon$ is much larger than $D(r) - \epsilon$ when r is much larger than the characteristic correlation length η for vorticity gradients,

$$I(r) \sim -6\, [F(r) - \epsilon]. \tag{3.51}$$

This approximation is possible only in two dimensions (see the appendix). Hence, using Eq. 3.48,

$$I(r) \sim \frac{3}{4}\alpha r^2 - \frac{1}{32}\beta r^4, \tag{3.52}$$

giving

$$\langle u_r^3 \rangle \sim \frac{1}{8}\alpha r^3 - \frac{1}{256}\beta r^5. \tag{3.53}$$

This is the solution of Eq. 3.3 at small scale. The first term represents the enstrophy 'cascade' to small scales, first conjectured by Batchelor (according to Bray, 1966), and also by Kraichnan (1967). Equation 3.53 has one further characteristic length scale,

$$\Delta_1 = \left(\frac{32\,\alpha}{\beta}\right)^{1/2}, \tag{3.54}$$

which is the largest length scale at which the enstrophy term dominates. From the definition of Q,

$$\Delta_1 \propto Q^{-1/2} L_1, \tag{3.55}$$

so the palinstrophy range expands as Q increases. This is because vortices inhibit enstrophy dissipation, implying that the turbulence transfers more enstrophy to large scales and less to small scales. The statistical structure then depends on Q; this probably explains, in part at least, the frequent disagreement between different numerical simulations of two–dimensional turbulence.

3.6 Solution at large scales

It is now easy to solve Eq. 3.3 at large scales, $L_1 << r << L_2$. In this range, $F_1(r)$ is negligible, by assumption. Since we assume that the turbulence transfers palinstrophy mainly to small scales, the first two terms in the Taylor series of $F_2(r)$ of dominate when $r << L_2$. To determine these terms, consider the equations for the conservation of mean kinetic energy and mean enstrophy,

$$\begin{aligned} \epsilon &= \langle \mathbf{u} \cdot \mathbf{f}_1 \rangle + \langle \mathbf{u} \cdot \mathbf{f}_2 \rangle \\ \alpha &= \langle \omega\, \phi_1 \rangle + \langle \omega\, \phi_2 \rangle, \end{aligned} \tag{3.56}$$

where ϕ, as before, is the component of the rotation of the forcing $\mathbf{f}$ perpendicular to the plane of the flow. Recall that we denote the rates of energy and enstrophy transfer at the

scale L_1 as follows,

$$\begin{aligned} E &= \langle \mathbf{u} \cdot \mathbf{f}_1 \rangle \\ A &= \langle \omega \, \phi_1 \rangle. \end{aligned} \tag{3.57}$$

Then

$$\begin{aligned} \langle \mathbf{u} \cdot \mathbf{f}_2 \rangle &= \epsilon - E \\ \langle \omega \, \phi_2 \rangle &= \alpha - A. \end{aligned} \tag{3.58}$$

Note that $E \geq \epsilon$ and $\mathbb{A} \geq \alpha$, provided that there is no mean transfer of kinetic energy or enstrophy at the scale L_2. When $r << L_2$,

$$F_2(r) \approx \epsilon - E - \frac{(\alpha - A)}{8} r^2. \tag{3.59}$$

Equation 3.3 then has the approximate large–scale solution,

$$\langle u_r^3 \rangle \sim \frac{3}{2} (E - \epsilon) \, r - \frac{1}{8} (A - \alpha) \, r^3. \tag{3.60}$$

The first term represents the inverse energy 'cascade', first conjectured by Kraichnan (1967), and not previously studied analytically; however, when Q increases, the second term dominates in a wider range. In fact, define

$$\Delta_2 = \left(\frac{E - \epsilon}{A - \alpha} \right)^{1/2}. \tag{3.61}$$

The energy transfer at large scales then corresponds to an inverse energy cascade in the range $L_1 << r << \Delta_2$ and an inverse enstrophy cascade in the range $\Delta_2 << r << L_2$.

3.7 Comparison with data

The rigorous estimates of the third–order moment are now used to support heuristic estimates of the energy spectrum $E(k)$. But we must first consider how intermittency, due to vortices, affects the energy spectrum. For this, denote by $P(r)$ the fraction of total space in which the energy transfer is active. Suppose that

$$P(r) \sim C \left(\frac{r}{L_1} \right)^q, \tag{3.62}$$

for some constant C. Denote by $v(r)$ the root–mean–square velocity difference u_r in the region where the energy transfer is active. Suppose now that the third–order moments $\langle u_r^3 \rangle$ is determined by the contribution from this region,

$$\langle u_r^3 \rangle \propto P(r)\, v(r)^3. \tag{3.63}$$

This is assumed in the so–called β–model for intermittency (Novikov & Stewart, 1964; Frisch, Sulem & Nelkin, 1978). Similarly, the intermittent part of the velocity field probably determines the energy spectrum (since the velocity field is more irregular here than in other regions),

$$E(K) \sim C\, P(k^{-1})\, k^{-1}\, v^2(k^{-1}), \tag{3.64}$$

where $v(r)$ was assumed a power–law and where C is another constant. From the three previous equations, together with the above results for the third–order moment,

$$E(k) \sim \begin{cases} C_1\, \alpha^{2/3}\, L_1^{-q/3}\, k^{-3-q/3} & 2\pi\eta^{-1} >> k >> 2\pi\Delta_1^{-1} \\ C_2\, \beta^{2/3}\, L_1^{-q/3}\, k^{-13/3-q/3} & 2\pi\Delta_1^{-1} >> k >> 2\pi L_1^{-1} \\ C_3\, (E-\epsilon)^{2/3}\, k^{-5/3} & 2\pi L_1^{-1} >> k >> 2\pi\Delta_2^{-1} \\ C_4\, (A-\alpha)^{2/3}\, k^{-3} & 2\pi\Delta_2^{-1} >> k >> 2\pi L_2^{-1} \end{cases} \tag{3.65}$$

The energy spectrum predicted by Kraichnan (1967) appears when $q = 0$ and Q is of order unity, so that Δ_1 is comparable with L_1; the meaning of these two conditions is that there should be no intermittency, and enstrophy should be transferred almost entirely to small scales. There is empirical support for both the enstrophy range (Ogura, 1958; Wiin–Nielsen, 1967; Maltrud & Vallis, 1991) and the energy range (Lilly, 1969; Frisch & Sulem, 1984; Herring & McWilliams, 1985; Sommeria, 1986; Maltrud & Vallis, 1991). Moreover, it has recently been shown rather conclusively that atmospheric turbulence has a k^{-3} range at wavelengths from about 600 to 3000km (e.g., Nastrom & Gage, 1985).

However, many simulations also indicate that the energy spectrum is steeper than k^{-3} when vortices are present. We can now explain this result, apart from the well–known effect of intermittency. Suppose, for the sake of definiteness, that the intermittency is in

the form of elongated vortex filaments. Then $q = 1$ and we get,

$$E(k) \sim \begin{cases} C_1\,\alpha^{2/3}\,L_1^{-1/3}\,k^{-10/3} & 2\,\pi\,\eta^{-1} >> k >> 2\,\pi\,\Delta_1^{-1} \\ C_2\,\beta^{2/3}\,L_1^{-1/3}\,k^{-14/3} & 2\,\pi\,\Delta_1^{-1} >> k >> 2\,\pi\,L_1^{-1} \\ C_3\,(E-\epsilon)^{2/3}\,k^{-5/3} & 2\,\pi\,L_1^{-1} >> k >> 2\,\pi\,\Delta_2^{-1} \\ C_4\,(A-\alpha)^{2/3}\,k^{-3} & 2\,\pi\,\Delta_2^{-1} >> k >> 2\,\pi\,L_2^{-1} \end{cases} \tag{3.66}$$

Maltrud & Vallis (1991) find that the energy spectrum for flows with vortices has two distinct ranges at wavenumbers larger than the forcing wavenumber $2\,\pi/L_1$. In the range at small wavenumbers, those next to the forcing wavenumber, the energy spectrum is, approximately, a power–law with exponent -4.5. On the other hand, in the range at large wavenumbers, those next to the dissipation wavenumber, the exponent is aproximately -3.6. Similar results were obtained by Santangelo, Benzi, & Legras (1989) for decaying turbulence. It is then plausible that the range at small wavenumbers is associated with intermittent palinstrophy transfer to small scales, while the range at large wavenumbers is associated with intermittent enstrophy transfer. Moreover, the inverse enstrophy transfer, and the corresponding k^{-3} range for the energy spectrum, was recently seen numerically (Borue, 1994); Borue even verified, by removing all large vortex patches, that this form of the spectrum is due to enstrophy transfer to large scales.

3.8 Appendix: the dissipation scale

To show that the dissipation scale for $I(r)$ scales like the correlation length η for vorticity gradients, let us first write the dissipation term as an integral over the correlation of vorticity gradients. From Eq. 3.3, or by direct calculation, it follows that any smooth function $f(r)$ satisfies,

$$r^{-2}\int_0^r y\left(\frac{d^2}{dy^2}+\frac{1}{y}\frac{d}{dy}\right)^{-1} f(y)\,dy = \left(\frac{d^2}{dy^2}+\frac{3}{y}\frac{d}{dy}\right)^{-1} r^{-2}\int_0^r y\,f(y)\,dy, \tag{3.67}$$

where the inverted differential operators are unique when the answer is assumed finite and zero at $r = 0$. Moreover,

$$\left(\frac{d^2}{dr^2}+\frac{3}{r}\frac{d}{dr}\right)^{-1} f(r) = \int_0^r u^{-3}\int_0^u v^3\,f(v)\,dv\,du, \tag{3.68}$$

so that Eq. 3.67 becomes

$$r^{-2} \int_0^r y \left(\frac{d^2}{dy^2} + \frac{1}{y} \frac{d}{dy} \right)^{-1} f(y)\, dy = \int_0^r u^{-3} \int_0^u v \int_0^v y\, f(y)\, dy\, dv\, du. \tag{3.69}$$

It was shown previously, in the proof of Eq. 3.3, that

$$D(r) = -2\nu r^{-2} \int_0^r y\, \nabla^2 R(\mathbf{y})\, dy, \tag{3.70}$$

where $y = |\mathbf{y}|$. Write

$$\begin{aligned} D(r) &= \epsilon - 2\nu r^{-2} \int_0^r y\, \nabla^{-2} \nabla^4 R(\mathbf{y})\, dy \\ &= \epsilon - 2\nu r^{-2} \int_0^r y \left(\frac{d^2}{dy^2} + \frac{1}{y} \frac{d}{dy} \right)^{-1} \nabla^4 R(\mathbf{y})\, dy. \end{aligned} \tag{3.71}$$

On reducing by means of Eq. 3.69 and Eq. 3.42,

$$D(r) = \epsilon - 2\nu \int_0^r u^{-3} \int_0^u v \int_0^v y \left\langle \nabla\omega(\mathbf{x}) \cdot \nabla\omega(\mathbf{x}+\mathbf{y}) \right\rangle dy\, dv\, du. \tag{3.72}$$

Note that $D''(0) = -\alpha/4 = -F''(0)$, which again agrees with the Taylor series of $F(r)$. When $y << \eta$,

$$\left\langle \nabla\omega(\mathbf{x}) \cdot \nabla\omega(\mathbf{x}+\mathbf{y}) \right\rangle \approx \left\langle (\nabla\omega)^2 \right\rangle, \tag{3.73}$$

giving

$$D(r) \approx \epsilon - \frac{1}{8} \alpha r^2, \tag{3.74}$$

because $|\mathbf{y}| \leq r$ in Eq. 3.72. Furthermore, for $r >> \eta$,

$$\frac{D(r) - \epsilon}{r^2} << -\frac{1}{8} \alpha. \tag{3.75}$$

Therefore, as we wanted to prove, $F(r) - \epsilon$ is much larger than $D(r) - \epsilon$ whenever r is much larger than the correlation length η for vorticity gradients. Note that this analysis is possible only in two dimensions, because otherwise α does not appear in both the expansion for $F(r)$ and the expansion for $D(r)$. In fact, when the turbulence is three–dimensional, the second term in the expansion for $D(r)$, which still represents viscous enstrophy dissipation, diverges as the Reynolds number R tends to infinity, and is soon much larger than α. The usual dimensional arguments for estimating η (e.g., Bray, 1966; Batchelor, 1969; Kraichnan, 1967) generally fail, because they require that the turbulence is not intermittent.

Comments.

It is assumed in this chapter that the distribution of velocity components is invariant under reflections of two given basis vectors about the origin. For instance, under the following reflections,

$$e_2 \mapsto -e_2 \qquad \text{and} \qquad e_3 \mapsto -e_3. \tag{4.39}$$

A more accurate term than 'reflectional symmetry in a plane' is then 'reflectional symmetry about an axis' (in this case, the axis through the origin parallel to e_1). In practice, this axis will be parallel to the mean flow. Full isotropy requires also reflectional invariance in the direction parallel to e_1, as well as rotational symmetry.

There is a mistake in (4.25). To show that the pressure term vanishes, assume that $\boldsymbol{r} = r\,\boldsymbol{e}_i$, where $\boldsymbol{e}_i$ is one of the two basis vectors that are reflected in the origin. Then it must be shown, for instance, that

$$\left\langle u_{1i}\,\frac{\partial p_0}{\partial x_{0i}} \right\rangle = 0. \tag{4.40}$$

But

$$\begin{aligned} \left\langle u_{1i}\,\frac{\partial p_0}{\partial x_{0i}} \right\rangle &= -\left\langle \frac{\partial u_{1i}}{\partial x_{0i}}\,p_0 \right\rangle \\ &= -\left\langle \frac{\partial u_{1i}}{\partial r_i}\,p_0 \right\rangle \\ &= -\frac{\partial}{\partial r_i}\left\langle u_{1i}\,p_0 \right\rangle \\ &= 0. \end{aligned} \tag{4.41}$$

The last equality was by reflectional symmetry. The other terms can be dealt with similarly. If it is assumed, moreover, that the correlation between velocity and pressure gradient is continuous in the separation r, all pressure terms vanish. However, in contrast to the statement in the chapter, this holds only when $\boldsymbol{r}$ is perpendicular to the axis of reflectional symmetry. For (4.34) to hold as it stands, reflectional symmetry in the e_1 direction is also required.

Chapter 4

The local structure of anisotropic turbulence

Kolmogorov's theory of locally isotropic turbulence (Kolmogorov, 1941 b) is extended to turbulence that is still homogeneous and stationary, but which, instead of being isotropic, is only reflectionally invariant in some plane. Equations are derived for the transfer of both kinetic energy and mean-square angular momentum. The combined solutions of these two equations give, when r is in the inertial range,

$$\langle u_r^3 \rangle \sim -\frac{8}{15}\,\epsilon\, r - \frac{4}{5\,r}\sum_i \langle u_i\, f_i \rangle\, r_i^2, \tag{4.1}$$

where ϵ is the mean rate of viscous energy dissipation per unit mass and where the brackets $\langle \cdot \rangle$ denote an average over space. Here the f_i denote components of the forcing. If the correlation between velocity and forcing is invariant under rotations of the coordinate system, then

$$\langle u_i\, f_i \rangle = \frac{1}{3}\,\epsilon, \tag{4.2}$$

and the above result reduces to that derived by Kolmogorov (1941 b) for locally isotropic turbulence. But in general, anisotropy at large scales results in anisotropy at small scales, though only in the coefficient of $\epsilon\, r$.

4.1 Introduction

It is natural to question whether isotropy is essential for Kolmogorov's (1941 b) classical work on the energy transfer in turbulence. After all, since homogeneity excludes mean energy transfer between different regions, it follows from stationarity that the flux of kinetic energy is approximately constant at inertial scales.

I consider this question by first deriving an equation for the transfer of kinetic energy and then an equation for the transfer of mean-square angular momentum (for velocity disturbances at different scales). The first equation holds when the turbulence is homogeneous and stationary; the second equation holds when the turbulence, in addition, is invariant under reflections in some plane. The inertial terms in these equations are divergences with respect to the separation between the points considered. Isotropy allows the inversion of these divergences without having to introduce undetermined functions. But inversion, without undetermined functions, is possible already under the much weaker condition of reflectional invariance in a plane.

Reflectional invariance in a plane is a plausible approximation in many contexts. For instance, turbulence in channels or pipes, at scales small compared with the distance to the wall, can probably be regarded as reflectionally invariant in the plane normal to the mean flow. The most significant consequence of reflectional invariance in a plane seems to be that the mean vorticity vanishes; since mean rotation usually affects turbulent structure, reflectional invariance in a plane, in contrast to full isotropy, has clear physical significance.

4.2 The transfer of kinetic energy

Let us first derive an equation for the mean energy transfer in turbulence that is homogeneous and stationary. Since stationarity is possible only when the turbulence is forced, consider an incompressible velocity field $\mathbf{u}$ that satisfies the Navier–Stokes equation with forcing $\mathbf{f}$,

$$\begin{aligned} \frac{\partial \mathbf{u}}{\partial t} + (\mathbf{u}\cdot\nabla)\mathbf{u} &= \nu\nabla^2\mathbf{u} - \frac{1}{\rho}\nabla p + \mathbf{f} \\ \nabla\cdot\mathbf{u} &= 0. \end{aligned} \tag{4.3}$$

The origin of forcing is of no concern here (but note that the forcing should be rotational, because homogeneity and incompressibility together imply that conservative forces, on average, transfer zero kinetic energy to the turbulence). Choose two points, $\mathbf{x}_0$ and $\mathbf{x}_1$. Define the relative position $\mathbf{r} = \mathbf{x}_1 - \mathbf{x}_0$. In the following, velocities and differential

operators with subscripts 0 and 1 denote values at the corresponding points. Similarly, the subscript r on differential operators denotes differentiation with respect to the relative position $\mathbf{r}$. The Navier–Stokes equation immediately shows that the velocity difference between these two points (the relative velocity) satisfies the equation

$$\frac{\partial}{\partial t}(\mathbf{u}_1-\mathbf{u}_0)+(\mathbf{u}_1\cdot\nabla_1)\mathbf{u}_1-(\mathbf{u}_0\cdot\nabla_0)\mathbf{u}_0=\nu\,\nabla_1^2\mathbf{u}_1-\nu\,\nabla_0^2\mathbf{u}_0-\frac{1}{\rho}\,\nabla_1 p_1+\frac{1}{\rho}\,\nabla_0 p_0+\mathbf{f}_1-\mathbf{f}_0. \quad (4.4)$$

Regard now $\mathbf{x}_0$ and $\mathbf{r}$ as independent variables. Differentiation with respect to $\mathbf{x}_1$ then equals differentiation with respect to $\mathbf{r}$, with $\mathbf{x}_0$ kept constant. It also equals differentiation with respect to $\mathbf{x}_0$, with $\mathbf{r}$ kept constant. Write the inertial term as the sum of a term that involves only velocity differences and a term that represents advection by the velocity field at $\mathbf{x}_0$,

$$\begin{aligned}(\mathbf{u}_1\cdot\nabla_1)\mathbf{u}_1 &= ([\mathbf{u}_1-\mathbf{u}_0]\cdot\nabla_r)[\mathbf{u}_1-\mathbf{u}_0]+(\mathbf{u}_0\cdot\nabla_1)\mathbf{u}_1\\ &= ([\mathbf{u}_1-\mathbf{u}_0]\cdot\nabla_r)[\mathbf{u}_1-\mathbf{u}_0]+(\mathbf{u}_0\cdot\nabla_0)\mathbf{u}_1, \quad (4.5)\end{aligned}$$

where the differentiation in the last term was changed from $\mathbf{x}_1$ to $\mathbf{x}_0$. We may similarly change the first Laplacians in Eq. 4.4 from $\mathbf{x}_1$ to $\mathbf{x}_0$. To simplify the notation, let $\mathbf{v}=\mathbf{u}_1-\mathbf{u}_0$ denote the relative velocity. Then

$$\frac{\partial\mathbf{v}}{\partial t}+(\mathbf{v}\cdot\nabla_r)\mathbf{v}+(\mathbf{u}_0\cdot\nabla_0)\mathbf{v}=\nu\,\nabla_0^2\mathbf{v}-\frac{1}{\rho}\,\nabla_0(p_1-p_0)+\mathbf{f}_1-\mathbf{f}_0, \quad (4.6)$$

To obtain an equation for the energy transfer, multiply by the relative velocity $\mathbf{v}$,

$$\frac{1}{2}\frac{\partial\mathbf{v}^2}{\partial t}+\frac{1}{2}\,\nabla_r\cdot[\mathbf{v}\,\mathbf{v}^2]+\frac{1}{2}\,\nabla_0\cdot[\mathbf{u}_0\,\mathbf{v}^2]=\nu\,\mathbf{v}\cdot\nabla_0^2\mathbf{v}-\frac{1}{\rho}\,\nabla_0\cdot[\mathbf{v}\,(p_1-p_0)]+\mathbf{v}\cdot(\mathbf{f}_1-\mathbf{f}_0), \quad (4.7)$$

where incompressibility of the velocity field, and hence the relative velocity, was used. Define averages over space by integrating (with respect to $\mathbf{x}_0$) over a sphere, divide by the volume, and let the radius tend to infinity. The average of the divergence of any vector with finite average is then zero. In particular,

$$\langle\,\nabla_0\cdot[\mathbf{u}_0\,\mathbf{v}^2]\,\rangle=\langle\,\nabla_0\cdot[\mathbf{v}\,(p_1-p_0)]\,\rangle=0, \quad (4.8)$$

where the brackets $\langle\cdot\rangle$ denote the average over space (since the turbulence is homogeneous, assume that ensemble averaging equals space averaging). Homogeneity and stationarity then give

$$\frac{1}{2}\,\nabla_r\cdot\langle\mathbf{v}\,\mathbf{v}^2\rangle=\nu\,\langle\,\mathbf{v}\cdot\nabla_0^2\mathbf{v}\,\rangle+\langle\,\mathbf{v}\cdot(\mathbf{f}_1-\mathbf{f}_0)\,\rangle, \quad (4.9)$$

Standard vector identities show that the viscous term can be written as follows,

$$\begin{aligned} \mathbf{v}\cdot\nabla_0^2\mathbf{v} &= -\mathbf{v}\cdot\nabla_0\times\nabla_0\times\mathbf{v} \\ &= -(\nabla_0\times\mathbf{v})^2+\nabla_0\cdot[\mathbf{v}\cdot\nabla_0\times\mathbf{v}]. \end{aligned} \tag{4.10}$$

The last term is a divergence with respect to $\mathbf{x}_0$ and its average is zero. Then

$$\frac{1}{2}\nabla_{\mathbf{r}}\cdot\langle\mathbf{v}\,\mathbf{v}^2\rangle = -\nu\,\langle(\omega_1-\omega_0)^2\rangle+\langle\mathbf{v}\cdot(\mathbf{f}_1-\mathbf{f}_0)\rangle. \tag{4.11}$$

Moreover, since the turbulence is stationary,

$$\langle\mathbf{u}\cdot\mathbf{f}\rangle = \nu\,\langle\omega^2\rangle, \tag{4.12}$$

so that, finally,

$$\frac{1}{2}\nabla_{\mathbf{r}}\cdot\langle\mathbf{v}\,\mathbf{v}^2\rangle = \nu\,\langle\omega_1\cdot\omega_0\rangle-\langle\mathbf{u}_0\cdot\mathbf{f}_1+\mathbf{u}_1\cdot\mathbf{f}_0\rangle. \tag{4.13}$$

This equation describes the energy transfer in homogeneous and stationary turbulence. As for isotropic turbulence, a dimensional estimate shows that the viscous term is small at scales much larger than the Kolmogorov dissipation scale $\eta = (\nu^3/\epsilon)^{1/4}$. Assume reflectional invariance in the plane spanned by $\mathbf{e}_2$ and $\mathbf{e}_3$. Equation 4.13 then has the inertial–range approximation,

$$\nabla_{\mathbf{r}}\cdot\langle\mathbf{v}\,\mathbf{v}^2\rangle \sim -4\,\epsilon, \tag{4.14}$$

with solution,

$$\langle\mathbf{v}\,\mathbf{v}^2\rangle \sim -\frac{4}{3}\,\epsilon\,\mathbf{r}+\nabla_r\times\mathbf{U}, \tag{4.15}$$

where $\mathbf{U}(\mathbf{r})$ is unknown. Since,

$$\mathbf{r}\cdot\nabla_r\times\mathbf{U} = \epsilon_{ijk}r_i\frac{\partial U_k}{\partial r_j} = 0, \tag{4.16}$$

we get,

$$\langle\mathbf{e}\cdot\mathbf{v}\,\mathbf{v}^2\rangle \sim -\frac{4}{3}\,\epsilon\,r, \tag{4.17}$$

where $\mathbf{e}=\mathbf{r}/|\mathbf{r}|$ and $r=|\mathbf{r}|$. The solution, however, involves several velocity components and we now seek statistics associated with only one velocity component. Von Kármán & Howarth (1938) use isotropy and tensor analysis for this purpose. I now describe an alternative approach, more general than tensor analysis.

4.3 The transfer of mean–square angular momentum

We seek an equation for the transfer of kinetic energy associated with only one velocity component. This is possible by observing that the total kinetic energy density is determined by the kinetic energy density associated with only one velocity component and then the mean–square angular momentum,

$$r^2\,\mathbf{v}^2 = (\mathbf{r}\cdot\mathbf{v})^2 + (\mathbf{r}\times\mathbf{v})^2. \tag{4.18}$$

Since we already have an equation for the transfer of the total kinetic energy, let us then derive an equation for the transfer of mean–square angular momentum. Simplify first the notation,

$$\begin{aligned} \mathbf{w} &= \mathbf{r}\times\mathbf{v} \\ \mathbf{p} &= \mathbf{r}\,(p_1 - p_0) \\ \mathbf{F} &= \mathbf{r}\times(\mathbf{f}_1 - \mathbf{f}_0), \end{aligned} \tag{4.19}$$

where $\mathbf{w}$ is the angular momentum associated with relative velocities and $\mathbf{F}$ is torque due to forcing. Note that

$$\begin{aligned} (\mathbf{v}\cdot\nabla_{\mathbf{r}})\mathbf{w} &= \mathbf{r}\times(\mathbf{v}\cdot\nabla_{\mathbf{r}})\mathbf{v} + \mathbf{v}\times\mathbf{v} \\ &= \mathbf{r}\times(\mathbf{v}\cdot\nabla_{\mathbf{r}})\mathbf{v}. \end{aligned} \tag{4.20}$$

That is, the cross product with $\mathbf{r}$ commutes with differentiation. Equation 4.6 then gives

$$\frac{\partial\mathbf{w}}{\partial t} + (\mathbf{v}\cdot\nabla_{\mathbf{r}})\mathbf{w} + (\mathbf{u}_0\cdot\nabla_0)\mathbf{w} = \nu\,\nabla_0^2\mathbf{w} - \frac{1}{\rho}\,\nabla_0\times\mathbf{p} + \mathbf{F}. \tag{4.21}$$

On multiplying by $\mathbf{w}$ and averaging, previous section show that

$$\frac{1}{2}\,\langle\mathbf{v}\cdot\nabla_{\mathbf{r}}\mathbf{w}^2\rangle = \nu\,\langle\mathbf{w}\cdot\nabla_0^2\mathbf{w}\rangle - \frac{1}{\rho}\,\langle\mathbf{w}\cdot\nabla_0\times\mathbf{p}\rangle + \langle\mathbf{w}\cdot\mathbf{F}\rangle, \tag{4.22}$$

using homogeneity and stationarity. Reflectional invariance now implies, together with homogeneity, that the pressure term vanishes. We have,

$$\begin{aligned} \mathbf{w}\cdot\nabla_0\times\mathbf{p} &= (\mathbf{r}\times\mathbf{v})\cdot(\mathbf{r}\times\nabla_0[p_1 - p_0]) \\ &= r^2\,\mathbf{v}\cdot\nabla_0[p_1 - p_0] - (\mathbf{r}\cdot\mathbf{v})(\mathbf{r}\cdot\nabla_0[p_1 - p_0]) \\ &= r^2\,\nabla_0\cdot(\mathbf{v}\cdot[p_1 - p_0]) - (\mathbf{r}\cdot\mathbf{v})(\mathbf{r}\cdot\nabla_0[p_1 - p_0]), \end{aligned} \tag{4.23}$$

where $\nabla_0 \times \mathbf{r} = 0$ was used for the first line and $\nabla_0 \cdot \mathbf{v} = 0$ for the second. The first term in the last equation, since it is a divergence with respect to $\mathbf{x}_0$, vanishes after averaging. Now

$$\langle (\mathbf{r}\cdot\mathbf{v})(\mathbf{r}\cdot\nabla_0[p_1 - p_0])\rangle = \sum_{ij} r_i r_j \left\langle v_i \frac{\partial}{\partial x_{0j}}[p_1 - p_0] \right\rangle, \tag{4.24}$$

where the x_{0j} are components of $\mathbf{x}_0$. Invariance under reflections of $\mathbf{e}_2$ and $\mathbf{e}_3$ implies that terms with $i \neq j$ vanish,

$$\begin{aligned} \langle (\mathbf{r}\cdot\mathbf{v})(\mathbf{r}\cdot\nabla_0[p_1 - p_0])\rangle &= \sum_{ii} r_i^2 \left\langle v_i \frac{\partial}{\partial x_{0i}}[p_1 - p_0] \right\rangle \\ &= \sum_{i} \left\langle \frac{\partial}{\partial x_{0i}} r_i^2 (v_i [p_1 - p_0]) \right\rangle, \end{aligned} \tag{4.25}$$

where incompressibility was used for the last line. This average is then a divergence with respect to $\mathbf{x}_0$ and then vanishes. Therefore, pressure does not contribute to the equation for the mean–square angular momentum,

$$\frac{1}{2}\langle \mathbf{v}\cdot\nabla_{\mathbf{r}}\mathbf{w}^2\rangle = \nu\langle \mathbf{w}\cdot\nabla_0^2\mathbf{w}\rangle + \langle \mathbf{w}\cdot\mathbf{F}\rangle. \tag{4.26}$$

The left side represents transfer of mean–square angular momentum by 'inertial torques', whereas the terms on the right side represent, respectively, transfers by 'viscous torques' and 'forcing torques'. The viscous term and the forcing term are given by

$$\begin{aligned} \nu\langle \mathbf{w}\cdot\nabla_0^2\mathbf{w}\rangle &= -2r^2\epsilon - 2r^2\nu\langle\omega_1\omega_0\rangle - 2\nu\langle(\mathbf{u}_0\cdot\mathbf{r})\nabla_0^2(\mathbf{u}_0\cdot\mathbf{r})\rangle \\ &\quad +\nu\langle(\mathbf{u}_1\cdot\mathbf{r})\nabla_0^2(\mathbf{u}_0\cdot\mathbf{r})\rangle + \nu\langle(\mathbf{u}_0\cdot\mathbf{r})\nabla_0^2(\mathbf{u}_1\cdot\mathbf{r})\rangle \\ \langle \mathbf{w}\cdot\mathbf{F}\rangle &= 2r^2\epsilon - r^2\langle\mathbf{u}_1\cdot\mathbf{f}_0 + \mathbf{u}_0\cdot\mathbf{f}_1\rangle - 2\langle(\mathbf{u}_0\cdot\mathbf{r})(\mathbf{f}_0\cdot\mathbf{r})\rangle \\ &\quad +\langle(\mathbf{u}_1\cdot\mathbf{r})(\mathbf{f}_0\cdot\mathbf{r})\rangle + \langle(\mathbf{u}_0\cdot\mathbf{r})(\mathbf{f}_1\cdot\mathbf{r})\rangle. \end{aligned} \tag{4.27}$$

The first terms on the right sides clearly cancel after adding the two equation. Moreover, since $\mathbf{r}$ is independent of $\mathbf{x}_0$, the third terms also cancel. Hence, on adding the two equations,

$$\begin{aligned} \nu\langle \mathbf{w}\cdot\nabla_0^2\mathbf{w}\rangle + \langle \mathbf{w}\cdot\mathbf{F}\rangle &= -2r^2\nu\langle\omega_1\omega_0\rangle + \nu\langle(\mathbf{u}_1\cdot\mathbf{r})\nabla_0^2(\mathbf{u}_0\cdot\mathbf{r})\rangle \\ &\quad +\nu\langle(\mathbf{u}_0\cdot\mathbf{r})\nabla_0^2(\mathbf{u}_1\cdot\mathbf{r})\rangle - r^2\langle\mathbf{u}_1\cdot\mathbf{f}_0 + \mathbf{u}_0\cdot\mathbf{f}_1\rangle \\ &\quad +\langle(\mathbf{u}_1\cdot\mathbf{r})(\mathbf{f}_0\cdot\mathbf{r})\rangle + \langle(\mathbf{u}_0\cdot\mathbf{r})(\mathbf{f}_1\cdot\mathbf{r})\rangle. \end{aligned} \tag{4.28}$$

The inertial–range approximation is then,

$$\frac{1}{2}\langle \mathbf{v}\cdot\nabla_{\mathbf{r}}\mathbf{w}^2\rangle \sim -r^2\langle \mathbf{u}_1\cdot\mathbf{f}_0+\mathbf{u}_0\cdot\mathbf{f}_1\rangle+\langle(\mathbf{u}_1\cdot\mathbf{r})(\mathbf{f}_0\cdot\mathbf{r})+(\mathbf{u}_0\cdot\mathbf{r})(\mathbf{f}_1\cdot\mathbf{r})\rangle, \tag{4.29}$$

and since r is much smaller than the forcing scale L,

$$\frac{1}{2}\langle \mathbf{v}\cdot\nabla_{\mathbf{r}}\mathbf{w}^2\rangle \sim -2r^2\epsilon+2\langle(\mathbf{u}\cdot\mathbf{r})(\mathbf{f}\cdot\mathbf{r})\rangle, \tag{4.30}$$

where subscripts on the right side are now unnecessary. Since $\mathbf{v}$ is incompressible, the left side can be written as a divergence with respect to $\mathbf{r}$. On inverting this divergence, as in the previous section,

$$\langle \mathbf{e}\cdot\mathbf{v}\,\mathbf{w}^2\rangle \sim -\frac{4}{5}\epsilon r^3+4\,\mathbf{e}\cdot\nabla_r^{-1}\cdot\langle(\mathbf{u}\cdot\mathbf{r})(\mathbf{f}\cdot\mathbf{r})\rangle, \tag{4.31}$$

where the inverse of the divergence is unique (the undetermined component is rotational and then vanishes by reflectional invariance). Since,

$$\langle(\mathbf{u}\cdot\mathbf{r})(\mathbf{f}\cdot\mathbf{r})\rangle=\sum_i\langle u_i\,f_i\rangle\,r_i^2, \tag{4.32}$$

and

$$\nabla_r^{-1}\cdot r_i^2=\frac{1}{5}r_i^2\,\mathbf{r}, \tag{4.33}$$

we get,

$$\langle \mathbf{e}\cdot\mathbf{v}\,\mathbf{w}^2\rangle \sim -\frac{4}{5}\epsilon r^3+\frac{4}{5}r\sum_i\langle u_i\,f_i\rangle\,r_i^2. \tag{4.34}$$

We have solved the equation for the transfer of mean–square angular momentum. If the turbulence was not reflectionally invariant, the mean vorticity could be non–zero, the mean–square angular momentum (with respect to some fixed point) would depend on the position, and we would expect transfer of mean–square angular momentum between different regions, rather than exclusively to small scales.

4.4 Conclusion

To confirm the conjecture that full isotropy has little significance for the energy transfer to small scales, let us finally extend Kolmogorov's 4/5–law to turbulence that is only

reflectionally invariant in a plane, though still assumed homogeneous and stationary. On combining Eqs. 4.17 and 4.34,

$$\langle u_r^3 \rangle \sim -\frac{8}{15}\epsilon\, r - \frac{4}{5} r^{-1} \sum_i \langle u_i\, f_i \rangle\, r_i^2. \tag{4.35}$$

When the turbulence is isotropic, $\langle u_i\, f_i \rangle = \epsilon/3$ for each i and Kolmogorov's 4/5–law appears. On the other hand, if only one component of the forcing (say f_1) is different from zero, then

$$\langle u_r^3 \rangle \sim -\frac{4}{3}\epsilon\, r, \tag{4.36}$$

when $\mathbf{r} = (r, 0, 0)$, and

$$\langle u_r^3 \rangle \sim -\frac{8}{15}\epsilon\, r, \tag{4.37}$$

when either $\mathbf{r} = (0, r, 0)$ or $\mathbf{r} = (0, 0, r)$. In particular, anisotropy at large scale generally remains at small scales and the turbulence does not approach isotropy as the Reynolds number tends to infinity. However, the order of magnitude of the third–order moment at small scales is the same as for isotropic turbulence.

It was indicated in the previous section that other types of energy transfer, rather than energy transfer to small scales, are possible if the condition of reflectional invariance in a plane is relaxed; it should be possible to extend the analysis in the present paper to some of these other types of energy transfer.

Chapter 6

A model for intermittency in homogeneous turbulence

Numerical studies show that intermittency in homogeneous turbulence appears when vortex sheets collapse into strained vortex tubes. Strained vortex tubes have helical streamlines, so that vortex sheets apparently transfer helicity to vortex tubes. It is then natural to conjecture that this helicity transfer controls the magnitude of the largest velocity differences for turbulence at high Reynolds number. Dimensional arguments suggests that the characteristic Reynolds number of the most intense vortex tubes increases like $R_\lambda^{1/3}$ as the Taylor micro–scale Reynolds number R_λ tends to infinity. The agreement with numerical results is reasonable. Moreover, if the structure functions are power–laws in the inertial range, their exponents ξ_p satisfy

$$\xi_p \sim \alpha + \frac{2-\alpha}{3} p, \tag{6.1}$$

as p tends to infinity. The exponent α describes the volume fraction in which the helicity transfer is active; it also controls the Reynolds–number scaling of the largest velocity differences at the Kolmogorov dissipation scale η. For $\alpha = 5/3$, there is good agreement with both experiments and numerical simulations. This value corresponds to the preceding estimate of the Reynolds numbers of vortex tubes. In addition, it is predicted that the most intense vortex tubes occupy a fraction of space that decreases like $R_\lambda^{-5/2}$, but no empirical results are available in this case.

6.1 Introduction

Kolmogorov (1941 a) and Obukhov (1941) consider the rate at which velocity disturbances in turbulence transfer kinetic energy to small scales and use it to estimate the characteristic velocity differences in the inertial range. But Batchelor & Townsend (1949) found that some velocity differences are much larger than the Kolmogorov–Obukhov theory predicts, so energy transfer at small scales is highly intermittent instead of uniform.

It has now been established that intermittency at small scales consists of slender vortex tubes (e.g., Siggia, 1981; Kerr, 1985; Vincent & Meneguzzi, 1991, 1994; Ruetsch & Maxey, 1992; Jiménez *et al.*, 1993). These tubes have radii that scale approximately like the Kolmogorov dissipation scale,

$$\eta = (\nu^3/\eta)^{1/4}, \tag{6.2}$$

where ϵ is the mean rate of viscous energy dissipation per unit mass, and lengths that scale approximately like the integral scale L (Jiménez *et al.*, 1993). This implies that intermittency does not transfer kinetic energy to small scales (since the kinetic energy associated with vortex tubes diverges logarithmically at infinity; Moffatt, 1984). But kinetic energy is not the only conserved quantity for Euler flows; so is the helicity,

$$H = \int \mathbf{u} \cdot \boldsymbol{\omega} \, dV, \tag{6.3}$$

where $\boldsymbol{\omega} = \nabla \times \mathbf{u}$ is the vorticity (Moreau, 1961; Betchov, 1961; Moffatt, 1969). Vortex tubes are strained by the surrounding flow (Jiménez *et al.*, 1993; Vincent & Meneguzzi, 1994) and the local streamlines resemble helices (She & Orszag, 1990). Moreover, large fluctuations in the local helicity density in homogeneous turbulence occur in smaller volume fractions as the scale decreases (Polifke, 1991). All this indicates that intermittency is associated with helicity transfer to small scales. Let us now consider the consequences of this hypothesis (the arguments in this chapter are heuristic).

6.2 Reynolds numbers of vortex tubes

Let us begin with a dimensional estimate of the characteristic Reynolds number of the most intense vortex tubes (i.e., those with the highest vorticity levels). For this purpose, consider first the mechanism by which vortex sheets may transfer helicity to vortex tubes. The Reynolds numbers of vortex tubes seem to increase with the Reynolds number of turbulence (Jiménez *et al.*, 1993), so that viscous forces presumably contribute little to

the helicity budget for vortex tubes in high–Reynolds number turbulence. Moreover, suppose that the rate of helicity transfer to vortex tubes is approximately steady (since vortex tubes are likely to approch rapidly a state of local statistical equilibrium; Batchelor & Townsend, 1949). Let $h = \mathbf{u} \cdot \omega$ be the helicity density. The Euler equation for steady flow then gives

$$\frac{dh}{dt} = \nabla \cdot [\omega \cdot \mathbf{u}^2], \tag{6.4}$$

where $d/dt = \partial/\partial t + \mathbf{u} \cdot \nabla$ and incompressibility was used. Consider now a fluid volume V and denote the helicity in this volume by H. After integrating Eq. 6.4 over V,

$$\frac{dH}{dt} = \int_S (\mathbf{n} \cdot \omega)\, \mathbf{u}^2\, dS, \tag{6.5}$$

where $\mathbf{n}$ is a unit normal vector on the surface S of the volume V. Suppose that the surface has two disjoint components, $S = S_1 \bigcup S_2$, such that $\mathbf{n} \cdot \omega$ is positive on S_1 and non–positive on S_2. Since the vorticity field is incompressible,

$$0 = \int_{S_1} (\mathbf{n} \cdot \omega)\, dS + \int_{S_1} (\mathbf{n} \cdot \omega)\, dS. \tag{6.6}$$

Suppose now that there is a characteristic vorticity magnitude ω_0 on the surface S, and a characteristic difference Δ in kinetic energy between points in S_1 and points in S_2. Then, in order of magnitude,

$$\frac{dH}{dt} \propto A(S)\, \omega_0\, \Delta. \tag{6.7}$$

provided that the areas, $A(S_1)$ and $A(S_2)$, are of equal magnitude. This heuristic discussion does support the hypothesis that vortex sheets transfer helicity to vortex tubes, because we would expect that the vortex lines associated with collapsing vortex sheets prefer to 'enter' vortex tubes at one end and to 'exit' at the other end.

Suppose now that, as vortex sheets form vortex tubes, the tubes rapidly approach an equilibrium state in which helicity transfer from tubes to the surrounding flow balances helicity transfer from sheets to tubes. Since the radii of vortex tubes fluctuate strongly along axes (Jiménez *et al.*, 1993), it is plausible that tubes shed small vorticity filaments, and thus reduce both the helicity and the total circulation associated with the core (somewhat similar to turbulent diffusion). Let u_v denote the characteristic velocity variation across the cores of the most intense vortex tubes. The left side of the following relation

is then a natural dimensional estimate for the rate of helicity transfer from tubes to the surrounding flow,

$$u_v^3 \eta^{-1} \propto \langle \omega^2 \rangle^{1/2} U^2. \tag{6.8}$$

Similarly, the right side is a natural estimate for the rate of helicity transfer from sheets to tubes. This estimate follows from Eq. 6.5 by assuming

$$\begin{aligned} \omega_0 &= \langle \omega^2 \rangle^{1/2} \\ \Delta &= U^2. \end{aligned} \tag{6.9}$$

In support, the numerical simulations of Vincent & Meneguzzi (1991) indicate that the typical vorticity in sheets is comparable with the root–mean–square vorticity. Furthermore, vortex tubes have lengths that scale like the integral scale L and the typical variation in the kinetic energy over a distance L is comparable with the mean kinetic energy U^2. Equation 6.8, together with standard relations for homogeneous turbulence (Tennekes & Lumley, 1990), now gives

$$u_v \propto R_\lambda^{-1/6} U. \tag{6.10}$$

Define a characteristic Reynolds number for the cores of vortex tubes,

$$R_v = u_v \eta / \nu. \tag{6.11}$$

Then

$$R_v \propto R_\lambda^{1/3}, \tag{6.12}$$

as the Taylor micro–scale Reynolds number R_λ tends to infinity. The agreement with numerical results (see Table 1 below) is reasonable.

R_λ	$R_v/R_\lambda^{1/2}$	$R_v/R_\lambda^{1/3}$
35.8	21.1	38.3
62.8	17.0	33.9
94.5	18.1	38.6
168.1	16.5	38.7

TABLE 1. Comparison of predictions for the Reynolds number of vortex tubes with the numerical results from Jiménez *et al.* (1993). The first column contains the Taylor micro–scale Reynolds number in four direct numerical simulations of homogeneous turbulence. The second column compares the numerical results with the scaling suggested by Jiménez *et al.*. The third column compares the numerical results with the prediction derived above.

6.3 A hypothesis for the structure functions

We have seen that the Reynolds numbers of vortex tubes are compatible with the hypothesis that intermittency is associated with helicity transfer to small scales. Let us now extend this analysis to all scales between η and L, so as to estimate the asymptotic behaviour of the structure functions as the order tends to infinity. As in previous chapters, we define the velocity difference u_r as follows,

$$\mathrm{u}_r = [\mathbf{u}(\mathbf{x} + r\,\mathbf{e}, t) - \mathbf{u}(\mathbf{x}, t)] \cdot \mathbf{e}, \tag{6.13}$$

where $\mathbf{e}$ is a unit vector. Assume that the pth order structure function is an approximate power–law in the inertial range,

$$\langle |u_r|^p \rangle \approx C_p \left(\frac{r}{L}\right)^{\xi_p} U^p, \tag{6.14}$$

where the C_p are non–dimensional constants and the brackets $\langle \cdot \rangle$ denote an ensemble average. Assume that this power–law fall–off holds in the range $\eta << r << L$ (this may fail if vortex sheets contribute to the largest velocity differences at scales comparable with the sheet thickness). Many theories have been proposed for intermittency (e.g., Kolmogorov, 1962; Obukhov, 1962; Novikov, 1961; Novikov & Stewart, 1964; Frisch, Sulem, & Nelkin, 1978; She & Orszag, 1991; She & Leveque, 1993; Dubrulle, 1994), but there is so far no agreement about the structure function exponents ξ_p for $p > 3$. It has also been suggested that intermittency is in the form of spirals (Lundgren, 1982), rather than simple tubes or sheets, but these spirals seem very unstable and, probably, do not appear in real turbulence (see appendix B).

Let us briefly review two of these theories of intermittency, as they have some common properties with the model considered below. The β–model (Novikov & Stewart 1964; Frisch, Sulem, & Nelkin 1978) develops the idea of Batchelor & Townsend (1949) that the volume fraction in which the energy transfer is active decreases like a power–law as the scale tends to zero. The β–model gives

$$\xi_p = \frac{p}{3} + \frac{1}{3}(3 - D)(3 - p), \tag{6.15}$$

where D characterises the typical number of offsprings for inertial–range 'eddies' (Frisch *et al.*, 1978). However, this prediction does not compare well with the higher order structure function exponents, as found experimentally by Anselmet *et al.* (1984) and numerically

by Vincent & Meneguzzi (1991). The β–model seems to fail at large p because of the implicit assumption that intermittency transfers kinetic energy down to small scales; it was remarked in the introduction that the kinetic energy associated with vortex tubes remains at large scales.

Both Anselmet *et al.* (1984) and Vincent & Meneguzzi (1991) find that the structure function exponents have the approximate form $\xi_p \sim p/9$ when the order p is large. She & Leveque (1993) and Dubrulle (1994) treat this asymptotic result as a hypothesis (expressed in terms of the largest rate of energy transfer). She & Leveque construct a model, without any physical basis, for which

$$\xi_p = \frac{p}{9} + 2\left[1 - \left(\frac{2}{3}\right)^{p/3}\right]. \tag{6.16}$$

This prediction is remarkably accurate at low orders of p. The factor 2 in Eq. 6.16 appears by assuming that the collection of vortex tubes typically occupies a region with box dimension equal to one (the codimension is then 2). This is not necessarily true. For instance, it is necessary that intense vortex tubes are not too strongly deformed when the Reynolds number is high, and this seems unlikely (particularly as the Reynolds numbers of the vortex tubes also increase). It is shown below that $\xi_p \sim p/9$ agrees with the hypothesis that the largest velocity differences are associated with helicity transfer to small scales.

Define the largest velocity difference $\max|u_r|$ and the probability $P(r)$ of finding velocity differences comparable with the largest velocity difference. The largest velocity difference is the limit

$$\max|u_r| = \lim_{p\to\infty} \langle |u_r|^p \rangle^{1/p}, \tag{6.17}$$

and it exists as a finite function whenever the higher order structure functions are finite (by Hölder's inequality). The probability $P(r)$ of finding large velocity differences is the volume fraction in which

$$|u_r| \geq \max|u_r| \tag{6.18}$$

(this definition makes sense because $\max|u_r|$ is only a characteristic velocity difference and larger velocity differences will occur). When the turbulence is in statistical equilibrium, the characteristic rate of helicity transfer by inertial forces associated with intermittency at scale r is comparable, on dimensional grounds, with the product of the probability $P(r)$ and the density $(\max|u_r|)^3/r^2$.

Hypothesis *Large velocity differences at length scales in the inertial range, from the integral scale L to the Kolmogorov dissipation scale η, are associated with intermittent helicity cascades in the sense that*

$$P(r)\,\frac{(\max|u_r|)^3}{r^2} \propto \frac{U^3}{L^2}, \tag{6.19}$$

as r tends to zero within the inertial range.

This hypothesis states that the mean rate of helicity transfer by inertial forces is constant in order of magnitude whenever r is both much smaller than the integral scale L and much larger than the Kolmogorov dissipation scale η. Previous works on helicity cascades, starting with Lesieur, Frisch & Brissaud (1971) consider energy spectra for helicity cascades that occupy all space. In general, such helicity cascades must be to large scales, because otherwise the energy cascade controls the energy spectrum (this is easily understood, on dimensional grounds, by noting that the energy spectrum associated with an energy cascade is much larger than the energy spectrum associated with a helicity cascade). However, we saw in the introduction that vortex tubes do not transfer kinetic energy to small scales; therefore, there is no conflict with energy cascades when the helicity cascade to small scales is associated with intermittency.

6.4 The structure function exponents

We now derive a prediction for the structure functions from the hypothesis that intermittency is associated with helicity cascades. Let us follow Batchelor & Townsend (1949) in assuming that the probability of finding high intermittent activity is a power–law,

$$P(r) \propto \left(\frac{r}{L}\right)^{\alpha}, \tag{6.20}$$

where $\alpha > 0$ is constant. The β–model is based on a similar assumption (Novikov & Stewart, 1964; Frisch, Sulem & Nelkin, 1978). The above hypothesis gives

$$\max|u_r| \propto \left(\frac{r}{L}\right)^{2/3-\alpha/3} U. \tag{6.21}$$

(Intermittent energy cascades, for comparison, give $1/3 - \alpha/3$ rather than $2/3 - \alpha/3$). It is shown in appendix A that

$$\langle|u_r|^p\rangle \sim C_p\,P(r)\,(\max|u_r|)^p, \tag{6.22}$$

where C_p is a non–dimensional constant, as p tends to infinity. Then

$$\xi_p \approx \alpha + \frac{2-\alpha}{3} p, \tag{6.23}$$

whenever p is sufficienty large; this relation between α and the higher order structure function exponents holds if, and only if, the distribution of large velocity differences is associated with intermittent helicity cascades.

Since the most intense vortex tubes have characteristic radii that scale like η, assume that $\max|u_\eta|$ scales like the characteristic velocity variation u_v across the cores of vortex tubes. It is then easy to show that

$$\begin{aligned} P(\eta) &\propto R_\lambda^{-5/2} \\ &\propto (\eta/L)^{5/3}. \end{aligned} \tag{6.24}$$

It does not seem that the Reynolds–number dependence of the volume fraction occupied by vortex tubes has been measured by experimenters. Returning to the structure functions, we see that $\alpha = 5/3$. Hence, we expect that

$$\xi_p \approx \frac{5}{3} + \frac{p}{9}, \tag{6.25}$$

as p tends to infinity. And, indeed, the agreement with experimental (Anselmet *et al.*, 1984) and numerical results (Vincent & Meneguzzi, 1991) is good when $12 \leq p \leq 22$ (Figure 6.1). When $p > 22$, the prediction in Eq. 6.25 disagrees with the numerical results. But the margin of error for the numerical results is, in this range, more than 20% (Vincent & Meneguzzi, 1991).

The estimate of the structure function exponents is not completely convincing. It seems plausible that vortex sheets affect these structure functions at scales larger than η. Certainly, the experimental results of Anselmet *et al.* (1984) indicate that the higher–order structure functions may have more than one inertial range (I am grateful to H. K. Moffatt for stressing this point). Nevertheless, I have included the prediction for the structure function exponents, as it is still too early to conclude that the structure functions are not simple power–laws.

6.5 Conclusion

We see that at least three independent empirical results agree reasonably with the hypothesis that intermittency is associated with helicity transfer to small scales. As far as I

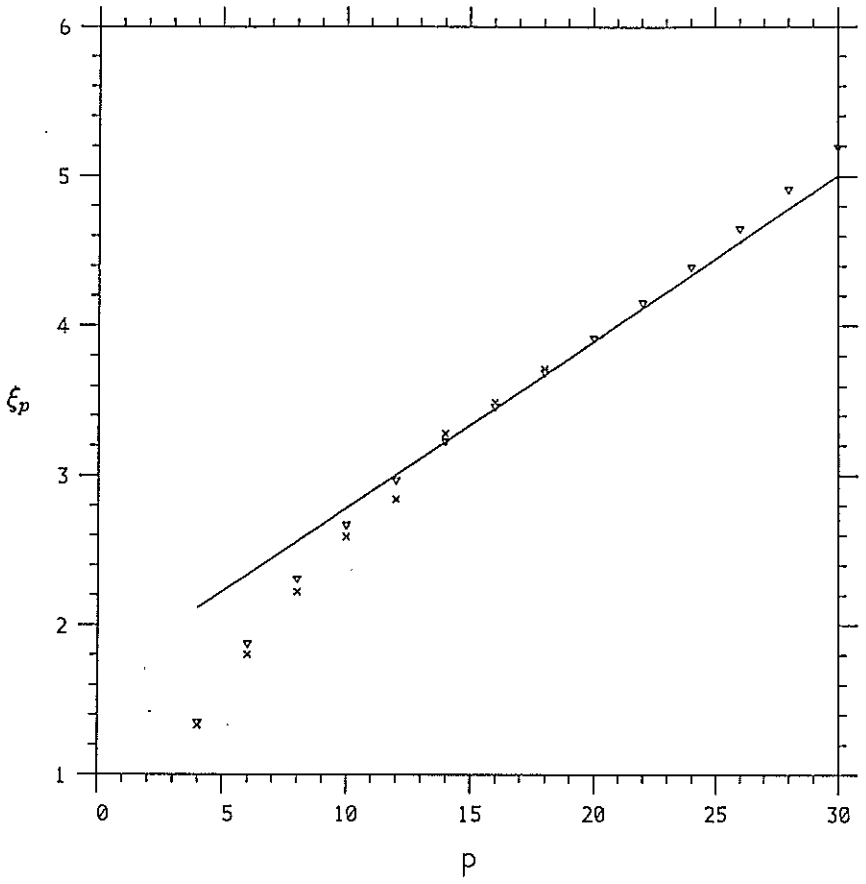

Figure 6.1: The structure function exponents ξ_p obtained by Anselmet *et al.* and by Vincent & Meneguzzi are represented, respectively, by crosses and triangles. The solid line is the prediction, $y = 5/3 + p/9$.

know, there are no other results available for comparison (other estimates of the structure function exponents do not reach sufficiently high orders, and there is little indication of the asymptotic slope).

6.6 Appendix A: the largest velocity differences

Let $p_r(x)$ denote the probability density function for the normalised velocity difference $x = |u_r|/U$. The pth order structure function is then

$$\langle |u_r|^p \rangle = U^p \int_0^\infty p_r(x)\, x^p\, dx. \tag{6.26}$$

Define the function

$$F_r(x) = \int_x^\infty p_r(u)\, du. \tag{6.27}$$

This is the probability that $|u_r| \geq x\, U$. Assume that the distribution $p_r(u)$ is continuous and everywhere positive; then F_r is differentiable and invertible. Notice that

$$F_r(0) = 1 \quad \text{and} \quad F_r(\infty) = 0. \tag{6.28}$$

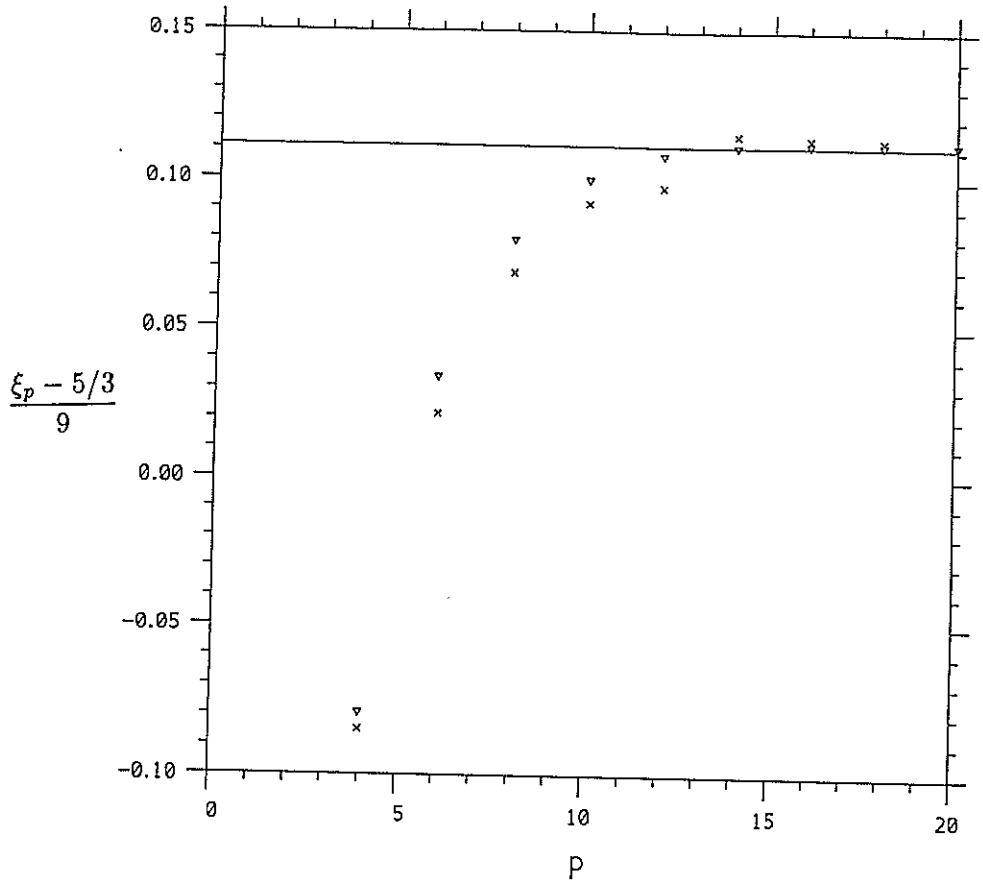

Figure 6.2: Plots of $(\xi_p - 5/3)/p$, based on the same data as the previous figure, but only up to $p = 20$. Crosses and triangles are used as before. The solid line is the prediction $y = 1/9$.

Since $dF_r = -p_r$,

$$\int_0^\infty p_r(x)\, x^p\, dx = \int_0^1 (F_r^{-1}(u))^p\, du, \tag{6.29}$$

where $F_r^{-1}(u)$ is the inverse function.

When p is large, the contribution to the pth order structure function is mainly from large x. Assume now that F_r, for large x, has the form

$$F_r(x) = f(x/x_0)\, y_0, \tag{6.30}$$

where x_0 and y_0 are functions of r only. The expression in Eq. 6.29 then becomes

$$\int_0^\infty p_r(x)\, x^p\, dx = y_0\, x_0^p \int_0^{y_0^{-1}} (f^{-1}(u))^p\, du. \tag{6.31}$$

The first function $x_0(r)$ characterises the largest velocity difference. We may assume that

$$x_0(r) = \frac{\max|u_r|}{U}. \tag{6.32}$$

To determine the second function y_0, note that

$$F_r(x_0) = f(1)\, y_0, \tag{6.33}$$

Since only the product $f(1)\, y_0$ has physical meaning, assume, without loss of generality, that $f(1) = 1$. Then, by definition of $P(r)$,

$$y_0(r) = P(r). \tag{6.34}$$

Assume now that $y_0(r)$ tends to zero as r tends to zero; this assumption is natural because intermitteny occurs in a smaller volume fraction as r decreases. Note that

$$f^{-1}(u) = F_L^{-1}\Big[u\, P(L)\Big], \tag{6.35}$$

and define the constant

$$C_p = P(L)^{-1} \int_0^\infty (F_L^{-1}(u))^p \, du. \tag{6.36}$$

Equation 6.31 then shows that

$$\langle |u_r|^p \rangle \sim C_p\, y_0\, x_0^p\, U^p, \tag{6.37}$$

as r/L tends to zero. The above expressions for x_0 and y_0 then give

$$\langle |u_r|^p \rangle \sim C_p\, P(r)\, (\max |u_r|)^p, \tag{6.38}$$

as r/L tends to zero. This equation holds when p is so large that the assumption in Eq. 6.30 can be used. This proves Eq. 6.22.

6.7 Appendix: a comment on spirals

Lundgren (1982) has suggested that the fine structure of turbulence is due to vortex sheets that collapse through instabilities of the Kelvin–Helmholtz type to form vortex tubes. Strikingly, his model gives an energy spectrum proportional to $k^{-5/3}$ in the inertial range, and this has motivated further work by others (Moffatt, 1984, 1993; Gilbert, 1988; Pullin & Saffman, 1993, 1994). Nevertheless, there is little evidence for spirals in turbulence at even moderate Reynolds numbers ($R_\lambda \sim 100$) and it is then legitimate to question whether such spirals are at all possible in fully–developed turbulence.

Velocity disturbances in the inertial range colllapse rapidly through inertial instabilities and it might seem, at first, that the spiral–model takes full account of these instabilities. But vortex sheets in real turbulence are subject to constant pertubations from the surrounding flow. Unless the central vortex tubes, around which vortex sheets collapse, are strong enough that such pertubations can be considered small, more instabilities will develop along the sheets and these will collapse into rows of vortex tubes.

Let us examine whether the vortex tubes observed numerically are so strong that they prevent further collapse of vortex sheets, that is, whether they are so strong that spirals can form. Let us assume that pertubations from the surrounding turbulence deform vortex sheets, or spirals, at a rate comparable with the root–mean–square strain rate (which is proprtional, when the turbulence is homogeneous, to the root–mean–square vorticity). This strain rate is characteristic of the smallest velocity disturbances; since pertubations of vortex sheets grow faster the smaller the wavelength (Batchelor, 1967), the smallest velocity disturbances are presumably the most significant for instability.

The condition that spirals form around vortex tubes is then that these tubes generate deformation rates that are, at least, comparable with the root–mean–square vorticity. This condition is easily checked. Denote by Γ the total circulation of characteristic vortex tubes in homogeneous turbulence and define the Reynolds number R_v (slightly different from the previous definition),

$$R_v = \frac{\Gamma}{\nu}. \tag{6.39}$$

The above condition must hold at distances up to the integral scale L, and the latter value gives a lower bound on R_v. In fact, suppose that the velocity induced by the vortex tube is similar to the velocity induced by a vortex line with similar total circulation. Then, at distances r larger than the dissipation scale η,

$$\mathbf{u}(\mathbf{r}) = \frac{\Gamma}{2\,\pi\,r}. \tag{6.40}$$

The deformation rate is then

$$\sigma(r) = -\frac{\Gamma}{2\,\pi\,r^2}, \tag{6.41}$$

so that

$$\sigma(r) = -\frac{R_v\,\nu}{2\,\pi\,r^2}. \tag{6.42}$$

For stability at distance L,

$$\sigma(L) \propto \langle\omega^2\rangle^{1/2}. \tag{6.43}$$

Since

$$\begin{aligned} \nu &= \langle\omega^2\rangle^{1/2}\,\eta^2 \\ L &\propto R_\lambda^{3/2}\,\eta, \end{aligned} \tag{6.44}$$

we finally get

$$\begin{aligned} R_v &\propto (L/\eta)^2 \\ &\propto R_\lambda^3. \end{aligned} \tag{6.45}$$

The stability of spirals then requires Reynolds numbers R_v that are several orders of magnitude larger than those found in numerical simulations (Jiménez *et al.*, 1993; see Table 1). Moreover, for turbulence in the atmospheric boundary layer, we have $L = 100m$ and $\eta = 0.01m$, at least in order of magnitude. Then R_v should be around 100 million for spirals to roll up around vortex tubes. Of course, this makes no sense physically, and it seems safe to conclude that such spirals do not occur when the Reynolds number is high.

Moreover, it seems that the whole approach, relating the energy cascade to the dynamics of large structures, will always encounter serious problems for the following reason. Since the enstrophy spectrum $\Omega(k)$ is related to the energy spectrum $E(k)$ as follows,

$$\Omega(k) = k^2\,E(k), \tag{6.46}$$

the enstrophy spectrum $\Omega(k)$ must decrease rapidly as k tends to zero. Otherwise, the mean kinetic energy (basically the total integral of the energy spectrum) is infinite. But such rapid decrease as k tends to zero generally fails for both vortex tubes and spirals. Physically, this is because the kinetic energy associated with vortex tubes is logarithmically singular at infinity (Moffatt, 1984). Since kinetic energy remains at large scales, the spiral–model does not represent energy transfer to small scales.

Chapter 7

The wavelet Gibbs phenomenon

The existence of a Gibbs Phenomenon for the continuous wavelet transform is demonstrated. The convergence properties of Grossmann–Morlet's inversion formula, which is a complex version of the 'reproducing' formula of Calderón, are also considered. An expression for the value of the overshoot is derived, and it is shown that the reconstructed function may have a number of local extrema that do not disappear as more small–scale wavelets are included. The wavelet overshoot is always less than the Fourier overshoot, and it is possible to choose the analysing wavelet such that there is no overshoot. The value of the overshoot is determined for some analysing wavelets that are in current use.

7.1 Introduction

When reconstructing periodic functions by means of their Fourier coefficients, it is common to use only those coefficients that correspond to frequencies smaller than some given frequency. As is well known, this filtered function has an overshoot of 17.9% in the neighbourhood of simple discontinuities. This is the so–called Gibbs Phenomenon (Wilbraham, 1848; Gibbs, 1899; Carslaw, 1925; Zygmund, 1959; Champeney, 1987). The Gibbs phenomenon for the discrete, orthonormal wavelet transform was examined by Jaffard (1989), who derived an expression for the overshoot. A similar result for wavelet integrals is the central result of this chapter. An expression is derived for the overshoot, and it is shown that the reconstructed function may have a number of local extrema that do not disappear

as more small–scale wavelets are included. The wavelet overshoot is always less than the Fourier overshoot, and it is possible to choose the analysing wavelet such that there is no overshoot. The value of the overshoot is determined for some analysing wavelets that are in current use.

7.2 The method of proof

Recall that the continuous wavelet transform produces a two–dimensional set of coefficients. In practice, only a finite number of coefficients can be calculated, and those coefficients that are not calculated are simply assumed to be zero when reconstructing the function. The function obtained using only the calculated coefficients is a filtered version of the original function, and the convergence properties of this filtered function, as the number of non–zero coefficients is increased, depends on the filter. The filter used here — probably the simplest possibility — discards all coefficients that have come about by dilating the analysing wavelet with a factor larger than some given positive number (the filter is defined in Eq. 7.5). In Fourier theory, this type of filter is called 'low–pass' (since only the low frequencies pass through), and I adopt this terminology for wavelets as well; the effect of a wavelet low–pass filter, however, is never identical to that of a Fourier low–pass filter.

The derivation of the Gibbs phenomenon for Fourier integrals is similar to the derivation for Fourier series, because both decompositions use Sine waves. This is not the case for wavelet integrals and wavelet series. Since wavelet integrals admit a much larger class of functions as admissible wavelets than do wavelet series, the derivation of the overshoot for wavelet integrals is different from the derivation of the overshoot for wavelet series. To find the overshoot for wavelet integrals, it is necessary to consider first the inversion formula for wavelet integrals. Grossman & Morlet (1984) gave a somewhat complicated proof of the inversion formula for wavelet integrals, and I have therefore found it worthwhile to construct a simple proof that uses nothing but elementary Fourier analysis. The idea of the proof is essentially due to Calderón (1964), but whereas his version does not clarify the convergence properties of the inverse wavelet transform, the proof presented here shows that the inverse wavelet transform converges pointwise almost everywhere and converges uniformly in intervals in which the function is continuous. These results on convergence make it easy to determine the overshoot by considering the inverse wavelet transform of Heaviside's function.

7.3 Inversion

In this section, the convergence properties of the inverse wavelet transform are discussed. In particular, a simple proof is given for the inversion formula derived by Grossman & Morlet (1984). It is shown that the constant shape of the wavelets, $g((t-r)/\lambda)$, implies that the wavelet low–pass filter, as defined in Eq. 7.6 below, is equivalent to convoluting the function with a summability kernel, which again is the same as integrating the product of the Fourier transform of the function and the Fourier transform of the summability kernel. A standard summability result is then used to find conditions under which the convergence of the inverse wavelet transform is uniform. These results appear to be new in the context of wavelet integrals. First, however, it is necessary to recall a few notions from Fourier analysis.

The Fourier transform of an integrable function always exists but is not necessarily integrable, so the inverse Fourier transform does not always exist in the usual sense. Inversion is possible, however, after multiplying the Fourier transform of the function with a dilated version of the Fourier transform of a *summability kernel* (Champeney, 1987); this yields a localised and parameter–dependent average of the function. A real–valued function $K(t)$ is a summability kernel if it satisfies the following four conditions (Champeney, 1987; Chandrasekharan, 1989; Zygmund, 1959):

(K1) $\tilde{K}(\omega) \in L^1(\mathbb{R}) \cap C^0(\mathbb{R})$

(K2) $\tilde{K}(\omega) = \tilde{K}(-\omega)$ at all $\omega \in \mathbb{R}$

(K3) $\tilde{K}(0) = 1$

(K4) there exists an $s > 1$, and an $A > 0$, such that $|K(t)| < A(1+|t|)^{-s}$ for all $t \in \mathbb{R}$.

The parameter–dependent averages are formed by convoluting the function, say $f(t)$, with dilated versions of the summability kernel,

$$K_\rho(t) = 1/\rho\, K(t/\rho). \tag{7.1}$$

For most 'reasonable' functions, it can be shown that this convolution tends to the Lebesgues value of the function almost everywhere as the parameter tends to zero:

Theorem 7.1 *Suppose that $f(t) \in L^p(\mathbb{R})$ for some $p \in [1,3]$, and that $K(\omega)$ satisfies con-*

ditions (K1) — (K4) above. It then follows that $f(t)$ has a Fourier transform $\tilde{f} \in L^q(\mathbb{R})$, where $p^{-1} + q^{-1} = 1$, and that

$$\frac{1}{\sqrt{2\pi}} \int_{-\infty}^{+\infty} \tilde{f}(\omega) K(\lambda\omega) e^{i\omega t}\, d\omega \tag{7.2}$$

converges to $f(t)$ in the following senses:

(1) to the Lebesgue value $f_L(t)$ at each Lebesgue point of $f(t)$;

(2) uniformly to $f(t)$ on an interval $[c, d]$ when $f(t)$ is continuous on (a, b), where $a < c < d < b$.

Recall that the Lebesgue values are the numbers $f_L(t)$ determined such that

$$\lim_{h \to 0} \frac{1}{h} \int_0^h |f(t+u) + f(t-u) - 2f_L(t)|\, du = 0, \tag{7.3}$$

and that the *Lebesgue points* are the points at which the Lebesgue values exist (Champeney, 1987; Chandrasekharan, 1989; Zygmund, 1959). If the function is locally integrable, then nearly every point is a Lebesgue point and $f_L(t)$ is nearly always equal to f(t) (Champeney, 1987). If $f(t+)$ and $f(t-)$ both exist, then

$$f_L(t) = \frac{1}{2}[f(t+) + f(t-)]. \tag{7.4}$$

In particular, if $f(t)$ is continuous at $t = t_0$, then $f_L(t_0) = f(t_0)$.

The above theorem is a rephrased version of a result that can be found, for instance, in §8 of Champeney (1987). This is not the most general form possible, though adequate for our purposes. We use the summability kernel defined by

$$\tilde{K}(\omega) = \frac{2\pi}{c_g} \int_{|\omega|}^{+\infty} \frac{|\tilde{g}(u)|^2}{u}\, du, \quad \omega \in \mathbb{R}. \tag{7.5}$$

It is shown below that $\tilde{K}(\omega)$ always satisfies conditions (K1) — (K3) when $g(t)$ is an analysing wavelet. Condition (K4), however, is not satisfied for all analysing wavelets and must therefore be added as an extra assumption. The summability kernel in Eq. 7.5 is derived from the wavelet low–pass filter, defined as follows,

$$f_\rho(t) = \frac{2}{c_g} Re\left[\int_{-\infty}^{+\infty} \int_{\rho}^{+\infty} W(\lambda, r)\, g\left(\frac{t-r}{\lambda}\right) \lambda^{-2}\, d\lambda\, dr\right], \tag{7.6}$$

where $\rho > 0$. This is a low–pass filter because the smallest scales have been discarded, just as in the low–pass filter for the Fourier transform. The convergence properties of $f_\rho(t)$ as $\rho \to 0$ depend on the analysing wavelet, as well as on the behaviour of the function $f(t)$ in a neighbourhood of the point $t = t_0$. The wavelet low–pass filter does not converge to the function $f(t)$ at every point, but, as shown below, it does converge to the Lebesgue value of $f(t)$ at all points where the Lebesgue value exists.

Theorem 7.2 *Suppose that $g(t)$ satisfies conditions (1) — (3) in Chapter 1, and that $K(t)$, as defined in Eq. 7.5, satisfies conditions (K1) — (K4). If $f(t) \in L^2(\mathbb{R})$, then*

$$f_\rho(t) = \frac{1}{\sqrt{2\pi}} \int_{-\infty}^{+\infty} f(\tau) K\left(\frac{t-\tau}{\rho}\right) \frac{1}{\rho}\, d\tau \to f_L(t) \text{ as } \rho \to 0, \tag{7.7}$$

at each Lebesgue point of $f(t)$, and the convergence is uniform on each closed interval $[b, c]$ such that $f(t)$ is continuous on some larger open interval (a, d), where $a < b < c < d$.

Remark

This result implies the pointwise convergence nearly everywhere of the inverse wavelet transform. To have uniform convergence when reconstructing functions from their Fourier series, or Fourier transforms, continuity is not a sufficient condition, so the wavelet transform is better behaved than the Fourier transform when faced with 'pathological' functions.

Proof.

Assume, for simplicity, that the analysing wavelet is progressive (that is, the Fourier transform vanishes for negative frequencies). First we show that $K(t)$ is a summability kernel. That $\tilde{K}(\omega)$ is integrable can be shown by using partial integration and condition (1), in Section 1.2,

$$\begin{aligned} \int_{-\infty}^{+\infty} |\tilde{K}(\omega)|\, d\omega &= 4\pi/c_g \int_0^\infty \int_\omega^\infty |\tilde{g}(u)|^2/u\, du\, d\omega \\ &= 4\pi/c_g \int_0^\infty |\tilde{g}(\omega)|^2\, d\omega < \infty. \end{aligned} \tag{7.8}$$

The Fourier transform $\tilde{K}(\omega)$ is, by its definition in Eq. 7.5, even and continuous: condition (K1) and (K2) are therefore satisfied. The definition of c_g in Section 1.3 shows

that $\tilde{K}(0) = 1$: condition (K3) is therefore also satisfied. It was assumed from the beginning that condition (K4) holds, so it follows that $K(t)$ is a summability kernel.

The next step is to show the equivalence of using the wavelet low–pass filter and of convoluting the function with the summability kernel defined in Eq. 7.5. It follows from the definition of the wavelet low–pass filter in Eq. 7.6 that

$$\begin{aligned} f_\rho(t) &= \frac{2}{c_g} Re\left[\int_{-\infty}^{+\infty}\int_{\rho}^{+\infty} W(\lambda,r) g\left(\frac{t-r}{\lambda}\right)\lambda^{-2}\,d\lambda\,dr\right] \\ &= \frac{\sqrt{8\pi}}{c_g} Re\left[\int_{0}^{+\infty}\int_{\rho\omega}^{+\infty} \tilde{f}(\omega)\,e^{i\omega t}\,\frac{|\tilde{g}(\lambda)|^2}{\lambda}\,d\lambda\,d\omega\right] \\ &= \sqrt{\frac{2}{\pi}} Re\left[\int_{0}^{+\infty} \tilde{f}(\omega) e^{i\omega t}\tilde{K}(\rho\omega)\right] d\omega, \end{aligned} \tag{7.9}$$

where Fubini's theorem was used to change the order of integration, and Plancherel's theorem was used to express the integral over r as an integral over the frequency. The function $f(t)$ is real–valued, which is equivalent to the condition that $\tilde{f}(-\omega) = \tilde{f}^*(\omega)$. The summability kernel $\tilde{K}(\omega)$ is real–valued and even, so the integration in the last line of Eq. 7.9 can be extended from $\mathbb{R}_+$ to $\mathbb{R}$ by

$$f_\rho(t) = \frac{1}{\sqrt{2\pi}}\int_{-\infty}^{+\infty} \tilde{f}(\omega) e^{i\omega t}\tilde{K}(\rho\omega)\,d\omega. \tag{7.10}$$

Condition (4) ensures that $K(t)$ is square integrable and Plancherel's theorem therefore shows that

$$f_\rho(t) = \frac{1}{\sqrt{2\pi}}\int_{-\infty}^{+\infty} f(\tau) K\left(\frac{t-\tau}{\rho}\right)\frac{1}{\rho}\,d\tau. \tag{7.11}$$

The result now follows from Theorem 7.1 above.

□

Theorem 7.2 is a wavelet version of Riemann's Localisation Theorem (Chandrasekharan, 1989; Zygmund, 1959), which states that the convergence of the inverse Fourier transform at a point $t = t_0$ depends only on the behaviour of the function $f(t)$ in an arbitrarily small neighbourhood of the point t_0. Since analysing wavelets are localised, it is not surprising that a similar result holds for wavelet transforms.

7.4 The wavelet Gibbs phenomenon

Before examining the wavelet Gibbs phenomenon, it is natural to enquire about the reasons for the Fourier Gibbs phenomenon. By inspecting the proof of the Gibbs phenomenon for Fourier series (see, e.g., Zygmund 1959), it is seen that the constant shape of the trigonometric basis and the oscillations in the Sine function are essential for the overshoot to occur. First, if we suppose, for simplicity, that

$$f(t) = \frac{1}{2}\,\mathrm{sign}(t), \quad t \in]-\pi, +\pi[\tag{7.12}$$

then $a_n = (n\pi)^{-1}$, when n is odd, and $a_n = 0$, when n is even. This power–law fall–off of the odd order coefficients is a consequence of the constant shape of the basis functions. When the number of terms in the truncated Fourier series, N_0, tends to infinity and t tends to zero such that tN_0 remains constant, the power–law fall–off of the odd order Fourier coefficients implies that the truncated Fourier series can be approximated by an integral. The approximation is given by

$$\frac{1}{\sqrt{2\pi}} \sum_{|n|\leq N_0} a_n e^{int} \approx \frac{1}{\pi} \int_0^{N_0 t} \frac{\sin x}{x}\, dx = \frac{1}{\pi}\mathrm{Si}(N_0 t), \tag{7.13}$$

where $\mathrm{Si}(t) = \int_0^t \sin x/x\, dx$ is the Sine integral (see Zygmund 1959 for more details). The truncated Fourier series for $N_0 = 4$ and $N_0 = 10$ are shown in figure 7.1. Second, the integrand, $\sin x/x$, changes sign whenever $x = n\pi$, where $n \in \mathbb{N}$, which shows that

$$\mathrm{Si}(\pi) > \mathrm{Si}(2\pi) > \mathrm{Si}(3\pi) > \ldots.$$

The oscillations in the Sine functions therefore imply that $x = \pi$ is a global maximum for the Sine integral and that $\mathrm{Si}(\pi) > \mathrm{Si}(\infty)$. This shows that the ratio of the supremum of the truncated Fourier series to the jump in the function, namely $1/2$, tends to $\mathrm{Si}(\pi)/\mathrm{Si}(\infty)$ as N_0 tends to infinity with $t = \pi/N_0$.

As pointed out in Chapter 1, analysing wavelets have zero integral and therefore 'oscillate'. Since the wavelets used in the wavelet transform are also of constant shape, the wavelet transform has both of the properties that lead to a Gibbs phenomenon for Fourier series and integrals (namely 'constant shape' and 'oscillations'). But square integrability of the analysing wavelet implies that the wavelets are localised; this is the only essential difference between the Fourier transform and the wavelet transform. The question is therefore: how does the localisation of the analysing wavelet affect the overshoot? Is the

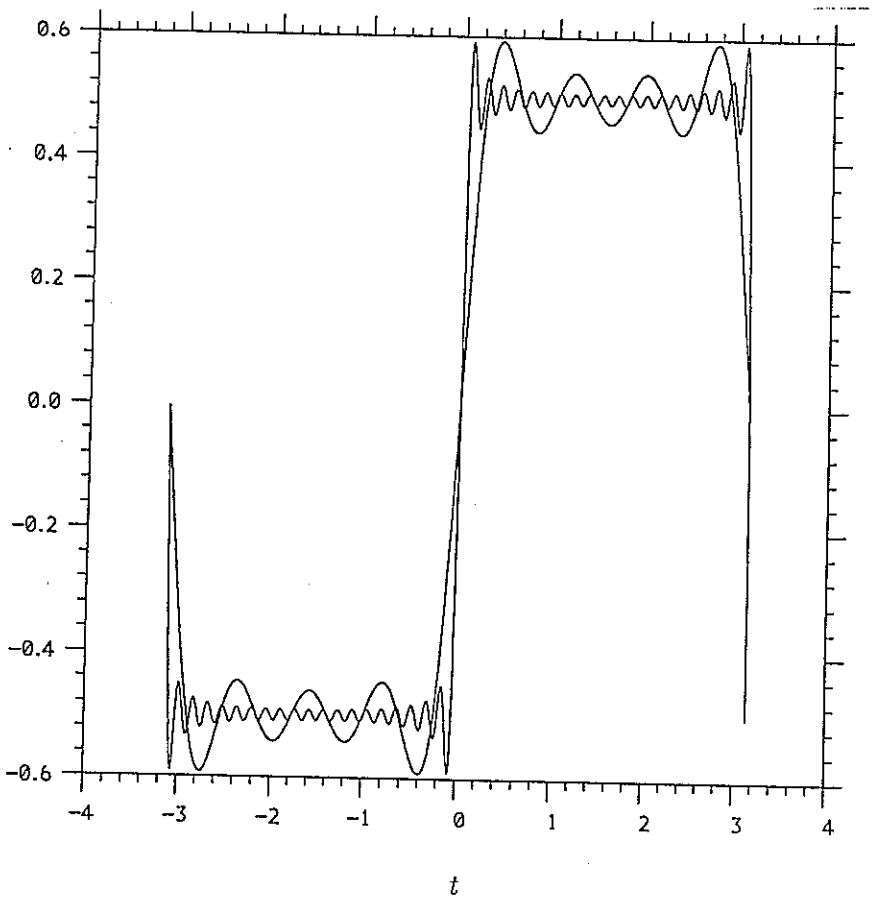

Figure 7.1: Examples of the truncated Fourier series for a step function (four terms, and twenty terms)

overshoot larger or smaller than the overshoot for Fourier transforms? It is tempting to try to answer these questions by direct calculations for particular analysing wavelets, since it can be done for Fourier series and integrals. However, if one attempts to find an expression for $W(\lambda, r)$ for Heaviside's function, for instance, and then inserts this expression in the inversion formula for the wavelet transform, it soon becomes a very complicated problem for even simple choices of the analysing wavelet. The reason is that the wavelet transform of Heaviside's function is generally a combination of special functions with arguments that depend in non–trivial ways on λ and r. It is shown below that the results from section 7.3 leads to a simple and general expression for the value of the overshoot for *all* analysing wavelets that satisfy the three conditions (1) – (3) in Chapter 1. Having derived a general expression for the value of the overshoot, the above questions can be answered.

Consider now a function with a simple discontinuity at $t = t_0$; this means that $f(t_0^+)$ and $f(t_0^-)$ both exist. Let $C = f(t_0^+) - f(t_0^-) > 0$ and suppose, for simplicity, that this is a positive number.

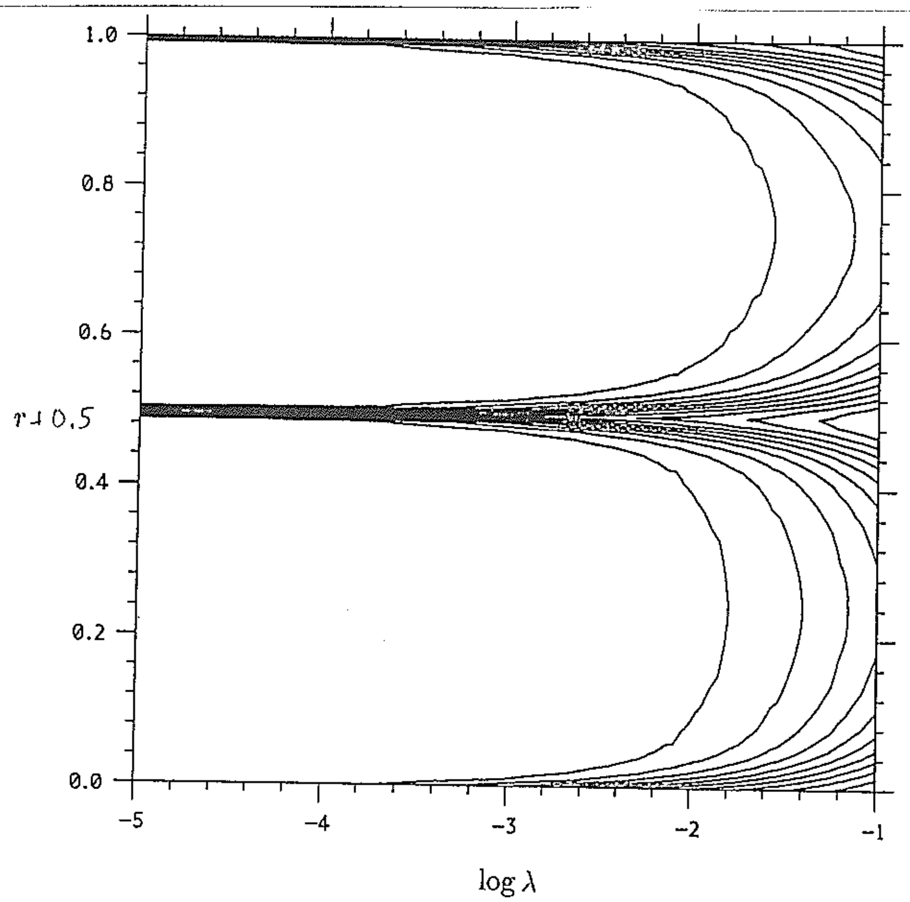

Figure 7.2: The wavelet transform of a step function with the complex–valued Mexican Hat wavelet

Definition 7.1 *The value of the overshoot is the number*

$$G_g = \frac{2}{C} \limsup_{\delta,\rho \to 0} \sup_{0< \quad <\delta} \left[f_\rho(t) - \frac{f(t_0^+) + f(t_0^-)}{2} \right], \qquad (7.14)$$

where $f_\rho(t)$ is defined in Eq. 7.6.

Remarks

1. The limit of the maximal amplitude in the filtered function is $100 \times (G_g - 1)\%$ larger than $|f(t_0^+) - f(t_0^-)|$. Some authors, e.g. Champeney (1987), measure the maximal amplitude by $50 \times (G_g - 1)\%$.

2. The value of the overshoot for Fourier series and integrals is

$$G_F = \frac{2}{\pi} \int_0^\pi \frac{\sin(t)}{t}\, dt = \mathrm{Si}(\pi)/\mathrm{Si}(\infty) \approx 1.179, \qquad (7.15)$$

(here F for Fourier). See also figure 7.1.

Before proceeding with the proof of the wavelet Gibbs phenomenon, it is useful to consider the wavelet transform of a discontinuous function. In figure 7.2, a part of the

wavelet transform of $f(t)$, which was defined in Eq. 7.12, is shown (the wavelet transform exists because $f(t)$ is bounded). The analysing wavelet used in this example is the Poisson wavelet with $m = 2$ (see Chapter 1 for the definition of the Poisson wavelets). The shape of the modulus of the wavelet transform is determined by the discontinuities at the points $t = n\pi$, $n \in \mathbb{N}$. Near these points the wavelet transform is excited at all scales and the shape of $|W(\lambda, r)|$ is asymptotically 'self–similar'.

Theorem 7.3 *Let the analysing wavelet $g(t)$ be progressive and satisfy conditions (1) — (3) in Chapter 1, and suppose that $f(t) \in L^2(\mathbb{R})$ is continuous in neighbourhoods to the right and to the left of $t = t_0$. If $C = f(t_0^+) - f(t_0^-) > 0$ exists and is finite, then there is an overshoot in the filtered function $f_\rho(t)$. The value of the overshoot, relative to C, is given by*

$$G_g = \sup_{M>0} \frac{4}{c_g} \int_0^\infty \frac{|\tilde{g}(\omega)|^2}{\omega} \mathrm{Si}(M\omega)\, d\omega. \tag{7.16}$$

Furthermore,

(1) $1 \leq G_g < G_F$

(2) If $|\tilde{g}(\omega)|^2/\omega$ is continuous for $\omega \in [0, \infty[$ and its Fourier Sine transform changes sign n times on the positive axis, then $f_\rho(t)$ has exactly n local extrema for $t > 0$ when $\rho \to 0$. In particular, if the Fourier Sine transform is negative for positive arguments, then there is no overshoot and $G_g = 1$.

Remarks

1. The Fourier Sine transform is here defined as the negative of the imaginary part of the Fourier transform.

2. Part of the following proof, Eqs. 7.22 — 7.25, uses only the four properties (K1) — (K4) for the summability kernel $K(t)$, so these calculations are identical to those for the inversion of Fourier transforms by summability kernels.

Proof.

We may assume: (1) the discontinuity occurs at $t_0 = 0$; (2) $f(t) = -1/2 + H(t) + r(t)$, where $H(t)$ denotes Heaviside's function and $r(t)$ is continuous in a neighbourhood of $t_0 = 0$. The wavelet transform and its inverse are both linear, so the general case follows by multiplying a function of this kind with an appropriate constant.

It was shown in Section 7.3 that

$$f_\rho(t) = \frac{1}{\sqrt{2\pi}} \int_{-\infty}^{+\infty} f(\tau) K\left(\frac{t-\tau}{\rho}\right) \frac{1}{\rho}\, d\tau, \tag{7.17}$$

and that

$$\int_{-\infty}^{+\infty} K(\tau)\, d\tau = \tilde{K}(0) = 1. \tag{7.18}$$

It is therefore possible to add and subtract $1/2$ from the right–hand side of the above equation in the following way:

$$f_\rho(t) = -1/2 + \frac{1}{\sqrt{2\pi}} \int_{-\infty}^{+\infty} [f(t+\tau) + 1/2]\, K\left(\frac{\tau}{\rho}\right) \frac{d\tau}{\rho}. \tag{7.19}$$

Using $f(t) = -1/2 + H(t) + r(t)$ this becomes

$$f_\rho(t) = -1/2 + \frac{1}{\sqrt{2\pi}} \int_0^{\infty} K\left(\frac{t-\tau}{\rho}\right) \frac{d\tau}{\rho} + \frac{1}{\sqrt{2\pi}} \int_{-\infty}^{+\infty} r(\tau)\, K\left(\frac{t-\tau}{\rho}\right) \frac{d\tau}{\rho}. \tag{7.20}$$

We now show that the last integral in Eq. 7.20 converges uniformly to $r(t)$ in a neighbourhood of the origin (this does not follow from Theorem 7.2 because the rest term $r(t)$ is not square integrable). Choose an $a > 0$ such that $r(t)$ is continuous in $]-a, a[$. Consider the two functions

$$r_1(t) = r(t)\, I_{]-a,a[}(t)$$

and

$$r_2(t) = r(t)\, I_{\mathbb{R}\setminus]-a,a[},$$

where]-a,a[denotes the open interval from $-a$ to a, and where $I_{]-a,a[}(t)$ is the indicator function on the set $]-a, a[$. Obviously, $r(t) = r_1(t) + r_2(t)$, which inserted in Eq. 7.20 leads to

$$\begin{aligned} f_\rho(t) \;=\; & -1/2 + \frac{1}{\sqrt{2\pi}} \int_0^{\infty} K\left(\frac{t-\tau}{\rho}\right) \frac{d\tau}{\rho} \\ & + \frac{1}{\sqrt{2\pi}} \int_{-\infty}^{+\infty} r_1(t)\, K\left(\frac{t-\tau}{\rho}\right) \frac{d\tau}{\rho} \qquad (7.21) \\ & + \frac{1}{\sqrt{2\pi}} \int_{-\infty}^{+\infty} r_2(t)\, K\left(\frac{t-\tau}{\rho}\right) \frac{d\tau}{\rho}. \qquad (7.22) \end{aligned}$$

The function $r_1(t)$ is continuous for $|t| \neq a$, so Theorem 7.2 implies that the second integral in Eq. 7.22 converges uniformly to $r(t)$ when the parameter t belongs to an interval on

the form $]-a+\epsilon, a-\epsilon[$, where $a > \epsilon > 0$. As $r_1(t)$ is continuous in this interval, it follows that $r_1(t)$ does not contribute to the asymptotic value of the overshoot.

Condition (K4) may be used to evaluate the last integral in Eq. 7.22. If we suppose that $t > 0$, then

$$\frac{1}{\sqrt{2\pi}}\Big|\int_{\mathbb{R}\setminus]-a,a[} r_2(t)\,K\Big(\frac{t-\tau}{\rho}\Big)\,\frac{d\tau}{\rho}\Big| \le \frac{A}{\sqrt{2\pi}}\int_{\mathbb{R}\setminus]-a,a[}|r_2(t)|\,\Big(1+|\frac{a-t}{\rho}|\Big)^{-s}\,\frac{d\tau}{\rho} \quad (7.23)$$

If $t \in]-a+\epsilon, a-\epsilon[$, as assumed for $r_1(t)$, then the right–hand side in Eq. 7.23 is uniformly of order $O(\rho^{s-1})$. It was required that $s > 1$, so the contribution from $r_2(t)$ converges uniformly to zero when $t \in]-a+\epsilon, a-\epsilon[$.

It has now been shown that the rest term $r(t)$ does not contribute to the asymptotic value of the overshoot, and we can therefore ignore the second integral in Eq. 7.20. The summability kernel $K(t)$ is even because $K(\omega)$ is even; the first integral in Eq. 7.22 therefore satisfies

$$\frac{1}{\sqrt{2\pi}}\int_0^\infty K\Big(\frac{t-\tau}{\rho}\Big)\,\frac{d\tau}{\rho} = 1/2 + \frac{1}{\sqrt{2\pi}}\int_0^{t/\rho} K(\tau)\,d\tau, \quad (7.24)$$

where $\int K(t)\,dt = 1$ was used. Equation 7.20 now shows that the value of the overshoot only depends on the supremum over t of the function

$$\frac{1}{\sqrt{2\pi}}\int_0^{t/\rho} K(\tau)\,d\tau. \quad (7.25)$$

For wavelet transforms, it is possible to express this function in terms of the analysing wavelet. If $K(\tau)$ is expressed as a Fourier integral, using the definition in Eq. 7.5, then partial integration of the function in Eq. 7.25 gives

$$\frac{1}{\sqrt{2\pi}}\int_0^{t/\rho} K(\tau)\,d\tau = \frac{1}{2}\frac{4}{c_g}\int_0^\infty \frac{|\tilde{g}(\omega)|^2}{\omega}\mathrm{Si}\Big(\frac{t\,\omega}{\rho}\Big)\,d\omega. \quad (7.26)$$

Since the supremum over t on the right–hand side in Eq. 7.26 is independent of ρ, we may take $\rho = 1$, so that the overshoot is given by the expression in Eq. 7.16, as we aimed to show.

We now prove the two inequalities in part 1) of Theorem 7.3. The first inequality holds because the right–hand side in Eq. 7.16 approaches unity as M tends to infinity.

The second inequality follows by noticing that the Sine integral, $\mathrm{Si}(x)$, is less than or equal to $\mathrm{Si}(\pi)$ everywhere:

$$\begin{aligned} G_g &= \sup_{M>0} \frac{4}{c_g} \int_0^\infty \frac{|\tilde{g}(\omega)|^2}{\omega} \mathrm{Si}(M\omega)\, d\omega \\ &= \frac{2\mathrm{Si}(\pi)}{\pi} + \sup_{M>0} \frac{4}{c_g} \int_0^\infty [\mathrm{Si}(M\omega) - \mathrm{Si}(\pi)] \frac{|\tilde{g}(\omega)|^2}{\omega}\, d\omega \\ &< \frac{2\mathrm{Si}(\pi)}{\pi} = G_F. \end{aligned} \tag{7.27}$$

The strict inequality in Eq. 7.27 holds because $\mathrm{Si}(M\omega) - \mathrm{Si}(\pi)$ is negative everywhere except at the point $\omega = \pi/M$, where it is zero. Part 1) of Theorem 7.3 has now been proved.

When proving the result in part 2) of Theorem 7.3, the contribution from the rest term can be ignored. This is justified in light of the remarks in the paragraph immediately below Eq. 7.23. With this simplification, the expression in Eq. 7.26 can be used directly, and we obtain, after differentiation with respect to t,

$$f'_\rho(t) = \frac{2}{c_g} \int_0^\infty \frac{|\tilde{g}(\omega)|^2}{t\omega} \sin(t\omega/\rho)\, d\omega. \tag{7.28}$$

It can be shown that differentiation under the integral sign is allowed when conditions (1) — (3) in Chapter 1 are satisfied. The function $|\tilde{g}(\omega)|^2/\omega$ is continuous by assumption and integrable by condition (3) in Chapter 1, so its Fourier transform is continuous (Chandrasekharan, 1989). Hence, if the Fourier Sine transform changes sign at a point $\omega = \omega_0$, then there exists an open interval (c, d) that contains ω_0, and such that the sign of the Fourier Sine transform in (c, ω_0) is the opposite of that in (ω_0, d). Equation 7.28 now shows that $f_\rho(t)$ has a local extremum at $t = \rho\omega_0$. If the Fourier Sine transform is negative for positive arguments, then $f'_\rho(t) > 0$ for $t > 0$. Since $f_\rho(0) = 0$, it follows that $f_\rho(t) > 0$ for all $t, \rho > 0$. Equation 7.25 and the asymptotic value of the Sine integral, $\mathrm{Si}(\infty) = \pi/2$, imply that $f_\rho(\infty) = 1/2$. Thus,

$$0 < f_\rho(t) < 1/2$$

for all $t, \rho > 0$, and there is no overshoot. Part 2) of Theorem 7.3 has now been proved.

□

The slope at $t = 0$, for $f(t) = H(t) - 1/2$, can be found by letting t tend to zero in Eq. 7.28,

$$f'_\rho(0) = \frac{2}{\rho} \frac{\|g\|_2^2}{c_g}. \tag{7.29}$$

The factor $\|g\|_2^2 \, c_g^{-1}$ is a measure of the amount of energy the analysis wavelet contains in frequencies smaller than unity. If most of the energy lies in this range of wavenumbers, the derivative $f'_\rho(0)$ is small.

7.5 Examples

The value of the overshoot and the number of local extrema are now determined for two kinds of analysing wavelets. The wavelets used below were all defined in Chapter 1. The number of extrema is compared with the result in Theorem 7.3. The expression in Eq. 7.26 shows that the value of the overshoot is equal to the supremum of

$$G_g(M) = \frac{4}{c_g} \int_0^\infty \frac{|\tilde{g}(\omega)|^2}{\omega} \, \mathrm{Si}(M\omega) \, d\omega \tag{7.30}$$

over positive M, which is also the exact expression for $f_\rho(t)$ when $t = \rho M$ and

$$f(t) = H(t) - 1/2.$$

Notice that $f_\rho(t)$ is well defined even though $f(t)$ is not square integrable. The number of local extrema is found by plotting $f_1(t) = 1/2 \, G_g(t)$ against t.

Example 1: *the Complex–Valued Mexican Hat Wavelet*
The filtered function $f_\rho(t)$ for the complex–valued Mexican Hat wavelet is shown in figure 7.3. We find that

$$G_g = \sup_{M>0} G_g(M) \simeq 1.069, \tag{7.31}$$

which shows that there is an overshoot of approximately 6.9 %. The Fourier Sine transform of $|\tilde{g}(\omega)|^2/\omega$ is (see p.495, Gradshteyn & Ryzhik, 1980)

$$-\frac{1}{\sqrt{2\pi}} \int_0^\infty \omega^3 \, e^{-\omega^2} \, \sin(u\omega) \, d\omega = \frac{1}{\sqrt{2}} \, \frac{6u - u^3}{16} \, \exp(-u^2/4) \tag{7.32}$$

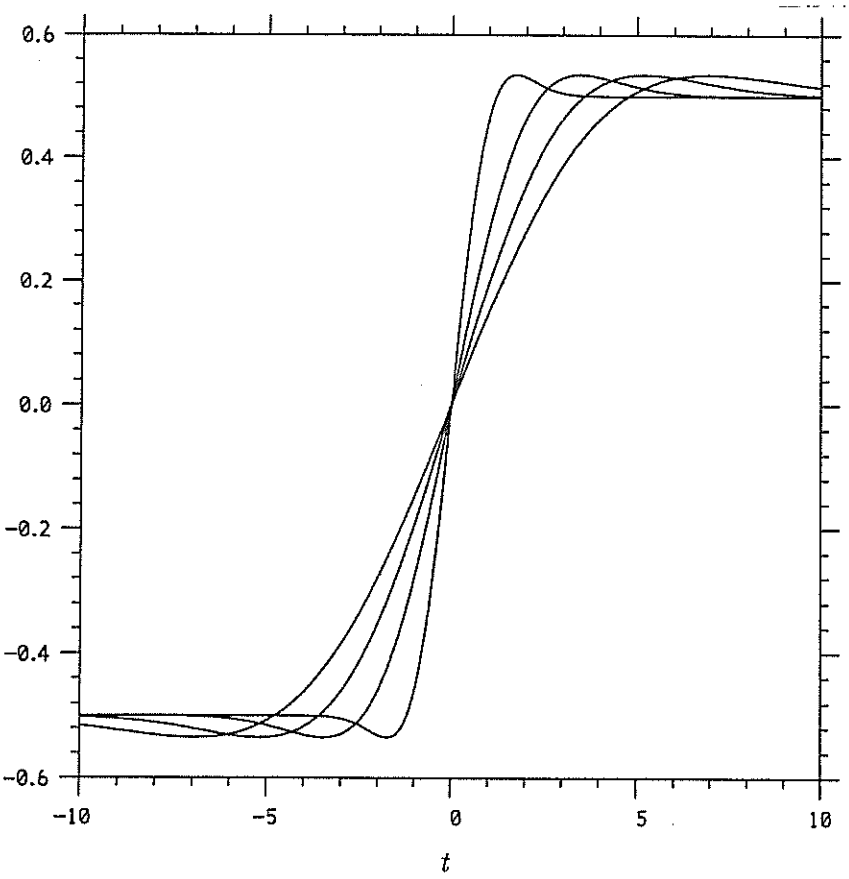

Figure 7.3: The filtered function $f_\rho(t)$ for the Mexican Hat wavelet, for various values of ρ.

and changes sign only once, namely when $u = \sqrt{6}$. According to Theorem 7.3 there should be only one local extremum in $f_1(t)$ for $t > 0$. This conclusion is supported by figure 7.3: there is only one local extremum, a maximum, and this seems to occur at $t = \sqrt{6}$.

Example 2: *The Poisson Wavelets*

Consider next the Poisson wavelets $g_m(t)$. The Fourier Sine transform of $|\tilde{g}_m(\omega)|^2/\omega$ is (p.490, Gradshteyn & Ryzhik, 1980)

$$-\frac{1}{\sqrt{2\pi}} \int_0^\infty \omega^{2m-1}\, e^{-2\omega}\, \sin(u\omega)\, d\omega = -\frac{\Gamma(2m)}{(4+u^2)^m} \sin(2m \tan^{-1}(u/2)). \qquad (7.33)$$

The number of zeros occuring for $u > 0$ in Eq. 7.33 is equal to the largest integer strictly smaller than m. For instance, if $0 < m \leq 1$, there are no zeros in the Fourier Sine transform, hence no local extrema and no overshoot (see figure 7.4).

Finally, let us show that the overshoot G_{g_m} for the poisson wavelet $g_m(t)$ converges toward G_F as m tends to infinity. To make c_g finite, it is necessary to assume that $m > 1/2$. The overshoot is determined by the function in Eq. 7.30. This function is an integral, and after changing variable of integration, $M\omega \mapsto \omega$, the integrand is the function

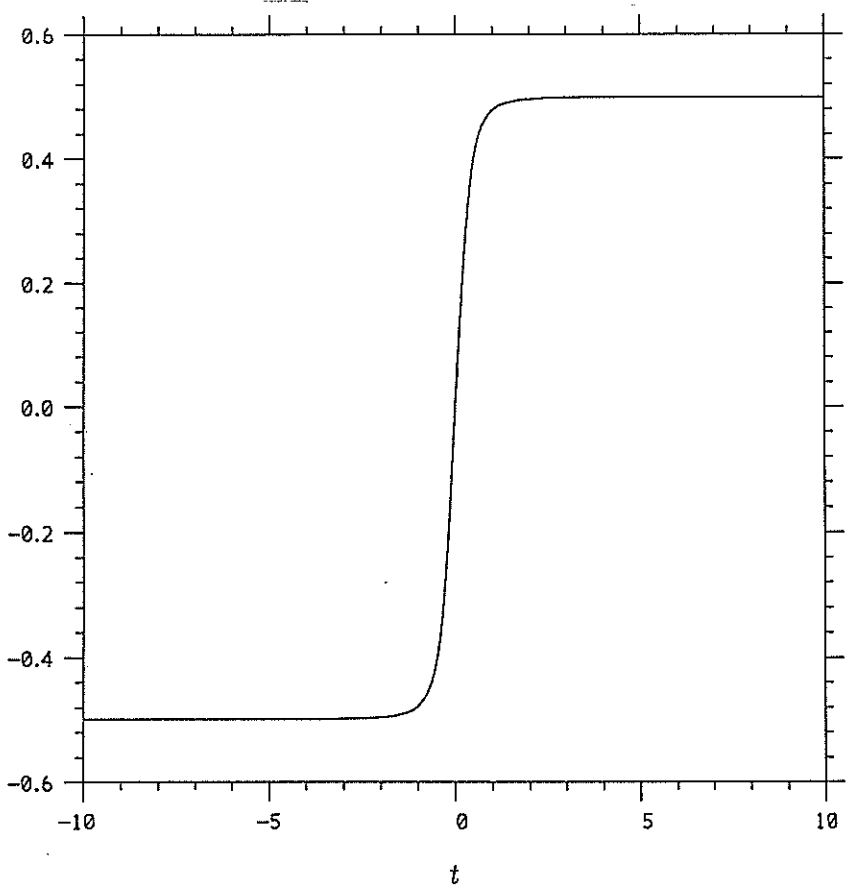

Figure 7.4: The filtered function $f_1(t)$ for the Poisson Wavelet with $m = 1$.

$h_m(\omega)$,

$$h_m(\omega) = \frac{|\,\tilde{g}_m(\omega/M)\,|^2}{\omega}, \tag{7.34}$$

where $M = \pi/(m - 1/2)$. The idea is now that this function converges in distribution toward a delta–function as m tends to infinity; of course, when $h_m(\omega)$ is a delta–function, the function defined in Eq. 7.30 reduces to the Sine integral and the overshoot is G_F. Now (see p. 317, Gradshteyn & Ryzhik, 1980),

$$c_g = \int_0^\infty h_m(\omega)\, d\omega = 2^{-2m+1}\, \pi\, \Gamma(m+1)^{-2}\, \Gamma(2m), \tag{7.35}$$

and Stirling's formula (e.g., Gradshteyn & Ryzhik, 1980) can be used to evaluate $\Gamma(2m)$ in the limit $m \to \infty$,

$$\frac{h_m(\omega)}{c_g} \sim \frac{1}{4\pi^2}\sqrt{\frac{m-1/2}{\pi}}\left(\frac{\omega e^{1-\omega/\pi}}{\pi}\right)^{2m-1} H(\omega), \tag{7.36}$$

for $\omega \geq 0$. Equation 7.35 shows that

$$\int_{-\infty}^{+\infty} \frac{h_m(\omega)}{c_g}\, d\omega = 1, \tag{7.37}$$

and it is easily shown that

$$\frac{h_m(\omega)}{c_g} \to 0 \tag{7.38}$$

as $m \to \infty$, provided $\omega \neq \pi$. Moreover, when $\omega = \pi$,

$$\frac{h_m(\omega)}{c_g} = \frac{1}{4\pi^2}\sqrt{\frac{m-1/2}{\pi}}. \tag{7.39}$$

Assuming that the convergence in Eq. 7.38 is uniform outside neighbourhoods of zero, it follows that $h_m(\omega)$ converges in distribution toward a delta–function. This explains why the the overshoot G_{g_m} converges toward G_F as m increases (see the numerical results in Table 7.1).

m	Overshoot in %
1	0.0
2	2.9
3	7.0
4	11.0
5	14.6
10	17.1
14	17.5

Table 7.1: $100 \times (C_g - 1)\%$ for various Poisson wavelets.

Chapter 8

Box dimensions and wavelet transforms

It is shown that wavelet coefficients can be used to characterise the box dimensions of graphs of continuous functions. The box dimensions of the classical Weierstrass functions are rederived and previous results for these functions are strengthened.

8.1 Introduction

Previous authors have noticed that wavelet transforms characterise the box dimensions of measure–theoretic supports (e.g., Holschneider, 1988; Ghez & Vaienti, 1989; Vaienti, 1991; Ghez & Vaienti, 1992). These results basically extend well known results on the scalings of local densities of measures (e.g., Falconer, 1990). But there has apparently not been any work on the connection between wavelet transforms and the box dimensions of the graphs of continuous functions. Recall from chapter 1 that the Hölder exponent for a function is the largest α such that

$$|f(x) - f(y)| \leq C\,|x - y|^{\alpha}, \tag{8.1}$$

for all x and y, and for some constant C. Since Hölder exponents give lower bounds on box dimensions (see Proposition 8.2), it is natural to conjecture that the absolute values of wavelet coefficients often determine box dimensions. I will now prove this conjecture for general conditions on the wavelet coefficients.

It is shown below that the existence and value of box dimensions of graphs of continuous functions can be determined from the corresponding wavelet transforms. The upper bound on the box dimension follows easily from standard results on the connection

between the Hölder continuity of functions and the box dimensions of their graphs (see Proposition 8.2 below), and from a recent result by Holschneider & Tchamitchian (1991) on the determination of Hölder continuity by means of wavelet transforms (see Chapter 1). The above conjecture on the connection between the fall–off of wavelet transforms and lower bounds on box dimensions is proved by exploiting the observation that a local lower bound on the wavelet transform leads to a lower bound on fluctuations in the function in an appropriately chosen interval. The lower bounds for the box dimension are equal to the upper bounds, showing that the wavelet coefficients determine the box dimension uniquely.

8.2 The determination of box dimensions

Box dimensions are easy to compute and are therefore often used to characterise scale invariance, though they are not 'dimensions' in any rigorous sense (Falconer, 1990). The box dimension of a set, when it exists, may be defined as follows (Falconer, 1990):

Proposition 8.1 *Suppose that* $\mathbb{F} \subseteq \mathbb{R}^2$ *is intersected by* n_k δ_k*–mesh cubes with* $\delta_k \searrow 0$ *as* $k \to \infty$, *and* $\delta_{k+1} \geq c\,\delta_k$ *for some* $0 < c < 1$. *Then the box dimension of* $\mathbb{F}$ *is given by*

$$D = \lim_{k \to \infty} \frac{\log n_k}{-\log \delta_k}, \tag{8.2}$$

provided the limit exists.

The notion of 'box dimension' was apparently first introduced by Kolmogorov (1956) in order to indicate the complexity of different function classes. (Strikingly, box dimensions were introduced to characterise the complexity of solutions of certain seventh–order equations, related to Hilbert's 13th problem, but are now used mainly in physics, such as the description of turbulent structure).

Rather than counting boxes directly, we rely on the following result (Falconer, 1990), relating the 'local envelope' of a continuous function to the box dimension:

Proposition 8.2 *Let* $f : [a, b] \to \mathbb{R}$, *where* $b > a$, *be a continuous function.*

(a) If f *is Hölder continuous with exponent* α *and the box dimension* D *exists, then* $D \leq 2 - \alpha$.

(b) Suppose that there are numbers $K_2 > 0$ *and* $0 \leq \alpha \leq 1$, *and a decreasing sequence as in Proposition 8.1, such that:*

for each $t_1 \in [a,b]$ *and* $k \in \mathbb{N}$ *there exists* $t_2 \in [a,b]$ *with* $|t_1 - t_2| \leq \delta_k$ *and*

$$|f(t_1) - f(t_2)| \geq K_2\, \delta_k^{\alpha}. \tag{8.3}$$

If the box dimension exists, then $D \geq 2 - \alpha$.

Remark

The box dimension exists if α in Eq. 8.3 may be chosen equal to the Hölder exponent.

To determine the box dimensions, we then need positive lower bounds on the 'typical' differences $|f(t_1)-f(t_2)|$ for given $|t_1-t_2|$. This is difficult because $|f(t_1)-f(t_2)|$ generally fluctuates when t_1 varies and $|t_1 - t_2|$ remains fixed. A similar problem with lower bounds occurs when considering the asymptotic behaviour at infinity of entire functions. In this case the problem is to obtain a lower bound on the maximum value of the function on a circle of given radius in the complex plane and centred at the origin. This is possible if the integral of the function along the circle can be estimated, because then the mean value theorem for integrals can be used: if $\int_a^b f(t)\,dt > c$, where $b > a$, then there is at least one point, $t_0 \in]a,b[$, such that $f(t_0) > c/(b-a)$. This trick[1] is now used to prove the following theorem.

Theorem 8.3 *Suppose that* $f : [a,b] \to \mathbb{R}$ *is continuous and that the analysing wavelet* g *satisfies the two conditions in Section 1.3. Let* $\{\lambda_k\}$, $k = 0, 1, \ldots$, *be a decreasing sequence with* $\lambda_k \searrow 0$, *as* $k \to \infty$, *and* $\lambda_{k+1} \geq c\,\lambda_k$ *for some* $0 < c < 1$ *and all* $k \in \mathbb{N}$. *Suppose that there is a collection of points* $\{r_{kl}\}$, *a* D *such that* $\max\{1, 2-m\} < D < 2$, *and* $\alpha, \beta > 0$ *with the following properties:* ↑ m from (1) p.9

(a) for each $t_0 \in [a,b]$ *and for some choice of* k *and* l,

$$|t_0 - r_{kl}| < \alpha\,\lambda_k; \tag{8.4}$$

(b) for all k *and* l,

$$|W(\lambda_k, r_{kl})| \geq \beta\,\lambda_k^{2-D}; \tag{8.5}$$

(c) and

$$|W(\lambda, r)| = O(\lambda^{2-D}), \tag{8.6}$$

[1] Littlewood was apparently the first to use the mean value theorem to derive such inequalities; the example mentioned here is part of his first paper (Littlewood, 1907).

uniformly in r.

Then the box dimension of the graph exists and is equal to D.

Remarks

1. The sequence $\{r_{kl}\}$ may be finite for each k.

2. The following proof does not require that r and λ are continuous parameters. The above theorem, therefore, also holds for discrete wavelet transforms.

Proof.
It is straightforward to get an upper bound on the box dimension. By Theorem 1.1 in Chapter 1, condition (c) above is equivalent to the function being uniformly Hölder continuous with exponent $2-D$. Condition (a) of Proposition 8.2 then shows that the box dimension, provided it exists, is less than or equal to $2-D$. Thus, it only remains to show that $2-D$ is also the lower bound for the box dimension and that the box dimension exists.

The proof for the lower bound on the box dimension is more complicated. To use the mean value theorem for integrals, notice first that

$$\int_{-\delta}^{+\delta} |f(t+t_0)-f(t_0)|\,dt \;\geq\; \frac{\lambda}{\sup|g|}\,\frac{1}{\lambda}\int_{-\delta}^{+\delta} |f(t+t_0)-f(t_0)|\,|g\Big(\frac{t}{\lambda}\Big)|\,dt. \tag{8.7}$$

The norm–inequality for integrals gives a lower bound on the right side of this inequality,

$$\begin{aligned}
&\frac{\lambda}{\sup|g|}\,\frac{1}{\lambda}\int_{-\delta}^{+\delta} |f(t+t_0)-f(t_0)|\,|g\Big(\frac{t}{\lambda}\Big)|\,dt \\
&\quad\geq\; \frac{\lambda}{\sup|g|}\,|\,\frac{1}{\lambda}\int_{-\delta}^{+\delta}[f(t+t_0)-f(t_0)]\,g^*\Big(\frac{t}{\lambda}\Big)\,dt\,| \\
&\quad=\; \frac{\lambda}{\sup|g|}\,|\,W(\lambda,t_0)-\frac{1}{\lambda}\int_{\mathbb{R}-[-\delta,+\delta]}[f(t+t_0)-f(t_0)]\,g^*\Big(\frac{t}{\lambda}\Big)\,dt\,|.
\end{aligned} \tag{8.8}$$

The last step followed by using the condition that the analysing wavelet has zero integral (condition (2) in Chapter 1).

We now evaluate the last term in Eq. 8.8 by using the Hölder continuity of $f(t)$ and the decay at infinity of the analysing wavelet. Condition (1) from the section on Hölder continuity in Chapter 1 implies that

$$\frac{1}{\lambda}\int_{\delta}^{\infty} |t|^{2-D}\,|g^*\Big(\frac{t}{\lambda}\Big)|\,dt \;\leq\; \frac{K}{m-1+D}\,\lambda^{1+m}\,\delta^{1-D-m}, \tag{8.9}$$

for some constant $K > 0$. To use this upper bound on the last integral in Eq. 8.8, the wavelet transform $|W(\lambda, t_0)|$ in the same line must be sufficiently large; this is the case when $t_0 = r_{kl}$. At these points,

$$\int_{-\delta}^{+\delta} |f(t + r_{kl}) - f(r_{kl})|\, dt \;\geq\; \frac{\lambda}{\sup |g|}\, \big|\, |W(\lambda, r_{kl})| - C\, \lambda^{1+m}\, \delta^{1-D-m}\, \big|, \qquad (8.10)$$

for some constant $C > 0$. To evaluate the right side, let $\lambda = \lambda_k$ and $\delta = 2\,\delta_k = 2\,\lambda_k\,\alpha\,h$, for some $h > 0$ which we can choose independently of k and l. The lower bound on the wavelet transform in condition (b) in Theorem 8.3 then implies that

$$\big|\, |W(\lambda_k, r_{kl})| - C\, \lambda_k^{1+m}\, \delta_k^{1-D-m} \big| \;\geq\; |\beta\, \alpha^{D-2}\, h^{D-2} - C\, \alpha^{-1-m}\, h^{-1-m}\, |\, 2^{2-D}\, \delta_k^{2-D}, \quad (8.11)$$

provided h is sufficiently large. By combining Eqs. 8.10 and 8.11, and then using the mean value theorem for integrals, it follows that there is a $t' \in]-\delta_k/2; \delta_k/2[$ such that

$$|f(t' + r_{kl}) - f(r_{kl})| \;\geq\; \frac{2^{2-D}}{\alpha\, h\, \sup |g|}\, |\beta\, \alpha^{D-2}\, h^{D-2} - C\, \alpha^{-1-m}\, h^{-1-m}|\, \delta_k^{2-D}. \qquad (8.12)$$

Condition (b) in Proposition 8.2 is then satisfied when $t_0 = r_{kl}$ and $t_1 = r_{kl} + t'$. Let us now show that this condition is satisfied for *all* $t_0 \in [a, b]$ (that is, there is always a $t_1 \in]t_0 - \delta_k; t_0 + \delta_k[$ such that the condition is satisfied). For given $t_0 \in [a, b]$ and $k \in \mathbb{N}$, condition (a) in the theorem shows the existence of an $r_{kl} \in [a, b]$ with $|t_0 - r_{kl}| < \delta_k/h$. Choose now a $t' \in]-\delta_k/2; \delta_k/2[$ such that Eq. 8.12 holds. Then $|t_0 - t_1| < \delta_k$, provided that $h \geq 2$. By taking either $t_1 = r_{kl}$ or $t_1 = t' + r_{kl}$, it follows that

$$|f(t_0) - f(t_1)| \;\geq\; \frac{1}{2\,\alpha\, h\, \sup |g|}\, |\beta\, \alpha^{D-2}\, h^{D-2} - C\, \alpha^{-1-m}\, h^{-1-m}\, |\, \delta_k^{2-D} \qquad (8.13)$$

and $|t_0 - t_1| < \delta_k$. This shows that condition (b) of Proposition 8.2 is satisfied. Since the exponent, $2 - D$, is an admissible Hölder exponent for the function, as shown earlier in this proof, it follows from the remark after Proposition 8.2 that the box dimension exists and is greater than or equal to D.

□

8.3 Weierstrass functions

On a historical note, the development of modern analysis was strongly motivated by the construction of continuous functions that are non–differentiable everywhere (Weierstrass,

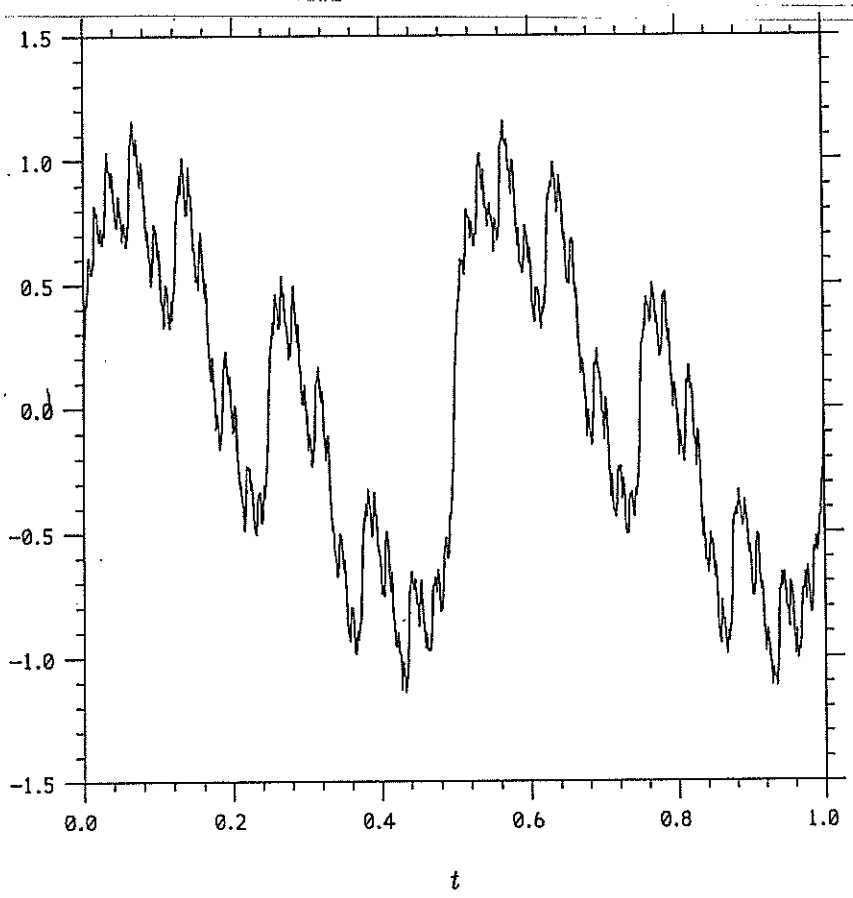

Figure 8.1: The periodic Weierstrass function with $a = 2$ and $b = 2^{1.4}$.

1872). Until then, most authors thought continuous functions would be differentiable everywhere, perhaps with the exception of a few isolated points. However, Weierstrass showed that the functions,

$$f(t) = \sum_{k=1}^{\infty} b^k \sin(a^k t), \quad t \in \mathbb{R}, \tag{8.14}$$

when a and b are chosen appropriately, are continuous yet non-differentiable everywhere. Hardy (1916) later showed that the Weierstrass functions are nowhere differentiable when $a\,b > 1$. Here we shall assume a integer, to make the functions periodic, and $0 < b < 1$. The Weierstrass functions are often used as examples of 'fractals' (e.g., Falconer, 1990) and it is then natural to illustrate the above theorem on these functions.

Corollary 8.4 *If $f : [0, 2\pi] \to \mathbb{R}$ is the Weierstrass function defined above, and if $ab > 1$, then the graph has box dimension*

$$D = 2 + \frac{\log b}{\log a}. \tag{8.15}$$

Remark

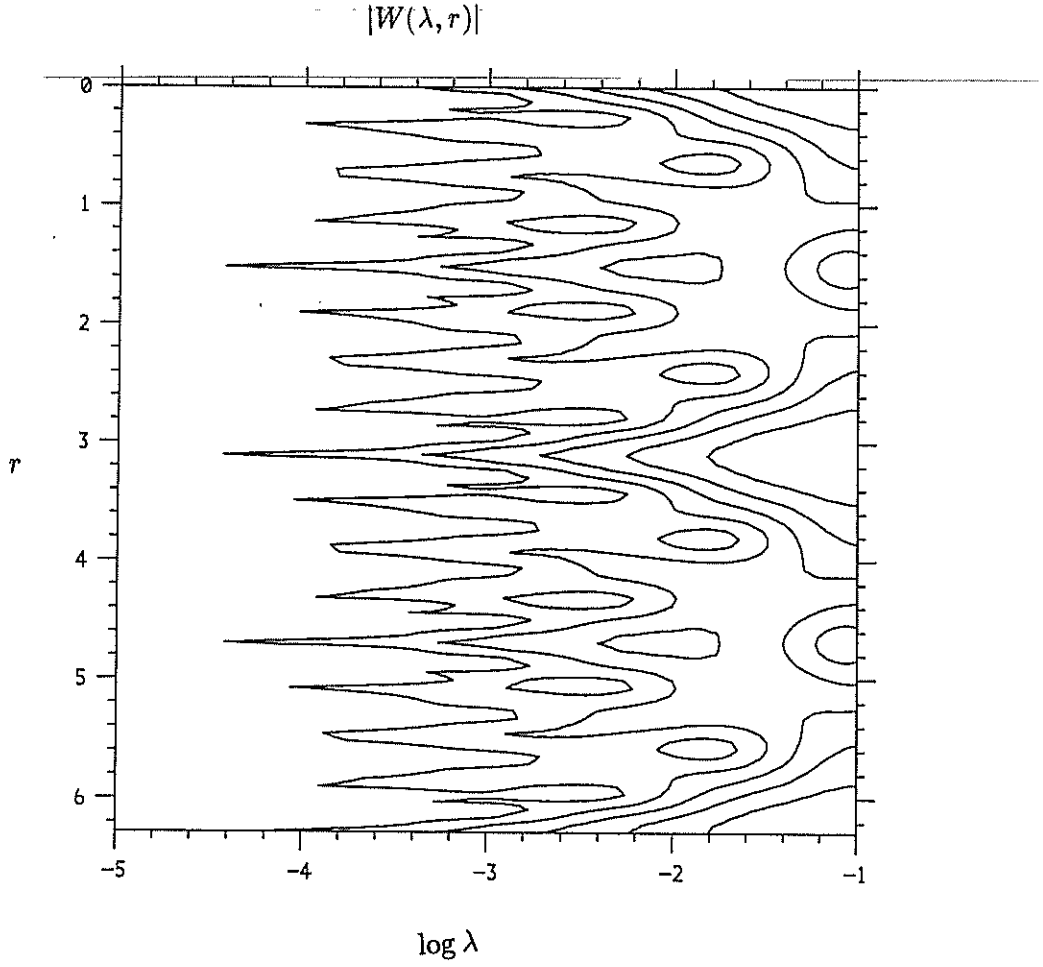

Figure 8.2: The wavelet transforms (complex–valued Mexican Hat wavelet) of the Weierstrass functions with $a = 2$ and $b = 2^{1.4}$.

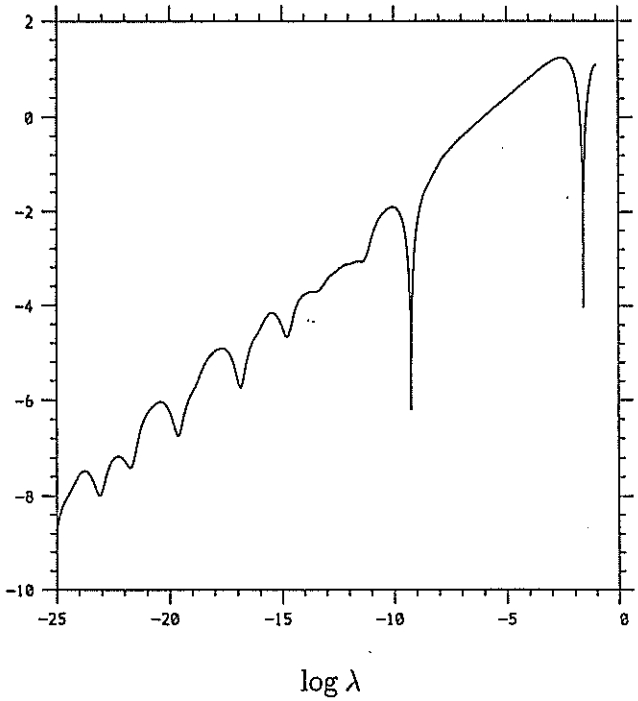

Figure 8.3: Logarithmic plot of the modulus of the wavelet transform with $r = 1/2$. The wavelet transform fluctuates around a power–law with exponent equal to $1.4 = \log b / \log a$.

1. This seems to strengthen previous results, for which it was required that a be 'large' (Falconer 1990).

2. The second part of the following proof (in which the Hölder continuity is determined) is due to Holschneider (private communication).

Proof.
For simplicity, define $f(t)$ on the entire real line, rather than just $[0, 2\pi]$. This does not affect the validity of the proof, because the contribution from 'infinity' is negligible when λ is small. Choose an analysing wavelet with bounded Fourier transform and support in the interval $[1, a[$. The wavelet transform of the Weierstrass function $f(t)$ is then given by

$$W(\lambda, r) = \frac{b^n}{2\pi} \tilde{g}(\lambda a^n) \exp[i r a^n], \tag{8.16}$$

where n is unique integer such that $\lambda a^n \in [1, a[$. Notice that

$$b = a^{\log b / \log a} \tag{8.17}$$

and that $0 > \log b/\log a > -1$. To show that conditions (a) and (b) in Theorem 8.3 are satisfied, Suppose that $\lambda = a^{-n}$, for some $n \in \mathbb{N}$. Equation 8.16 is then

$$W(a^{-n}, r) = \frac{a^{-n \log b / \log a}}{2\pi} \tilde{g}(1) \exp[i r a^n]. \tag{8.18}$$

Define,

$$r_{np} = \frac{a^n - p}{a^n} 2\pi,$$

where p is an integer from the set $[1, \ldots, a^n - 1]$. Since a is an integer,

$$a^n r_{np} = 0 \mod 2\pi, \tag{8.19}$$

so that

$$W(a^{-n}, r_{np}) = \frac{a^{-n \log b / \log a}}{2\pi} \tilde{g}(1). \tag{8.20}$$

We see that conditions (a) and (b) are satisfied. Since $\lambda > a^{-n}$, and because the Fourier transform of the analysing wavelet is bounded, there exists a positive constant C_0 such that

$$|W(\lambda, r)| \leq C_0 \lambda^{-\log b / \log a}. \tag{8.21}$$

We have now shown that $f(t)$ is Hölder continuous with exponent $-\log b/\log a$, so that condition (c) of Theorem 8.3 is satisfied.

□

Bibliography

[1] ANSELMET, F., GAGNE, Y., & HOPFINGER, E. J. 1984, High–order velocity structure functions in turbulent shear flows, *J. Fluid Mech.* **140**, 63 – 89.

[2] BATCHELOR, G. K. 1947, Kolmogoroff's theory of locally isotropic turbulence, *Proc. Cambr. Phil. Soc.* **43**, 533 – 559.

[3] BATCHELOR, G. K. 1953, The Theory of Homogeneous Turbulence, (CUP, 1953).

[4] BATCHELOR, G. K. 1969, Computation of the energy spectrum in homogeneous two–dimensional turbulence, *Phys. Fluids* **12**, Suppl. II, 233 – 239.

[5] BATCHELOR, G. K. 1967, *An Introduction to Fluid Mechanics* (Cambridge University Press).

[6] BATCHELOR, G. K. & TOWNSEND, A. A. 1947, Decay of vorticity in isotropic turbulence, *Proc. Roy. Soc.* A**190**, 534 – 550.

[7] BATCHELOR, G. K. & TOWNSEND, A. A. 1949, The nature of turbulent motion at large wave–numbers, *Proc. Roy. Soc.* A**199**, 238 – 255.

[8] BETCHOV, R. 1961, Semi–isotropic turbulence and helicoidal flows, *Phys. Fluids* **4**, 925 – 926.

[9] BORGAS, M. S. & SAWFORD, B. L. 1991, The small–scale structure of acceleration correlations and its role in the statistical theory of turbulent diffusion, *J. Fluid Mech.* **228**, 295 – 320.

[10] BOUBNOV, B. M., DALZIEL, S. B., & LINDEN, P. F. 1994, Source–sink turbulence in a stratified fluid, *J. Fluid Mech.* **261**, 273 – 303.

[11] BORUE, V. 1994, Inverse energy cascade in stationary two–dimensional homogeneous turbulence, *Phys. Rev. Lett.* **72**, 1475 – 1478.

[12] BRAY, R. W. 1966, A study of turbulence and convection using Fourier and numerical analysis, Ph. D. thesis, University of Cambridge (DAMTP).

[13] CALDERÓN, A. P., & ZYGMUND, A. 1961, Local properties of solutions of elliptic partial differential equations, *Studia Math.* **20**, 171–225 .

[14] CALDERÓN, A. P. 1964, Intermediate spaces and interpolation, the complex method, *Studia Math.* **24**, 113 – 190.

[15] CARSLAW, H. S. 1925, A Historical Note on Gibbs Phenomenon. *Bull. Amer. Math. Soc.* **31**, 420 – 424.

[16] CHAMPENEY, D. C. 1987, *A Handbook of Fourier Theorems* (Cambridge University Press).

[17] CHANDRASEKHARAN, K. 1989, *Classical Fourier Transforms*, (Springer-Verlag).

[18] DRITSCHEL, D. G. 1993, Vortex properties of two–dimensional turbulence, *Phys. Fluids* **A5**, 984 – 997.

[19] DUBRULLE, B. 1994, Intermittency in fully developed turbulence: log–Poisson statistics and scale invariance, *Phys. Rev. Letter* **73**, 959 – 962.

[20] EINSTEIN, A. 1905, On the movement of small particles suspended in a stationary liquid demanded by the molecular–kinetic theory of heat, *Ann. d. Physik* **17**, p. 549(or, in *Investigations on the theory of the Brownian movement*, Dover, 1956).

[21] FALCONER, K. J. 1990, *Fractal Geometry*, (John Wiley and Sons).

[22] FARGE, M. 1992, Wavelet Transforms and Their Applications to Turbulence, *Ann. Rev. Fluid Mech.*, 395–457.

[23] FJØRTOFT, R. 1953, On the changes in the spectral distribution of kinetic energy for two–dimensional, nondivergent flow *Tellus* **5**, 225 – 230.

[24] FORNBERG, B. 1977, A numerical study of two–dimensional turbulence, *J. Comput. Phys.* **25**, 1 – 31.

[25] FRISCH, U. & SULEM, P. L. 1984, Numerical simulation of the inverse cascade in two–dimensional turbulence, *Phys. Fluids* **28**, 1921 – 1923.

[26] FRISCH, U., SULEM, P–L., & NELKIN, M. 1978, A simple model of intermittent fully–developed turbulence, *J. Fluid Mech.* **87**, 719 – 736.

[27] GHEZ, J. M., & VAIENTI, S. 1989, On the Wavelet Analysis for Multifractal Sets, *J. Stat. Phys.* **57**:415.

[28] GHEZ, J. M., & VAIENTI 1992, S. 1992, Integrated Wavelets on Fractal Sets, I & II, *Nonlinearity* **3**:777 and 791.

[29] GIBBS, J. W., Nature, LXIX (1899).

[30] GILBERT, A. D. 1988, Spiral structures and spectra in two–dimensional turbulence, *J. Fluid Mech.* **193**, 475 – 497.

[31] GRADSHTEYN, I. S., & RYZHIK, I. M. 1980, *Table of Integrals, Series, and Products* (Academic Press Inc.).

[32] GROSSMAN, A., & MORLET, J. 1984, Decomposition of Hardy Functions into Square Integrable Wavelets of Constant Shape, *SIAM J. Math. Anal.*, (4) **15**, 723 – 736.

[33] HAMA, F. R. 1953, The spectrum equation of two–dimensional isotropic turbulence, *Proc. 3rd Midwestern Conference on Fluid Mech.* (University of Minnesota), 427 – 433.

[34] HANNA, S. R. 1980, Lagrangian and Eulerian time–scale relations in the daytime boundary layer, *J. Appl. Met.* **20**, 242 – 249.

[35] HARDY, G., LITTLEWOOD, J. E., & PÓLYA, G. 1934, *Inequalities* (Cambridge University Press).

[36] HERRING, J. R. & McWILLIAMS, J. C. 1985, Comparison of direct numerical simulation of two–dimensional turbulence with two–point closure: the effects of intermittency, *J. Fluid Mech.* **153**, 229 – 242.

[37] HOLSCHNEIDER, M. 1988, On the Wavelet Transformation of Fractal Objects, *J. Stat. Phys.*, (5/6) **50**, 963 – 993.

[38] HOLSCHNEIDER, M., & TCHAMITCHIAN, P. 1991, Pointwise analysis of Riemann's "non–differentiable" function, *Invent. Math.* **105**, 157 – 175.

[39] INOUE, E. 1951, On the turbulent diffusion in the atmosphere, *J. Meteor. Soc. Japan* **29**, 246 – 252.

[40] INOUE, E. 1952, On the Lagrangian correlation coefficient for turbulent diffusion and application to atmospheric diffusion phenomena, *Geophys. Res. Rap.* **19**, 397 – 412.

[41] JAFFARD, S. 1993, Orthonormal and continuous wavelet transform: Algorithms and applications to the study of pointwise properties of functions, *Proceedings of the IMA Conference on Wavelets, Fractals and Fourier Transforms: New Developments and New Applications*, (Oxford University Press).

[42] JIMÉNEZ, J., WRAY, A. A., SAFFMAN, P. G., & ROGALLO, R. S. 1993, The structure of intense vorticity in homogeneous isotropic turbulence, *J. Fluid Mech.* **255**, 65 – 90.

[43] VON KÁRMÁN, T. & HOWARTH, L. 1938, On the statistical theory of isotropic turbulence, *Proc. R. Soc. Lond.* A **164**, 192 – 215.

[44] KERR, R. M. 1985, Higher order derivative correlation and the alignment of small scale structures in isotropic numerical turbulence, *J. Fluid Mech.* **153**, 31 – 58.

[45] KOLMOGOROV, A. N. 1941a, The local structure of turbulence in incompressible viscous fluid for very large Reynolds numbers, *Dokl. Akad. Nauk SSSR* **30**, 301 – 305; see also *Proc. R. Soc. London Ser. A* **434** (1991).

[46] KOLMOGOROV, A. N. 1941 b, Dissipation of energy in the locally isotropic turbulence, *Dokl. Akad. Nauk SSSR* **32**; see also *Proc. R. Soc. London Ser. A* **434** (1991).

[47] KOLMOGOROV, A. N. 1962, A refinement of previous hypotheses concerning the local structure of turbulence in a viscous incompressible fluid at high Reynolds number, *J. Fluid Mech.* **13**, 82 – 85.

[48] KOLMOGOROV, A. N. 1956, Some fundamental problems in the approximate and exact representation of functions of one or several variables, in *Proc. III Math. Congress USSR* Vol. 2, 28 – 29 (MGU Press, Moscow), (in Russian); an english translation can be found in Vol. 1 of his *Collected Works*, (Kluwer Academic Publishers, 1985).

[49] KRAICHNAN, R. H. 1967, Inertial ranges in two–dimensional turbulence, *Phys. Fluids* **10**, 1417 – 1423.

[50] LANDAU, L. D., & LIFSHITZ, E. M. 1944, Fluid Mechanics (in Russian) (translated in 1959; Pergamon Press, London).

[51] LEGRAS, B., SANTANGELO, P., & BENZI, R. 1988, High resolution numerical experiments for forced two–dimensional turbulence, *Europhys. Lett.* **5**, 37 – 42.

[52] LEITH, C. E. 1968, Diffusion approximation for two–dimensional turbulence, *Phys. Fluids* **11**, 671 – 673.

[53] LESIEUR, M., FRISCH, U., & BRISSAUD, A. 1971, Théorie de Kraichnan de la Turbulence, *Ann. Geophys.* **25**, 151 – 165.

[54] LILLY, D. K. 1969, Numerical simulation of two–dimensional turbulence, *Phys. Fluids* **12**, Suppl. II, 240 – 249.

[55] LITTLEWOOD, J. E. 1907, *Lond. Math. Soc.* Jan. 1.

[56] LUNDGREN, T. S. 1982, Strained spiral vortex model for turbulent fine structure, *Phys. Fluids* **25**, 2193 – 2203.

[57] MELANDER, M. V., ZABUSKY, N. J., & McWILLIAMS, J. C. 1988, Symmetric vortex merger in two dimensions: causes and conditions, *J. Fluid Mech.* **115**, 303 – 340.

[58] MEYER, Y. 1990, *Ondelettes et Operateurs I – III*, (Hermann, Paris).

[59] McWILLIAMS, J. C. 1984, The emergence of isolated coherent vortices in turbulent flows, *J. Fluid Mech.* **146**, 21 – 43.

[60] MALTRUD, M. E. & VALLIS, G. K. 1991, Energy spectra and coherent structures in forced two–dimensional and beta–plane turbulence, *J. Fluid Mech.* **228**, 321 – 342.

[61] MOFFATT, H. K. 1969, The degree of knottedness of tangled vortex lines, *J. Fluid Mech.* **35**, 117 – 129.

[62] MOFFATT, H. K. 1984, Simple topological aspects of turbulent vorticity dynamics, in *Turbulence and chaotic phenomena in fluids*, (ed. T. Tatsumi, Elsevier).

[63] MOFFATT, H. K. 1993, Spiral structures in turbulent flow, in *Proceedings of the Monte Veritá conference* (eds. Dracos & Tsinober; Birkhäuser).

[64] MOREAU, J. J. 1961, Constantes d'un flot tourbillonnaire en fluid parfait barotrope, *C. R. Acad. Sci. Paris* **252**, 2810.

[65] MONIN, A. S. & YAGLOM, A. M. 1975, *Statistical fluid mechanics: the mechanics of turbulence*, (Cambridge, Mass.; MIT Press).

[66] NASTROM, G. D. & GAGE, K. S. 1985, A climatology of atmospheric wavenumber spectra of wind and temperature observed by commercial aircraft, *J. Atmos. Sci.* **42**, 950 – 960.

[67] VON NEUMANN, J. 1949, Recent theories of turbulence, In *Collected Works* vol. VI (Pergamon Press, 1963).

[68] NOVIKOV, E. A., & STEWART, R. W. 1964, Intermittency of turbulence and spectrum of fluctuations in energy–dissipation, *Izv. Akad. Nauk SSSR*, Ser. Geofiz. **3**, 408 – 413 (in Russian).

[69] NOVIKOV, E. A. 1963, Random force method in turbulence theory, *Sov. Phys.* JETP **17**, 1449 – 1454.

[70] OBUKHOV, A. M. 1941, On the distribution of energy in the spectrum of turbulent flow, *Dokl. Akad. Nauk SSSR* **32**, 22 – 24.

[71] OBUKHOV, A. M. 1959, Description of turbulence in terms of Lagrangian variables, *Adv. Geophys.* **6**, 113 – 116.

[72] OBUKHOV, A. M. 1962, Some specific features of atmospheric turbulence, *J. Fluid Mech.* **13**, 77 – 81.

[73] OGURA, Y. 1958, On the isotropy of large–scale disturbances in the upper troposphere, *J. Meteorol.* **15**, 375 – 382.

[74] POLIFKE, W. 1991, Statistics of helicity fluctuations in homogeneous turbulence, *Phys. Fluids* **3**, 115 – 129.

[75] PULLIN, D. I., & SAFFMAN, P. G. 1993, On the Lundgren–Townsend model of turbulent fine scales, *Phys. Fluids* **5**, 126 – 145.

[76] PULLIN, D. I., BUNTINE, J. D., & SAFFMAN, P. G. 1994, On the spectrum of a stretched spiral vortex, *Phys. Fluids* **6** (9), 3010 – 3027.

[77] RASMUSSEN, H. O. 1993a, The wavelet Gibbs phenomenon in *Wavelets, Fractals, and Fourier Transforms, Cambridge December 1990*, (Eds. Farge, Hunt, & Vassilicos; Clarendon Press, 1993).

[78] RASMUSSEN, H. O. 1993b, The determination of box dimensions by means of wavelet transforms, *J. Stat. Phys.* **71** Nos. 3/4, 817 – 823.

[79] RASMUSSEN, H. O. 1995a, The local structure of anisotropic turbulence, submitted to *Proc. Roy. Soc. London.*

[80] RASMUSSEN, H. O. 1995b, Lagrangian structure of forced turbulence, submitted to *Proc. Roy. Soc. London.*

[81] RASMUSSEN, H. O. 1995c, A comment on spirals, submitted to *Phys. Fluids.*

[82] RASMUSSEN, H. O. 1995d, The Reynolds numbers of vortex tubes, submitted to *Phys. Rev. Lett..*

[83] RASMUSSEN, H. O. 1995e, A model for the higher–order structure function exponents of homogeneous turbulence, submitted to *Phys. Rev. Lett..*

[84] RASMUSSEN, H. O. 1995f, The energy transfer in forced turbulence, in preparation.

[85] RASMUSSEN, H. O. 1995g, The local structure of two–dimensional turbulence, in preparation.

[86] REYNOLDS, O. 1883, An experimental investigation of the circumstances which determine whether the motion of water shall be direct or sinuous, and of the law of resistance in parallel channels, *Phil. Trans. R. Soc. London* **174**, 935 – 982.

[87] REYNOLDS, O. 1894, On the dynamical theory of incompressible viscous fluids and the determination of the criterion, *Phil. Trans. R. Soc. London* **186**, 123 – 161.

[88] RICHARDSON, L. F. 1922, *Weather Prediction by Numerical Process*, (Dover, New York).

[89] RICHARDSON, L. F. 1926, Atmospheric diffusion shown on a distance–neighbour graph, *Proc. Roy. Soc.* A **110**, 709 – 737.

[90] RODEAN, H. C. 1991, The universal constant for the Lagrangian structure function, *Phys. Fluids* A **3** (6), 1479 – 1480.

[91] RUETSCH, G. R., & MAXEY, M. R. 1992, The evolution of small–scale structures in homogeneous isotropic turbulence, *Phys. Fluids* **4**, 2747 – 2760.

[92] SANTANGELO, P., BENZI, R., & LEGRAS, B. 1989, The generation of vortices in high resolution, two–dimensional decaying turbulence and the influence of initial conditions on the breaking of self–similarity, *Phys. Fluids* A1, 1027 – 1034.

[93] SAWFORD, B. L. 1991, Reynolds number effects in Lagrangian stochastic models of turbulent diffusion, *Phys. Fluids* A **3** (6), 1577 – 1586.

[94] SHE, Z–S. & LEVEQUE, E. 1993, Universal scaling laws in fully developed turbulence, *Phys. Rev. Lett.* **72**, 336 – 339.

[95] SHE, Z–S., & ORSZAG, S. A. 1991, Physical model of intermittency in turbulence: inertial–range non–Gaussian statistics, *Phys. Rev. Lett.* **66**, 1701 – 1704.

[96] SIGGIA, E. D. 1981, Numerical study of small scale intermittency in three dimensional turbulence, *J. Fluid Mech.* **107**, 375 – 406.

[97] SOMMERIA, J. 1986, Experimental study of the two–dimensional inverse energy cascade in a square box, *J. Fluid Mech.* **170**, 139 – 168.

[98] TATSUMI, T. 1980, Theory of Homogeneous Turbulence, *Advances in Applied Mechanics* **20**, 39 – 133.

[99] TAYLOR, G. I. 1921, Diffusion by continuous movements, *Proc. Lond. Math. Soc.* **20** (2), 196 – 211.

[100] TAYLOR, G. I. 1935, Statistical theory of turbulence I - V, *Proc. Roy. Soc.* **A151**, 421 – 478.

[101] TENNEKES, H., & LUMLEY, J. L. 1990, *A First Course in Turbulence*, (MIT).

[102] VINCENT, A., & MENEGUZZI, M. 1991, The spatial structure and statistical properties of homogeneous turbulence, *J. Fluid Mech.* **225**, 1 – 20.

[103] VINCENT, A., & MENEGUZZI, M. 1994, The dynamics of vorticity tubes in homogeneous turbulence, *J. Fluid Mech.* **258**, 245 – 254.

[104] WEIERSTRASS, K. 1872, Über continuierliche Functionen eines reellen Argumentes, die für keinen Werth des letzteren einen bestimmten Differentialquotienten besitzen, *Mathematische Werke* II (Königl. Akad. Wiss.), 71–74.

[105] WIIN–NIELSEN, A. 1967, On the annual variation and spectral distribution of atmospheric energy, *Tellus* **19**, 540 – 559.

[106] WILBRAHAM 1848, *Camb. and Dublin Math. Journal,* **III**, 198 – 201 (I have not found a copy of this journal).

[107] YAKHOT, V. 1992, 4/5 Kolmogorov law for statistically stationary turbulence: application to high–Rayleigh–number Bénard convection, *Phys. Rev. Lett.* **69**, 769 – 771.

[108] YEUNG, P. K. & POPE, S. B. 1989, Lagrangian statistics from direct numerical simulations of isotropic turbulence, *J. Fluid Mech.* **207**, 531 – 586.

[109] ZOCCHI, G., TABELING, P., MAURER, J., & WILLAIME, H. 1994, Measurement of the scaling of the dissipation at high Reynolds numbers, Submitted to *Phys. Rev. E.*

[110] ZYGMUND, A. 1959, *Trigonometric Series*, (Cambridge University Press).